NOAA Technical Memorandum ERL SEL-62

A SUMMARY OF SOLAR 1-8Å MEASUREMENTS FROM THE SMS AND GOES SATELLITES, 1977-1981

S. D. Bouwer
R. F. Donnelly
J. Falcon
A. Quintana
G. Caldwell

Space Environment Laboratory
Boulder, Colorado
July 1982

noaa NATIONAL OCEANIC AND ATMOSPHERIC ADMINISTRATION / Environmental Research Laboratories

NOAA Technical Memorandum ERL SEL-62

A SUMMARY OF SOLAR 1-8Å MEASUREMENTS FROM THE SMS AND GOES SATELLITES, 1977-1981

S. D. Bouwer
R. F. Donnelly
J. Falcon
A. Quintana
G. Caldwell

Space Environment Laboratory
Boulder, Colorado
July 1982

UNITED STATES
DEPARTMENT OF COMMERCE
Malcolm Baldrige,
Secretary

NATIONAL OCEANIC AND
ATMOSPHERIC ADMINISTRATION
John V. Byrne,
Administrator

Environmental Research
Laboratories
George H. Ludwig
Director

Table of Contents

A SUMMARY OF SOLAR 1-8Å MEASUREMENTS FROM THE SMS AND GOES SATELLITES, 1977-1981

S. D. Bouwer*, R. F. Donnelly†, J. Falcon†, A. Quintana+, G. Caldwell†

Abstract

The 1-8Å band of synodic full-disc solar x-rays (1-8Å) $W \cdot m^{-2}$ have been measured nearly continuously from 1975 to 1981 aboard the SMS-1, SMS-2, GOES-1, GOES-2, and GOES-3 satellites. These measurements are scheduled to continue in an on-going series of GOES satellites. The 1-8Å band of X-rays are proportional to the emission measure at coronal heights at temperatures greater than 2×10^6 K. In the past, attention has been centered on using solar x-ray measurements in the detection and description of solar flares and their ionospheric effects. Here we center on a practical method of describing solar 1-8Å mean and background X-ray measurements in a continuous time series to describe long-term solar variability. Intercomparisons of the satellites using linear regression techniques and a useful background coronal index are described. Sources of error and statistical information on relative accuracy are discussed. Data are presented in monthly plots of hourly averages, in tables of daily mean and background indices, and in comparison to the Ottawa 10.7 cm radio flux.

Key Words: Solar X-Rays, SMS-GOES Satellites, Coronal Background Index, Linear Regression, Ottawa 10.7 cm flux.

*Cooperative Institute for Research in Environmental Sciences, University of Colorado, Boulder, Colorado; †Environmental Research Laboratories, Boulder, Colorado; + COOP Student, Environmental Research Laboratories, Boulder, Colorado

1. INTRODUCTION

1.1 Overview of SMS and GOES solar X-ray measurements.

SMS and GOES are acronyms for the NASA Synchronous Meteorological Satellites and the NOAA Geostationary Operational Environmental Satellites. The instruments making the X-ray measurements are part of the Space Environment Monitoring System (SEMS). Two bands of X-rays (1/2-4Å, 1-8Å) are measured in three second intervals. Energetic particles and magnetic field measurements are the remainder of the SEMS system. The satellites are geostationary and spin stabilized. The design is discussed by Grubb (1975), the details of calibration by Unzicker and Donnelly (1974) and Donnelly et al., (1977). The 1-min measurements are presented in graphical format by Donnelly and Bouwer (1981), and Donnelly (1981).

The data are available from the World Data Center A for Solar-Terrestrial Physics, NOAA-EDIS, Boulder, Colorado, 80303, in the form of hourly graphs, microfilm, print-outs, and magnetic tapes.

The data presented here are based on the one-minute averages from SMS-2, GOES-1, GOES-2, and GOES-3 measurements. The 1/2-4Å band is not included here because they are very sensitive to the spectra assumption (Donnelly et al., 1977) and because frequent data gaps make the 1/2-4Å band unsuitable for long time series analysis.

Figure 1.1 illustrates the time coverage of each of the satellites, indicating in shading the primary source of data used in this report. Most of the primary data are from two SMS-2 and GOES-2 satellites. SMS-1 measurements are not used here because of severe photo-electron bias and low flux problems. Data prior to January 1977 is also not discussed due to frequent data gaps and low-flux problems. Data from GOES-1 and GOES-3, are used when the data from SMS-2 or GOES-2 contain data gaps. The secondary data sources (denoted by open

rectangles in Figure 1.1) were also used in deriving linear regression coefficients for the satellite comparisons.

An important consideration are the four gain ranges used by each satellite. In order to provide a large dynamic range and high intensity resolution, satellite electronics provide four overlapping amplifier gain ranges for each ion chamber. The net effect of these ranges on sources of errors will be discussed in section 2.

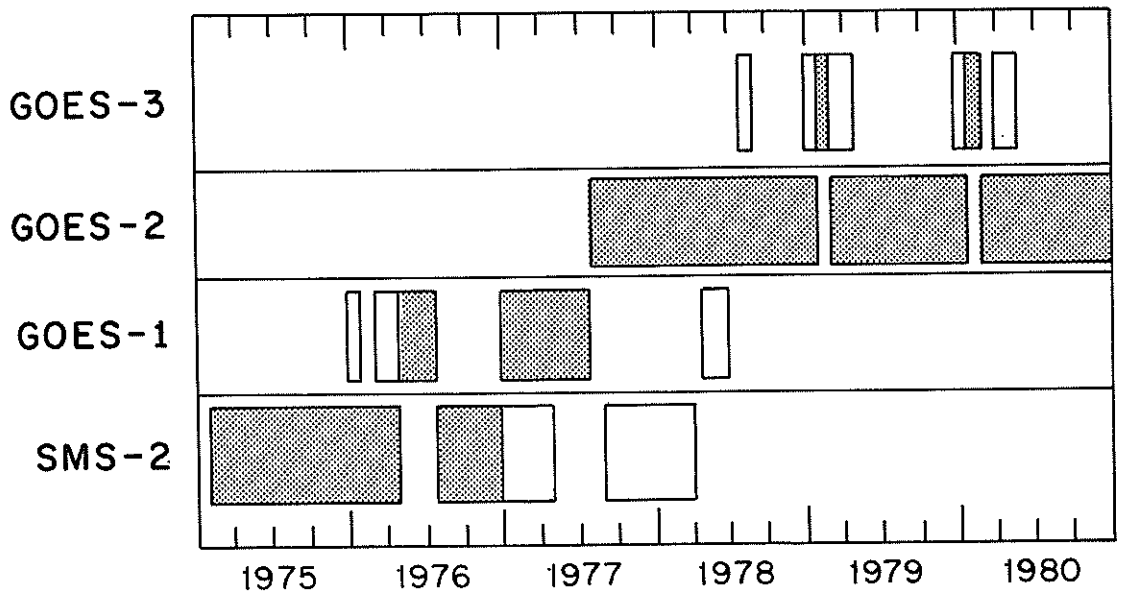

Fig 1.1 Effective data availability of X-ray flux from the SMS and GOES satellites. The shaded portions indicate the primary data sources, the open rectangles the secondary data sources.

1.2 A Continuous and Noise-free Time Series.

In order to complete studies of time and frequency domain analysis of the 1-8Å solar X-rays, it was first necessary to develop a continuous and consistant time series from the four satellites. The frequency domain analysis is now in progress, and will soon be submitted for publication. Using simple linear regression techniques, the GOES-1 and GOES-2 measurements were adjusted to be like those from the SMS-2 satellite. The GOES-3 measurements were then

adjusted to the (adjusted) GOES-2 measurements, which nominally adjusts GOES-3 to SMS-2. Known sources of spurious noise were carefully removed from the data. The adjusted flux values were then compared again, and in general, a worst-case relative error of 20% in the daily values was found between concurrent satellites. A more complete description of the linear regression techniques are described in the next section.

After a long, nearly continuous time series of $\Phi(1\text{-}8\mathring{A})$ was developed, one problem remained with respect to the use of $\Phi(1\text{-}8\mathring{A})$ in statistical and frequency-domain analysis: large, time-dependent variance. The effective dynamic ranges of all the SMS and GOES X-ray instruments are 10^{-8} to 10^{-3} $W \cdot m^{-2}$, or a factor of 10^5. The daily average X-ray flux varies from 10^{-10} to 10^{-5} $W \cdot m^{-2}$ from sunspot minimum to maximum (Keplin et al., 1977). An impulsive flare can rise rapidly from a pre-flare background to a brief maximum by a factor of about 10^2 with a more gradual decay. See Figure 1.2.

The result of these large variations in time series analysis are: (1) An average of $\Phi(1\text{-}\mathring{8})$ over more than a few hours is often dominated by the high flare flux, as opposed to a slowly-varying background (resulting in autocorrelated residuals), and (2) the relatively large, rapid increase of $\Phi(1\text{-}8\mathring{A})$ by a factor of 100-200 with a slow exponential decay results in non-constant variance.

Two methods were used to reduce the effects of autocorrelation and non-constant variance. One method is a simple sampling technique to reduce autocorrelated residuals resulting from the linear regression, described in section 4. The other method is the use of a logarithmic transformation of $\Phi(1\text{-}8\mathring{A})$ described in the sections on statistical comparisons and the X-ray index.

At this point it is important to discuss the meaning behind the term "index". Ideally, an index is the measurement of a single quantity that tends to characterize the "whole" of a physical process. Furthermore, an index should ideally be such that it is convenient and practical to use. The X-ray index

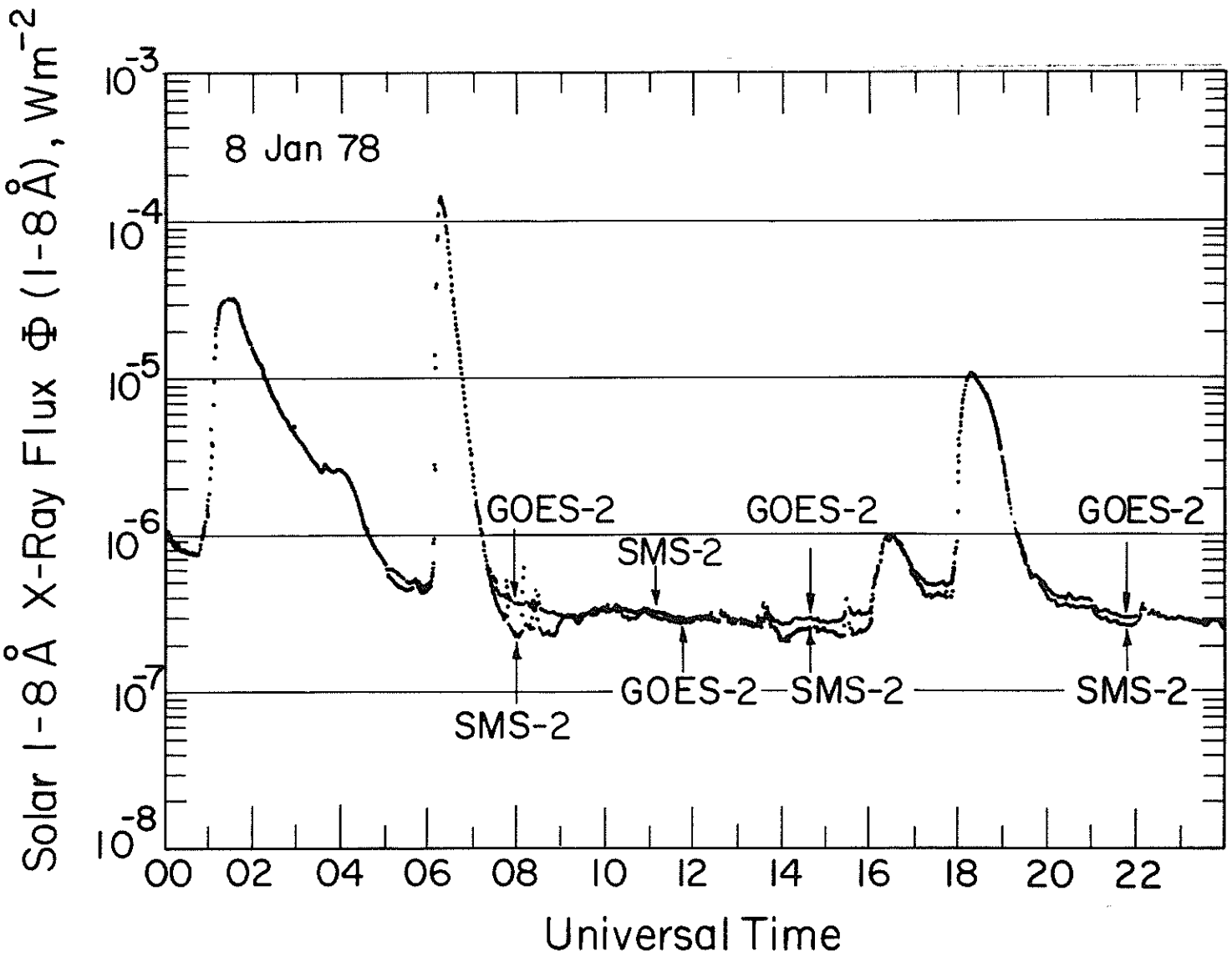

Fig 1.2 Comparison plot of one-minute 1-8Å X-ray flux averages from GOES-2 to SMS-2.

described later fulfill these criteria, and has the added advantage of easily being transformed back to the physically more meaningful $\Phi(1\text{-}8\mathring{A})$.

2. SOURCES OF ERRORS

In the technical memorandum by Donnelly et al, (1977), specific errors in SMS-GOES X-ray measurements are estimated. Recent analysis indicated that only two minor revisions to that list are required. Table 2.1 lists the errors pertinent to the 1-8Å band from Donnelly's original table.

Table 2.1 Estimated Errors for SMS-GOES X-ray Measurements

A. Transfer Function Accuracy	$\simeq \pm$ 20%
B. Effective Spectral Shape	$\simeq \pm$ 10%
C. SMS-1 Ultraviolet-Photoelectron Effect (see below)	
D. Telescope Pointing Errors	+2% to -0%
E. Intensity Resolution	
1. Flux intensity at the high end of a gain range.	∿0.3%
2. Flux intensity of the low end of a gain range when $\Phi\ (1\text{-}8\mathring{A}) \gtrsim 10^{-6}\ W \cdot m^{-2}$	∿3%
F. Occasional Sources of Error	
1. Range switch transients	
2. Eclipse temperature decreases	<3%
3. Isolated bad points	

The ultraviolet-photoelectron effect is due to solar ultraviolet flux shining on the ion chambers inducing photoelectron ejection - which in turn generates a current that is weakly coupled into the ion chamber circuit, causing an apparent "negative flux" when the solar X-ray flux is low. Originally SMS-1 was thought to be the only satellite effected, because SMS-2 and all the GOES satellites had electronic revisions to reduce the coupling. Later analysis suggested that SMS-2 was similarly effected, but to a much lesser degree. The photoelectron effect was reduced to negligible levels on the GOES telescopes by the

addition of a thin absorbtion window to block UV radiation while possible introducing a minimum flux bias. Figure 2.1, a selected scatter plot for a particular day, illustrates the photoelectron effect by the decrease of SMS-2 flux with respect to a given GOES-2 flux value at 10^{-7} W·m^{-2}. This effect can appear whenever the Φ (1-8Å) $\lesssim 10^{-6}$ W·m^{-2} and when a GOES satellite is used with respect to SMS-2.

Overall, the relative error of the SMS-2 photoelectron effect is less than 3% for Φ (1-8Å) $\gtrsim 10^{-6}$ W·m^{-2}. At $\approx 5 \times 10^{-7}$ W.m^{-2}, the error increases to 30%, at $\approx 1 \times 10^{-7}$ W·m^{-2} the relative error is about 60%, and at $\Phi \lesssim 10^{-7}$ W·m^{-2} the error is greater than 100%. It is important to note that the original analysis by Donnelly et al, (1977) considered only flux of terrestrial importance, i.e. $\gtrsim 10^{-6}$ W·m^{-2}.

Another source of error apparent at Φ (1-8Å) $<10^{-6}$ W·m^{-2} is energetic particle contamination of the ion chamber, resulting in measured SMS-2 flux increasing above the true X-ray flux. Figure 1.2 indicates that SMS-2 flux measured an increase in flux between 9-14 UT, when GOES-2 did not. In Figure 2.1 the decrease in GOES-2 flux relative to SMS-2 flux at 10^{-7} W·m^{-2} is due to energetic particle contamination. This effect has been noted by Grubb (1975), Donnelly et al, (1977), and Donnelly & Bouwer, (1981). SMS-2 seems to be more susceptible than the GOES satellites, and generally the error is about 1/2 that of the photoelectron effect, depending on the magnitude and time of particle flux at geostationary altitudes.

The photoelectron effect and particle contamination makes simple linear regression fits of GOES measurements to SMS-2 measurements unsuitable at low flux levels. The effects of autocorrelated residuals requires careful sampling, as discussed in Section 2 where different sampling algorithms in regression studies are discussed.

The transfer function accuracy depends on specific engineering assumptions

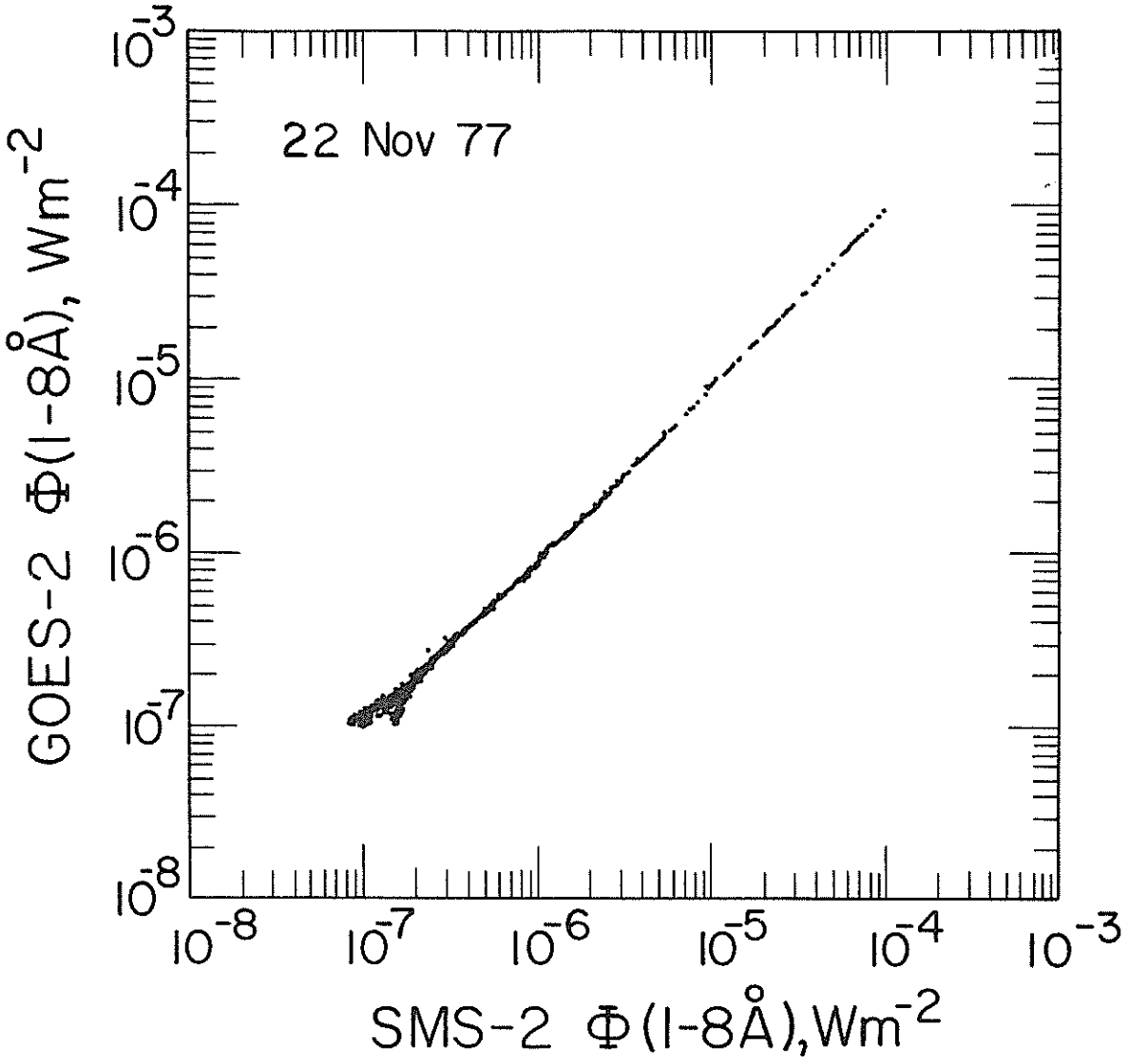

Fig 2.1 Scatter plot of a typical day of one-minute X-ray flux averages. The low-flux spread to the left of a straight line is due to the SMS-2 photoelectron effect, and to the right due to particle contamination.

of the X-ray telescope and ion chamber, and has been discussed in detail by Donnelly et al., (1977), and Unzicker and Donnelly (1974). The errors associated with the transfer function are absolute errors (e.g. with respect to an absolute physical standard) and are largely time and satellite independent. We assume it is a negligible source of relative error (e.g. between two times).

The effective spectral shape errors are most apparent during flares when the solar X-ray spectrum varies rapidly. The window filters on SMS-2 and the GOES series differ slightly, resulting in different responses ($\gtrsim$ 10%) between satellites during flares.

The occasional sources of errors in table 2.1 were removed from most of the data on a case-by-case basis using an interactive graphics computer.

Any errors caused by potential long-term drift have not been observed between satellites nor are they expected on the basis of a 5-year instrument lifetime (Grubb, 1975). On a time scale of 10 and 18 months of concurrent satellite measurements (SMS-2 vs. GOES-1, GOES-2 vs GOES-3 respectively) virtually no change in the background flux or flare response was observed by one satellite relative to another. It is unlikely that three satellites could degrade in exactly the same manner and rate, thus we suggest that there are no significant long-term instrument degradations.

In terms of relative errors between satellites, the overall accuracy for Φ (1-8Å) $\gtrsim 10^{-6} W \cdot m^{-2}$ is $\pm$ 20% (individual errors added in quadrature).

3. THE SOLAR 1-8Å X-RAY INDEX

As both a convenience and a helpful statistical method a simple logarithmic transformation of X-ray flux measurements was developed. Originally introduced by Donnelly (1982) as a convenient tool to scale plots and report data, it was later found to satisfy a statistical assumption for the equality of variance in the intercomparison of GOES-2 to SMS-2. This assumption will be discuss-

ed in detail in section 4. In essence, the transformation of flux ($W \cdot m^{-2}$) measurements to dimensionless index units stabilizes the variance by removing the standard deviations dependency on the mean (Cochran and Snedecor, 1967). However, it is important to note that for most physical calculations, X-ray flux must be transformed from index units to units of $W \cdot m^{-2}$. To convert flux ($W \cdot m^{-2}$) units to X-ray index units, the transformation is:

(1) $X = 100 \log_{10} [\Phi\ (1\text{-}8\mathring{A}) \times 10^{10}]$.

To convert X-ray index units to flux ($W \cdot m^{-2}$) units necessary for most calculations, the reverse transformation is:

(2) $\Phi\ (1\text{-}8\mathring{A}) = 10^{\frac{(x-1000)}{100}}$.

3.1 Calculation of the Daily Background Index

To estimate the non-flare daily X-ray flux an algorithm similar to the Ottawa background 10.7 cm flux was developed. Based on hourly averages of the X-ray one-minute averages, the algorithm was written as a computer routine to avoid subjective interpretations on a daily basis. Instead of a daily minimum X-ray flux, a selected mid-day minimum is used to weight the time of the daily value near 12 UT, $\pm$ 4 hrs. All calculations are done in flux ($W \cdot m^{-2}$) units, then converted to index unit form. The algorithm is:

(1) Divide 24 hourly averages into three equal "bins" of 8 hours.

(2) Select the minimum hourly average from each bin.

(3) Perform a simple linear interpolation between the minima of the outside bins for an interpolated minimum halfway (in time) between the outside minima.

(4) Select the lower minimum from either the middle bin or the interpolated minimum. This selected mid-day minimum is defined as the daily background X-ray flux.

To the extent any non-flare index can represent a true "background" flux, inspection of Figure 3.1 suggests this algorithm is highly effective for removing

the obvious effects of flares, while retaining a degree of daily phase coherence.

In a comparison between the daily minimum hourly average to the daily background flux, a relative amplitude difference of just a few percent between the two indices was found. In Figure 3.1, the index scale on the right also indicates the traditional C, M and X flare classifications associated with 1-8Å X-ray flux at the 10^{-6}, 10^{-5}, and 10^{-4} $W \cdot m^{-2}$ levels, respectively.

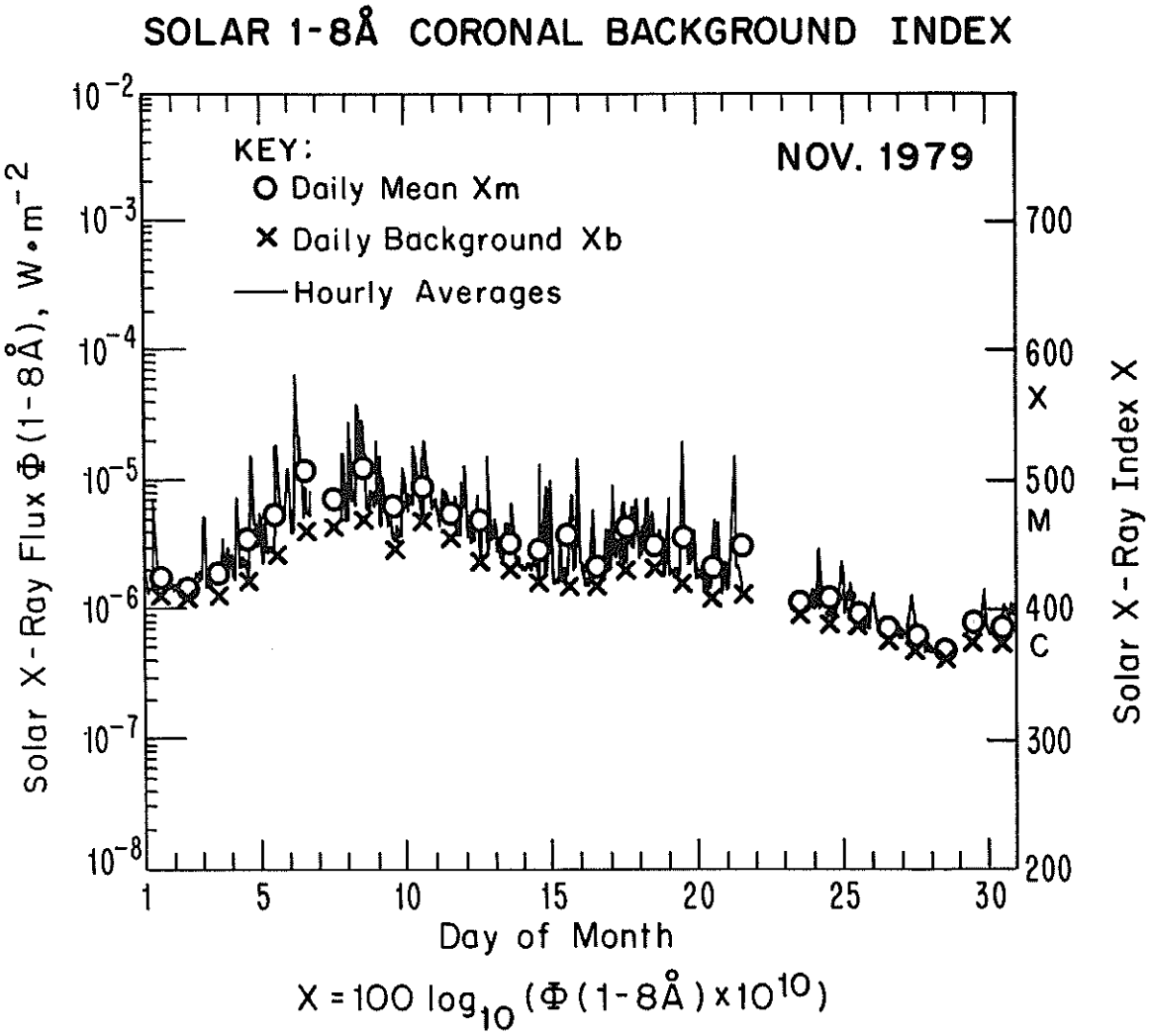

Fig 3.1 Time series plot of the X-ray flux maximum most closely corresponding to the Dec 79 smoothed sunspot maximum.

4. STATISTICAL COMPARISON OF GOES-2 TO SMS-2 MEASUREMENTS

Since the majority of flux measurements for this report are from the GOES-2 satellite, careful attention is first paid to the low flux statistical comparison of GOES-2 to the earlier SMS-2 measurements. In this comparison, the SMS-2 data is the dependent variable, and GOES-2 data is the independent variable. A linear least squares fit was found to be the most appropriate. We considered only low flux values $< 1.2 \times 10^{-6}$ $W \cdot m^{-2}$ during 1977-1978 (see Figure 1.1), resulting in ten randomly selected days from September 1977 to March 1978. As will be shown later, a logarithmic transformation for index units was necessary for satisfying the assumption of equality of variance, a critical assumption for forming confidence intervals.

From initial comparisons of minute-to-minute samples, we found high autocorrelations among successive residuals from the fit. Autocorrelation among the residuals indicates a violation of the assumption of independence, which must be satisfied for the resulting confidence intervals to be correct.

The easiest way to get around this problem is to increase the time between successive data points until the autocorrelation between the residuals is negligible. Thus, we began by analyzing one minute values which were an hour apart. The correlation between residuals which were one hour apart was 0.23 with a large lag standard error of 0.12. For residuals two hours apart, the correlation was 0.34 with a large lag standard error of 0.12, and for three hours apart the correlation was 0.17 with a large lag standard error of 0.13. The large lag standard error is interpreted as the standard error of the correlation coefficient only if the correlation between residuals further apart in time than the lag being tested is negligible. Using normal theory one can test if the correlation is negligible by checking if the absolute value of the correlation is less than 1.96 times the large lag standard error. Using this technique we found the autocorrelation was negligible among residuals which were three or

more hours apart. So by only fitting data points which are three hours or more apart, the assumption of independence among residuals will be satisfied.

For the fitting process we want to obtain at least 30 observations so that the normal distribution can be used for inferences. By using 9 days of data we obtained 39 one-minute values where each value was at least 3 hours apart. A linear fit of this data explained 97% of the variation in SMS-2 when GOES-2 was known. The intercept term was 11.57 and had a standard deviation of 11.02. This implies that the intercept term is not significantly different from zero based on this data. Conversely, the slope was 0.99 and its standard error was 0.03, so the slope is a crucial term in the model.

The true linear model which we are trying to estimate can be represented by:

$$y_i = \alpha + \beta x_i + \varepsilon_i \qquad (4.1)$$

where x_i is the independent variable which is known and corresponds to the GOES-2 observation; y_i is the dependent variable which corresponds to the SMS-2 value we will estimate; α is the true, but unknown intercept term; β is the true but unknown slope; and ε_i is the true, but unknown error in the model. In order to apply standard confidence intervals to our estimates $\hat{\alpha}$, $\hat{\beta}$, and $\hat{y}$ (our estimated SMS-2 value), certain assumptions must be satisfied about the errors ε_i. The usual assumptions are that the errors are independent, have zero mean, a constant variance, and follow a normal distribution. Thus, if our fitted model is correct, the residuals should exhibit tendencies that tend to confirm the assumptions we have made, or at least, should not exhibit a denial of the assumptions. The principal ways of testing our assumptions are by graphing the residuals which are estimates of the errors in the model, ε_i.

In Figure 4.1a is a plot of the standardized residuals over time. However, not all the data is equally spaced in time, although it has been plotted that way. The residuals are centered about zero in a random fashion and there

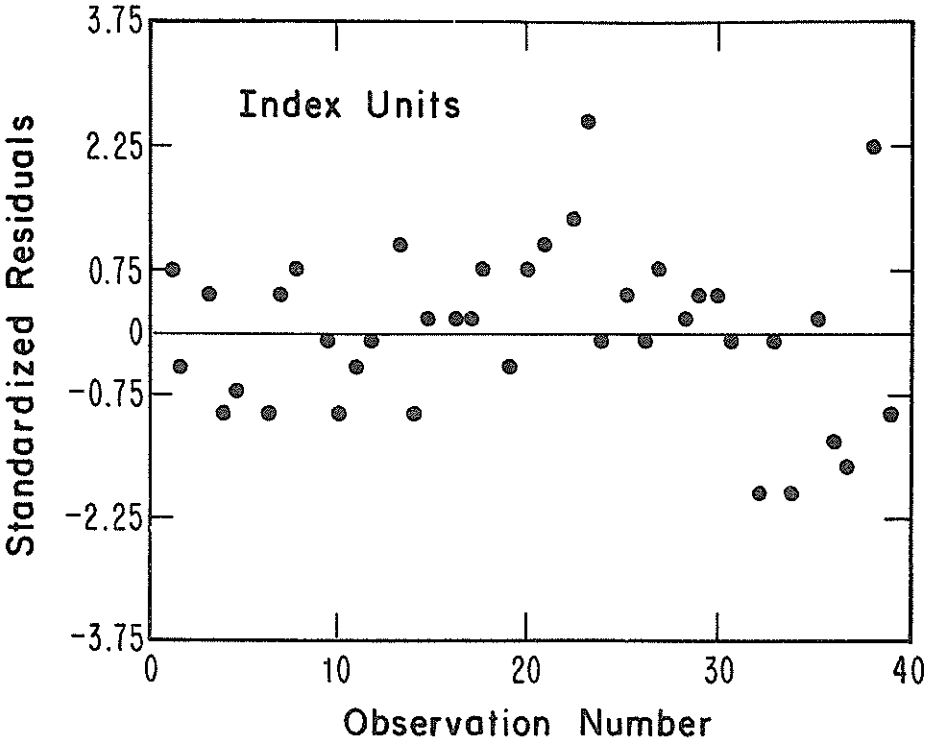

Fig 4.1a The standarized residuals as a function of the observational number from the GOES-2 to SMS-2 comparison.

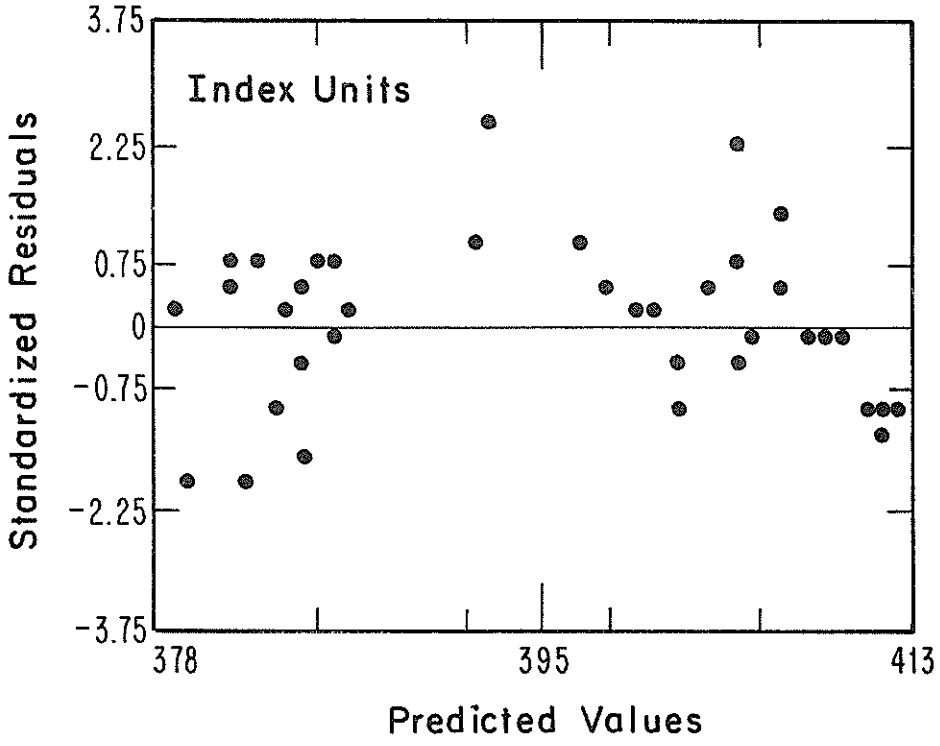

Fig 4.1b The standarized residuals as a function of the predicted values in the GOES-2 to SMS-2 comparison.

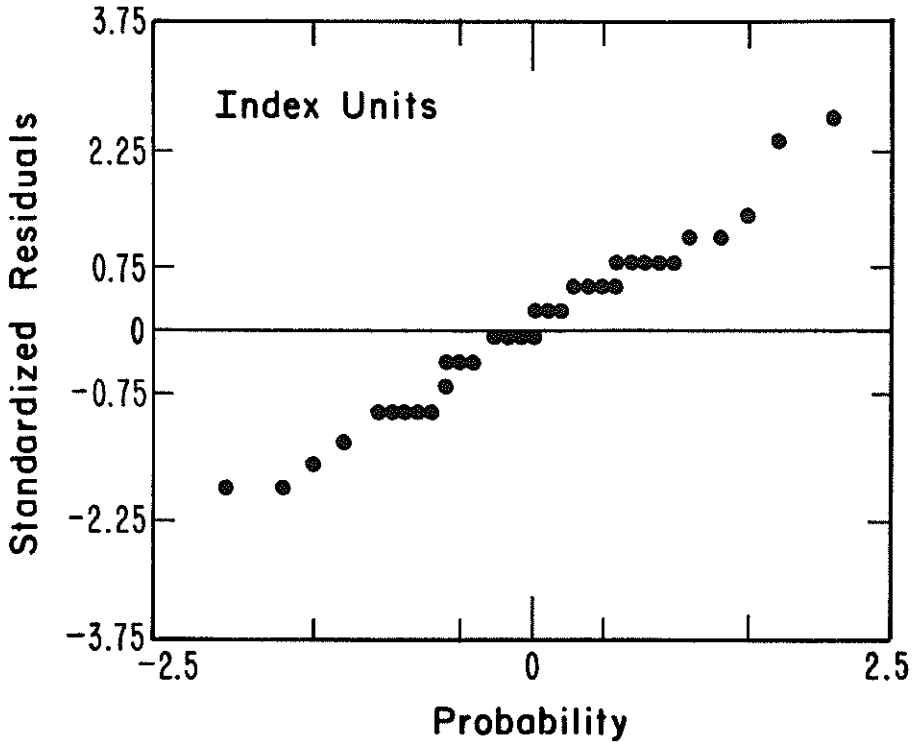

Fig 4.2a The standarized residuals falling on a relatively straight line indicate normality when index units are used in linear regressions.

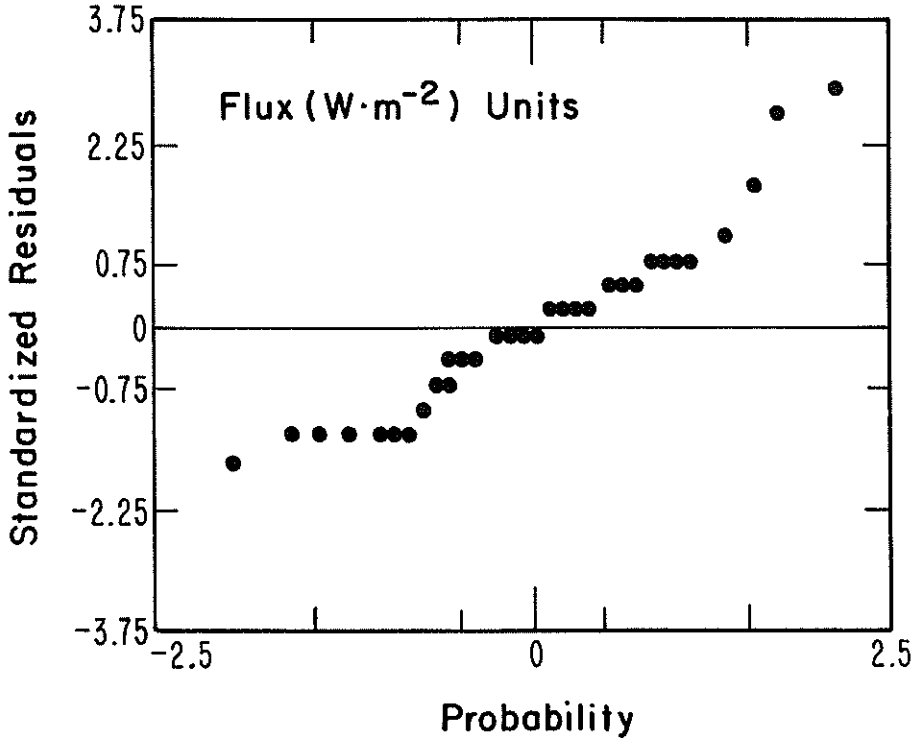

Fig 4.2b The standarized residuals do not fall on a straight line, indicating a lack of normality when flux (W·m^{-2}) units are used in linear regressions.

is no evidence of time cycles or of increasing or decreasing variance in the data over time.

In Figure 4.1b the standarized residuals are plotted versus the predicted values. In this figure there is some indication that a quadratic term should be included in the model. However, in other comparisons where a different time period was used, the addition of a quadratic term was not significant, indicating that the quadratic term is not real and should not be included.

Figure 4.2a is a probability plot of the standardized residuals which can be used to check if the residuals are normally distributed. If they are normally distributed then they should fall along a straight line. Figure 4.2a indicates that there were not as many large residuals as would be expected for the normal distribution; however, this only means that the confidence intervals will be conservative.

In Figure 4.2b the probability plot of the standardized residuals are given for data expressed in flux ($W \cdot m^{-2}$) units instead of the index units. This normal probability plot indicates a definite lack of normality. Transforming the dependent variable by taking the log often induces normality as well as equality of the variances. The solar index was used since it achieved these purposes as well as being more convenient (see Donnelly, 1982).

In estimating the confidence interval of for a typical background index value from GOES-2, we will only take into account the random sources of errors. However, as discussed in section 2 there is no indication of any long-term systematic variations. That is, we do not expect long-term systematic drifts or time-dependent bias at Φ (1-8Å) $\gtrsim 10^{-6}$ $W \cdot m^{-2}$.

A two-sided 95% confidence interval on an estimated $\hat{y}$ (estimated SMS-2 value) where more than 30 values were used in the fit is:

$$\hat{y} - 1.96\, S_{\hat{y}} \leq y \leq \hat{y} + 1.96\, S_{\hat{y}} \qquad (4.2)$$

where y is the true (but unknown) SMS-2 value and is estimated by $\hat{y} = a + b\, x_0$,

where x_o is the GOES-2 value used to predict the SMS-2 value y, and a and b are the intercept and slope terms respectively. The $S_{\hat{y}}$ term in (4.2) is the standard error of a predicted value, and was calculated using

$$S_{\hat{y}} = \sqrt{(RSD)^2 + (SDPV)^2} \quad , \tag{4.3}$$

where RSD stands for the residual standard deviation and SDPV is the standard deviation of the predicted values.

Assuming a typical observed value for GOES-2 of $x_o = 395.0$, $S_{\hat{y}}$ was calculated to be 2.16. The corresponding SMS-2 value $\hat{y} = 402.62$.

Thus a 95% two-sided confidence interval on the estimated SMS-2 value, excluding variation due to systematic components is:

$$402.62 - (1.96)\ (2.16) \leq y \leq 402.62 + (1.96)\ (2.16)$$

or

$$398.4 \leq y \leq 406.9;$$

an excellent result.

The most important result from this detailed comparison came when we extrapolated the linear regression to high flux ($\lesssim 10^{-5}$ W·m^{-2}) and compared this line with the earlier results of a comparison in which only one-minute flare data was used (e.g. Φ (1-8Å) $\gtrsim 10^{-5}$ W·m^{-2}). The relative difference between the two comparisons was negligible, of the order of a few percent difference in Φ (W·m^{-2}).

The major utility of this detailed statistical comparison is that it outlined the method by which each range in each satellite comparison was to be used to derive the linear regression coefficients. The results are presented in the next section.

5. RESULTS OF COMPARISONS

From the results of the statistical calibration described in the prior section, the following algorithm was selected to derive the regression

coefficients for adjusting each of the four ranges for each of the three GOES measurements to the estimated SMS-2 value. First, from scatter plots of concurrent satellite measurements only those times and flux levels were selected that were free from known sources of noise (i.e. particle contamination, photoelectron effect, etc.). Then, for each range, one-minute average values were selected (in flux units) at those lags where the autocorrelation of the residuals was negligible. Figures 5.1, 5.2, and 5.3 illustrate the actual data values used.

For both the GOES-1 and GOES-2 to the SMS-2 comparisons, a lower cut-off flux value was used to reduce the low-flux errors. Note that for both GOES-1 and GOES-2 the scatter plot indicates that only a single regression line for all three observed ranges is required. For GOES-3, however, there is a clear need for a regression line for each range. Also note that for GOES-3, there are no low-flux errors apparent like those in the GOES-1 or GOES-2 to SMS-2 scatter plots.

Table 5.1:

Independent satellite x	Range numbers	Range in measured flux, $W \cdot m^{-2}$	Regression line slope b
GOES-1	1-4	$10^{-8} < \Phi\ (1\text{-}8\mathring{A}) \lesssim 10^{-3}$	1.005
GOES-2	1-4	$10^{-8} < \Phi\ (1\text{-}8\mathring{A}) \lesssim 10^{-3}$	1.098
GOES-3	1	$\Phi\ (1\text{-}8\mathring{A}) \leq 1.15 \times 10^{-6}$	1.268
	2	$1.15 \times 10^{-6} < \Phi \leq 1.3 \times 10^{-5}$	1.253
	3	$1.3 \times 10^{-5} < \Phi \leq 1.5 \times 10^{-4}$	(1.041)
	4	$1.5 \times 10^{-4} < \Phi \lesssim 10^{-3}$	(1.078)

Table 5.1 lists the final regression coefficients for the 1-8Å solar X-ray flux, in $W \cdot m^{-2}$, for each of the satellites. The coefficient b is applied with the formula y=bx, where the dependent variable y represents the adjusted flux

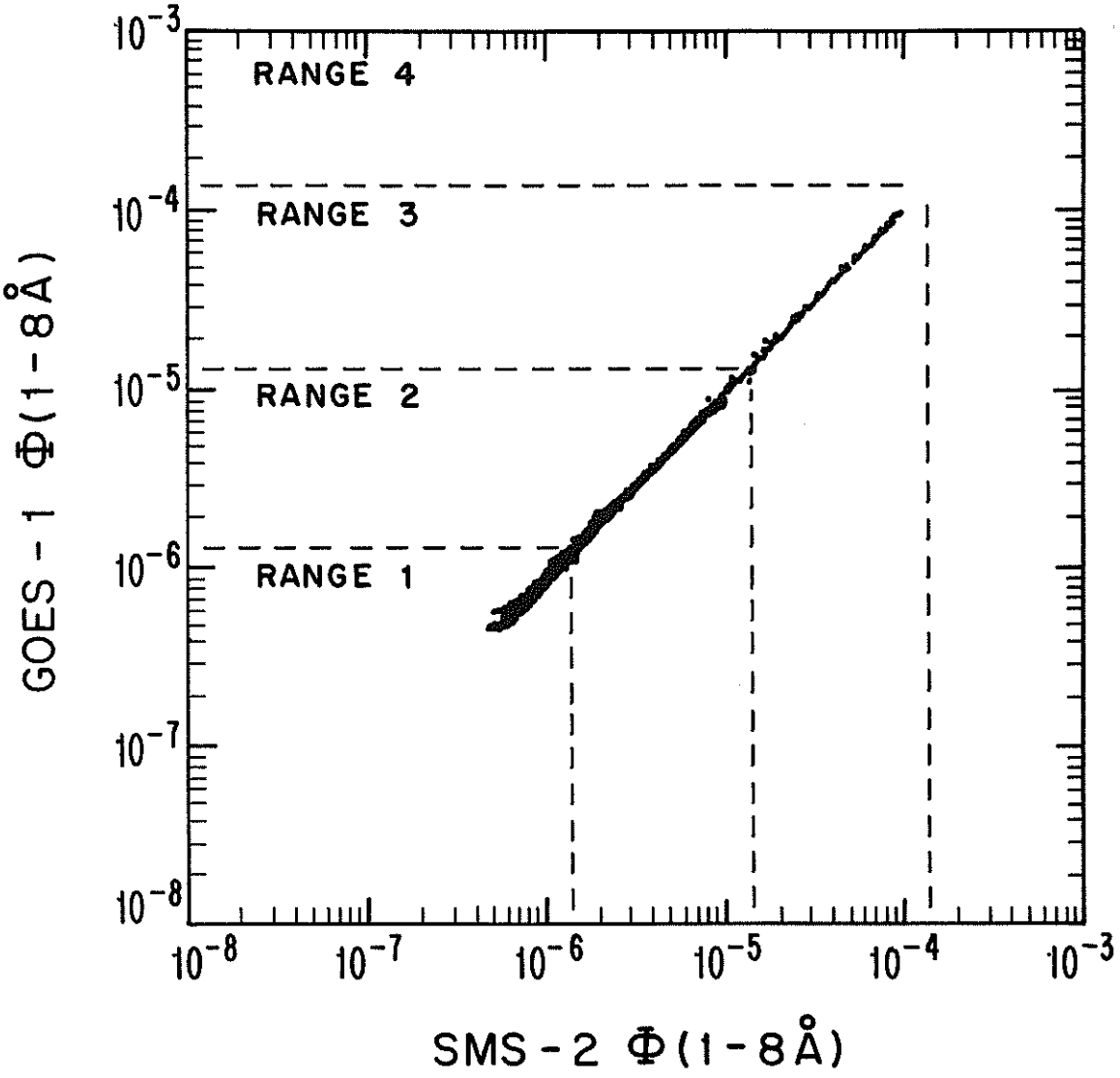

Fig 5.1 Scatter plot illustrating the one-minute values used in deriving the GOES-1 regression coefficients.

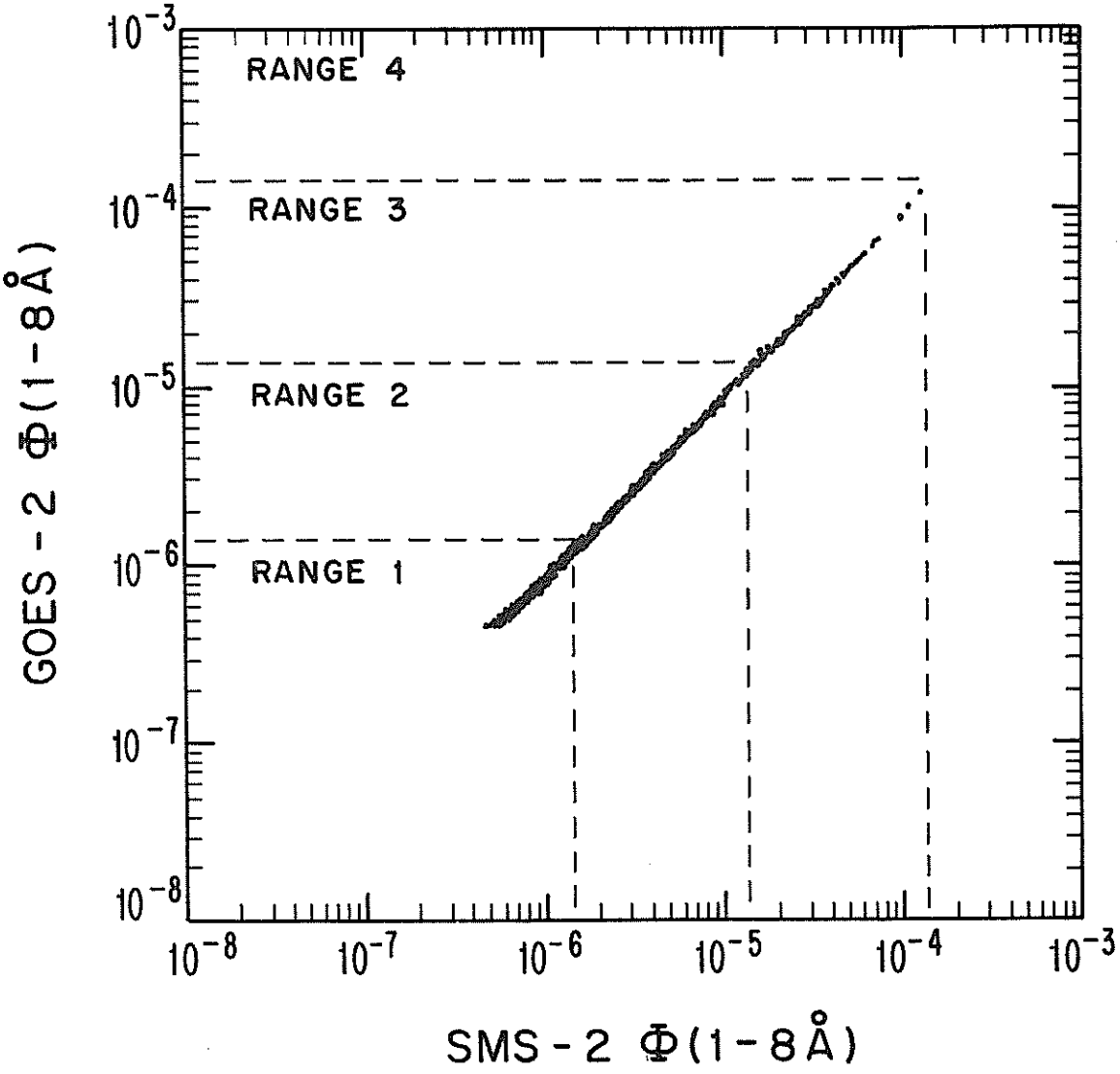

Fig 5.2 Scatter plot illustrating the one-minute values used in deriving the GOES-2 regression coefficients.

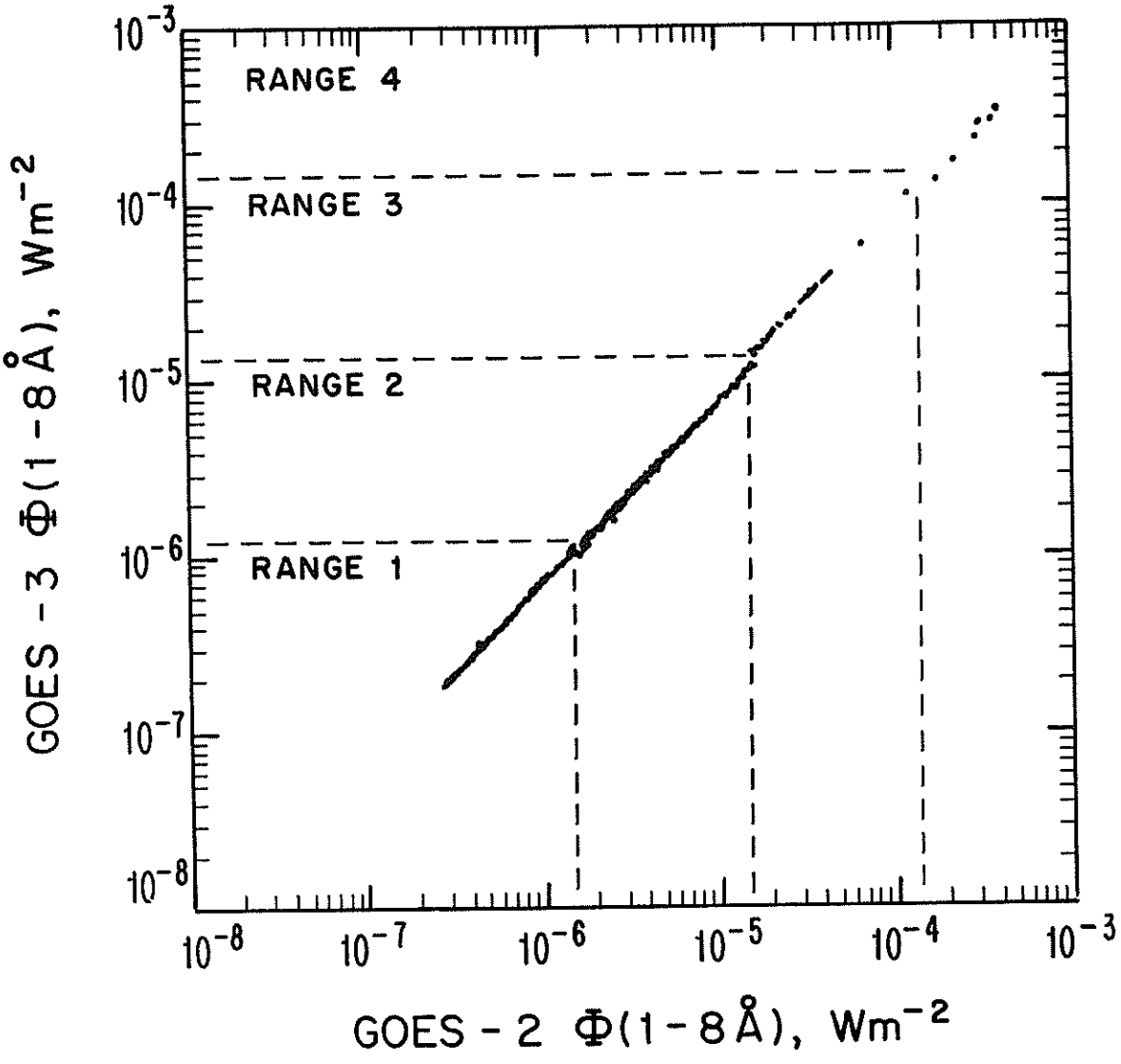

Fig 5.3 Scatter plot illustrating the one-minute values used in deriving the GOES-3 regression coefficients.

measurement in terms of SMS-2 flux. The correlation coefficients for each fit are at least 0.985, with ranges 3 and 4 from GOES-3 the most uncertain (due to a limited sample period). In all fits the $y = a + bx$ model (in $W \cdot m^{-2}$ units) was used, but in all cases the a intercept term was not significant. The insignificant intercept term also provides supporting evidence that long-term drift problems are undetectable in the GOES series of satellites for the time period studied.

All the flux values reported here have had the appropriate adjustments made to the estimated SMS-2 value, providing (See Figure 1.1) a nearly continuous time series from January 1977 to September 1981, independent of the satellite.

Figure 5.4 illustrates the daily mean and background solar 1-8Å X-ray flux for nearly five years of measurements. The rise from solar minimum to solar maximum (Dec. 79 is the 6-month smoothed sunspot maximum), is clearly evident. The unusually high, sustained average after solar maximum is real (i.e. not due to long-term satellite drift). These values have not been corrected to one A.U. (the correction would result in at most a $\pm$ 3.3% flux difference). Measurements for a period after September 1981 cannot be used from GOES-2 because X-ray telescope pointing errors suddenly began resulting in up to 100% relative flux errors.

6. MONTHLY AVERAGE COMPARISON OF SOLAR 1-8Å X-RAY FLUX TO THE OTTAWA 10.7 CM FLUX

Since both solar X-ray flux and the Ottawa 10.7 cm flux are intended to be coronal indices, it is of interest to compare the two. Donnelly (1982) has compared the nonflare 1-8Å X-ray flux with 10.7 cm radio flux in detail. In brief, he has shown a strong central meridian dependence in 10.7 cm radio flux not present in X-rays, and a large 10.7 cm quiet-sun flux from the chromosphere-corona transition region not present in X-rays.

In averaging by the month, the major effects of solar rotation are removed.

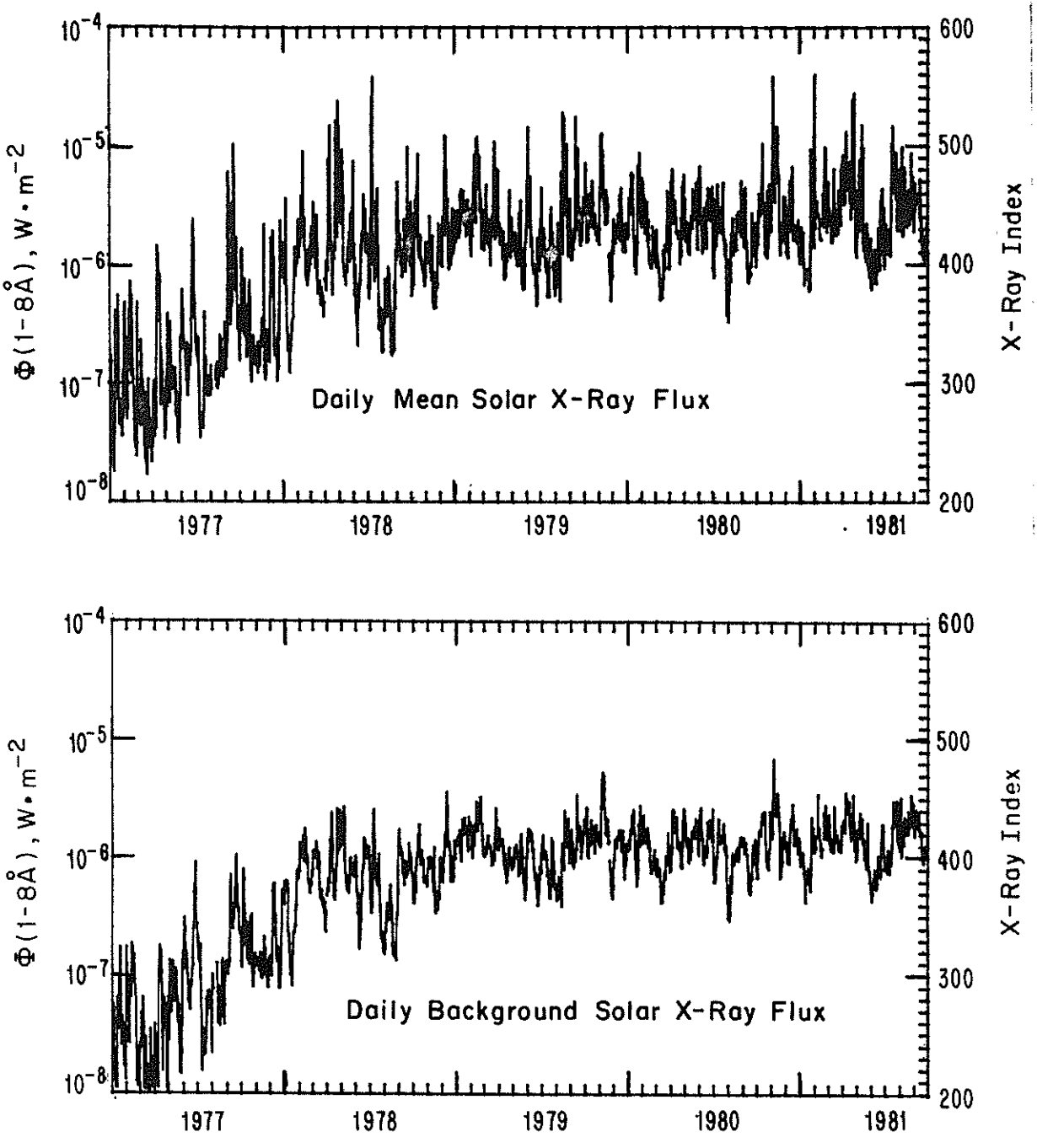

Fig 5.4 Time series plots of the daily mean and background (non-flare) X-ray flux. All values have been adjusted to be like those of the SMS-2 flux.

Figure 6.1 illustrates how the concurrent monthly averages plot in time. In general, the peaks and valleys in the time series line up well. The 10.7 cm (2800 MHz) radio flux values are taken from the non-burst values published in the brief reports of Geomagnetic and Solar Data in the Journal of Geophysical Research.

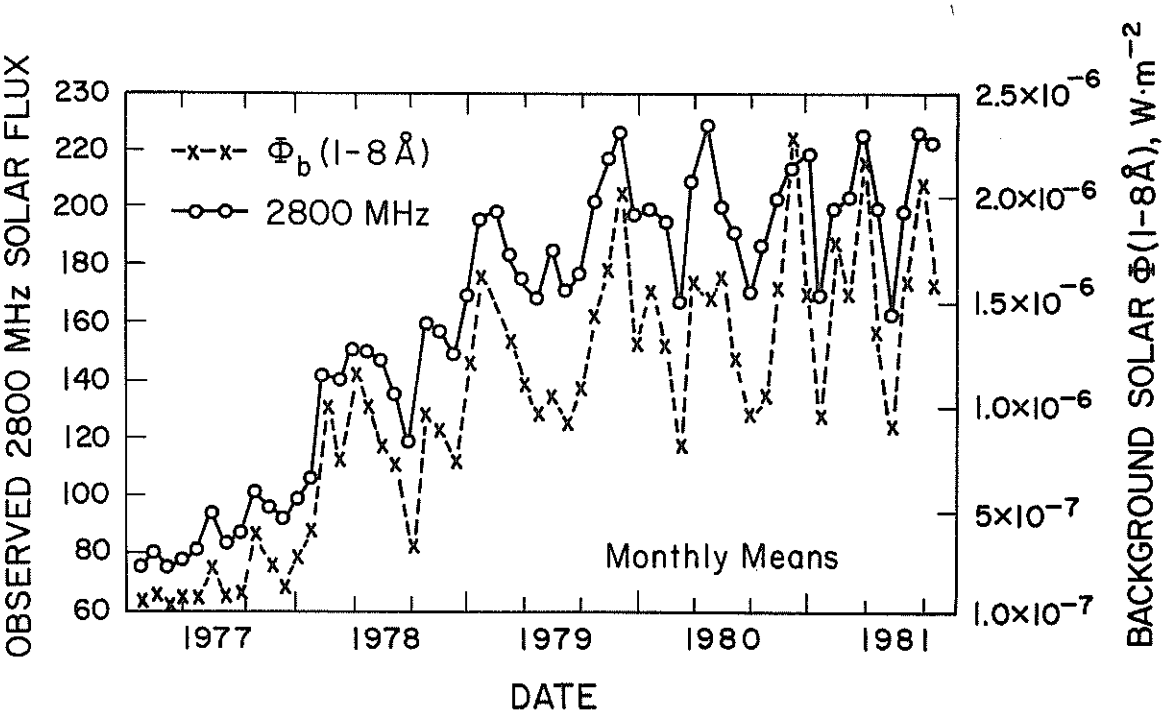

Fig 6.1 Time series plot comparing monthly mean values of 1-8Å X-ray flux to the Ottawa 2800 MHz background flux.

Figure 6.2 illustrates the scatter plot between the X-ray and radio flux, and the linear regression line existing between the two indices. A high correlation coefficient of .95 results. However, in Figure 6.3 a plot of the residuals reveals some interesting problems in assuming a linear fit between the two indices. The standard deviation in Figure 6.3 is indicated by the dashed line. Inspection of the residuals reveal three principle problems: (1) The variance increases as a function of time, (2) the residuals are highly autocorrelated (e.g. not independent) prior to solar maximum, and (3) an additional quadratic term is suggested in the model. The apparent solar-cycle dependence between X-ray and radio flux suggest that the two coronal indices are not linearly related, most

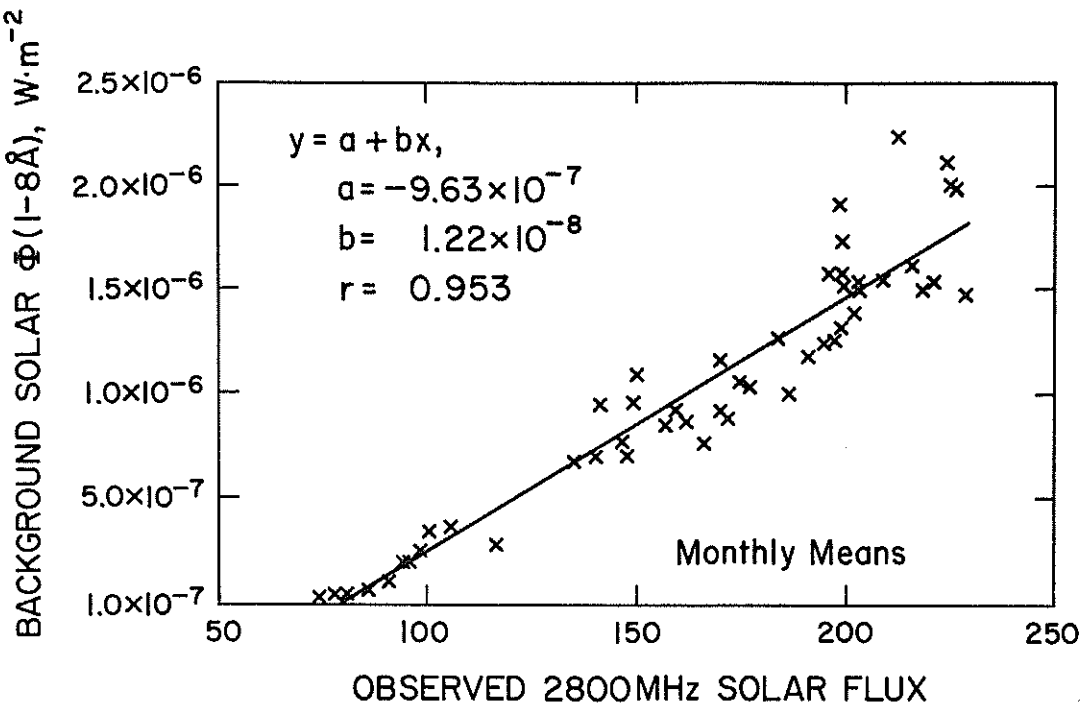

Fig 6.2 Scatter plot of monthly X-ray flux to the monthly Ottawa 2800 MHz flux. For comparison purposes, a linear regression line is fitted.

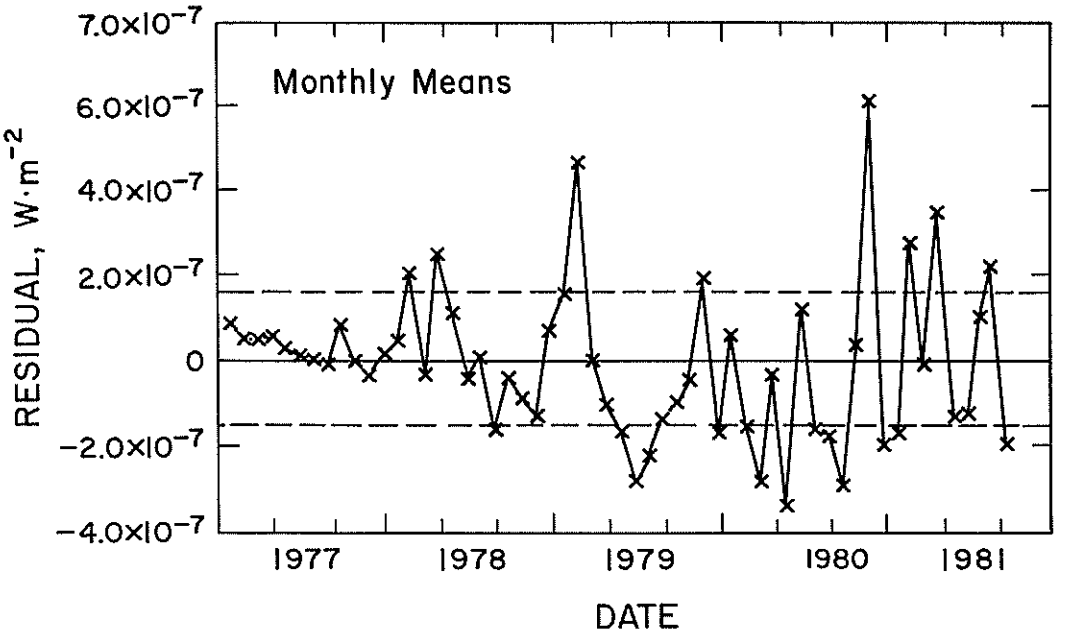

Fig 6.3 The residuals from the linear fit in Figure 6.2 illustrating the non-linearity of the two solar indices.

probably due to real physical differences.

7. SOLAR 1-8Å MEASUREMENTS FROM JANUARY 1, 1977 TO SEPTEMBER 30, 1981

The following figures and tables present the adjusted (to SMS-2) 1-8Å full-disk X-ray flux. Known sources of noise have been removed by deleting the hourly values known to be effected. The X-ray flux is presented with the values above the Earth's atmosphere for terrestrial applications and have not been corrected to one A.U., which results in a $\pm$ 3.3% relative variation from perihelion to aphelion. Note that in averaging by the hour, the true maximum flare flux is averaged out. Many major flares up to November, 1980 are presented in their one-minute values by Donnelly (1981) and Donnelly and Bouwer (1981).

Section 7.1 contains computer-drawn plots of the hourly averages. Section 7.2 lists the daily background solar index values, which can be converted to physically meaningful flux units by relation (2) in section 3.1. Section 7.3 tables the daily mean index values. Note that the daily mean was calculated in flux ($W \cdot m^{-2}$) units, not the dimensionless index units they are reported as. Missing daily values are indicated by dashed lines in the tables.

7.1 Monthly Plots of Hourly Averages

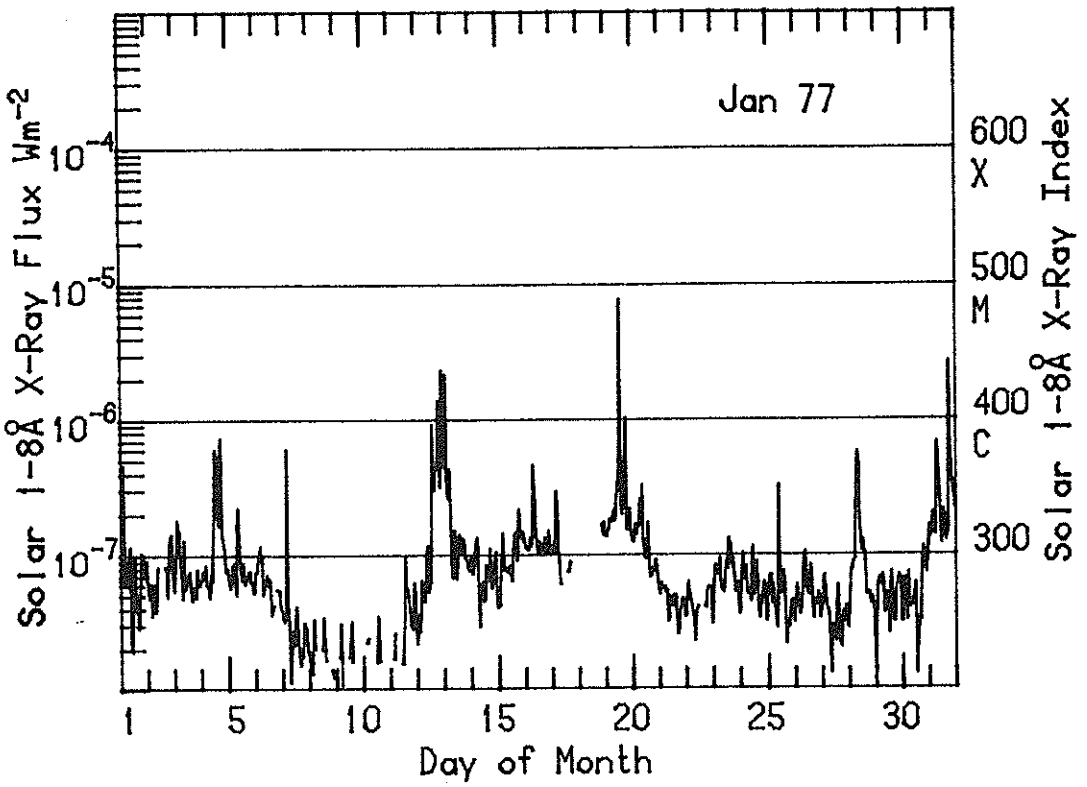
Jan 77
Solar 1-8Å X-Ray Flux Wm-2
10-4
10-5
10-6
10-7
600
X
500
M
400
C
300
Solar 1-8Å X-Ray Index
1
5
10
15
20
25
30
Day of Month

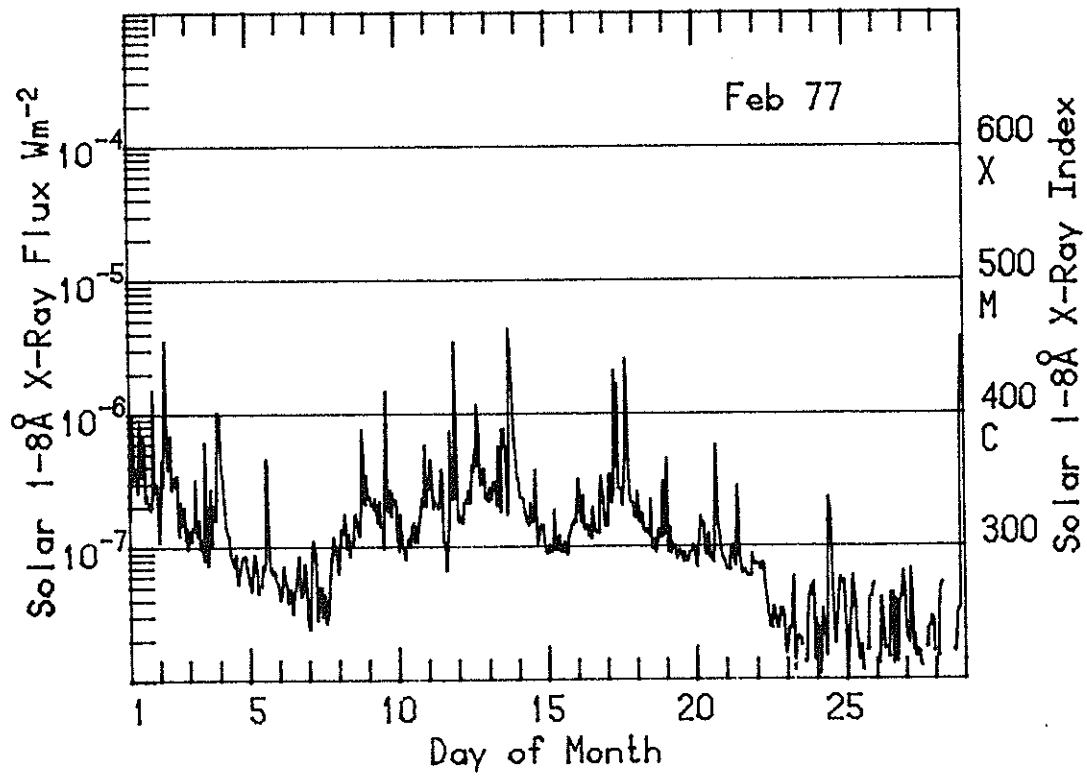
Feb 77
Solar 1-8Å X-Ray Flux Wm-2
10-4
10-5
10-6
10-7
600
X
500
M
400
C
300
Solar 1-8Å X-Ray Index
1
5
10
15
20
25
Day of Month

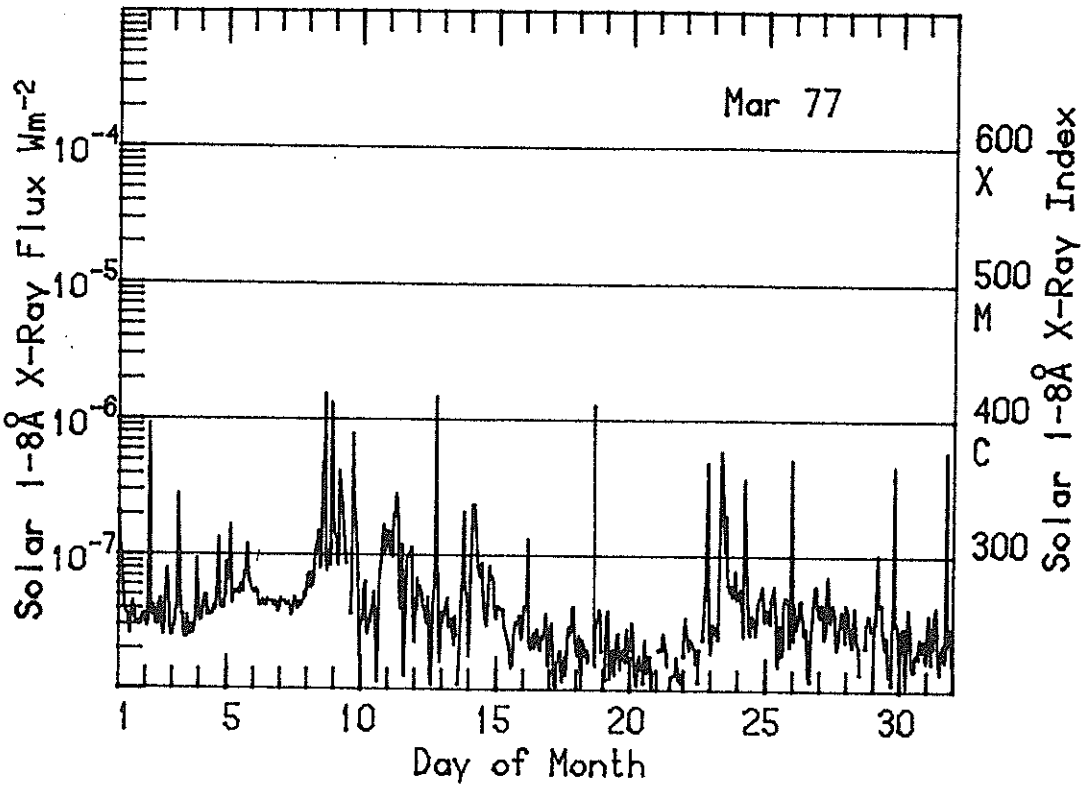
Mar 77
Solar 1-8Å X-Ray Flux Wm⁻²
10⁻⁴
10⁻⁵
10⁻⁶
10⁻⁷
600
X
500
M
400
C
300
Solar 1-8Å X-Ray Index
1
5
10
15
20
25
30
Day of Month

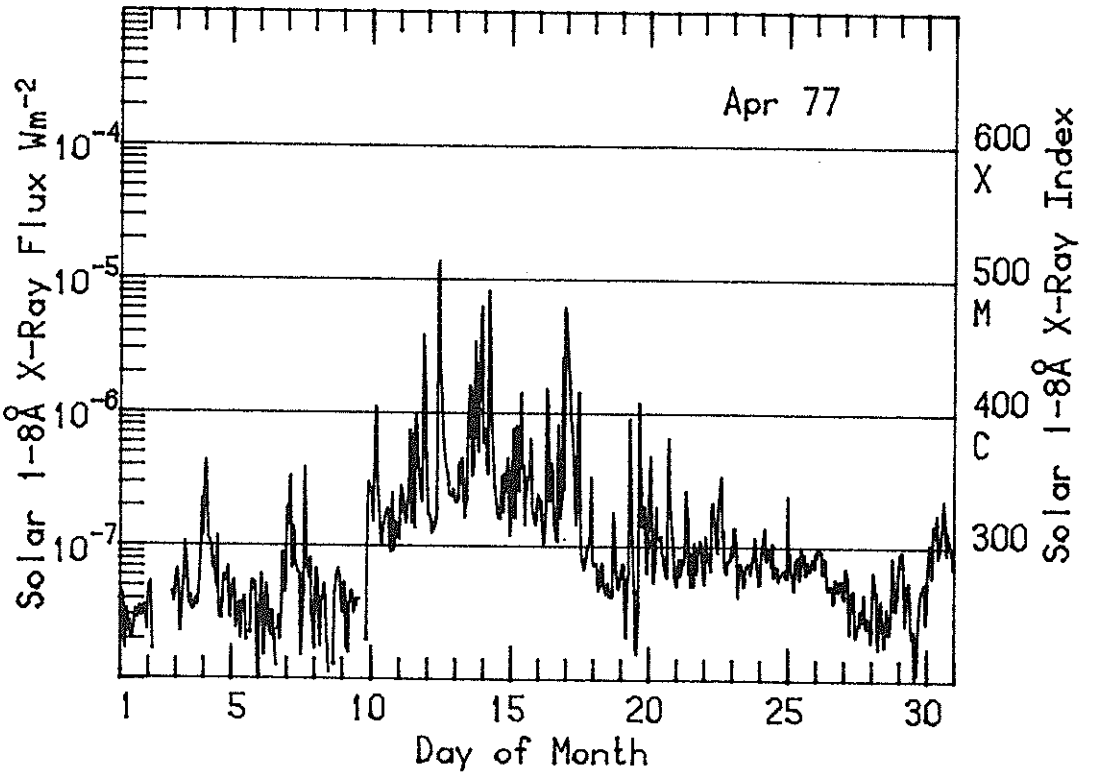
Apr 77
Solar 1-8Å X-Ray Flux Wm⁻²
10⁻⁴
10⁻⁵
10⁻⁶
10⁻⁷
600
X
500
M
400
C
300
Solar 1-8Å X-Ray Index
1
5
10
15
20
25
30
Day of Month

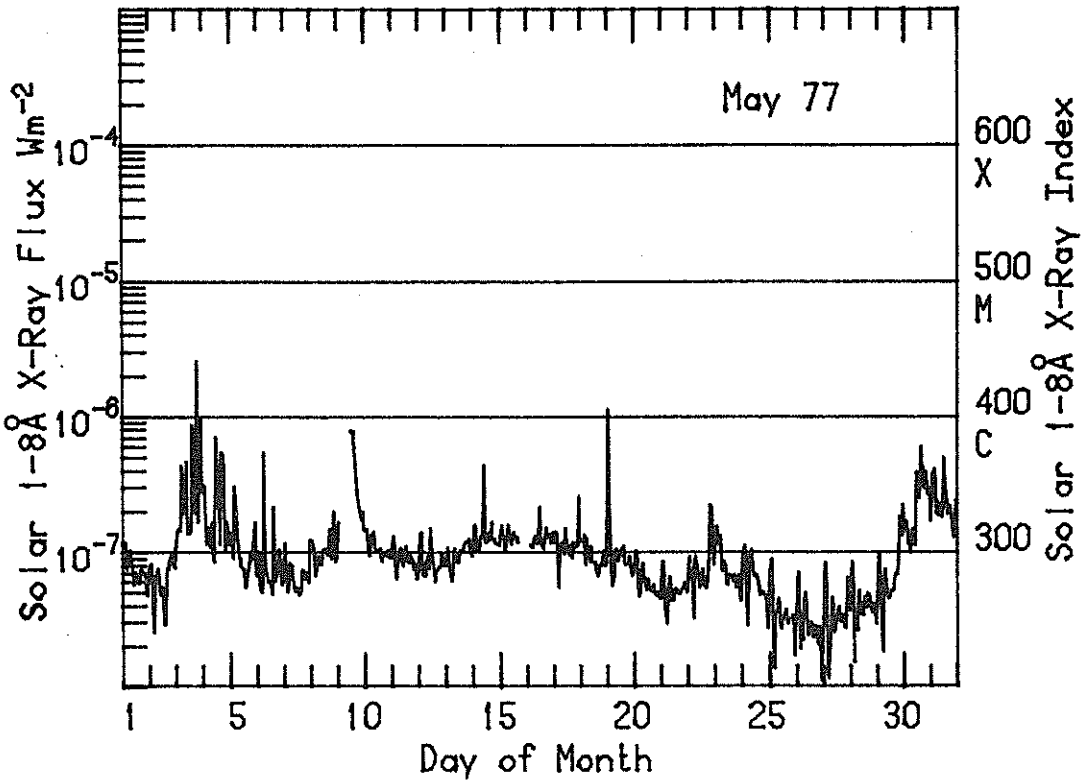
May 77
Solar 1-8Å X-Ray Flux Wm-2
10-4
10-5
10-6
10-7
600
X
500
M
400
C
300
Solar 1-8Å X-Ray Index
1
5
10
15
20
25
30
Day of Month

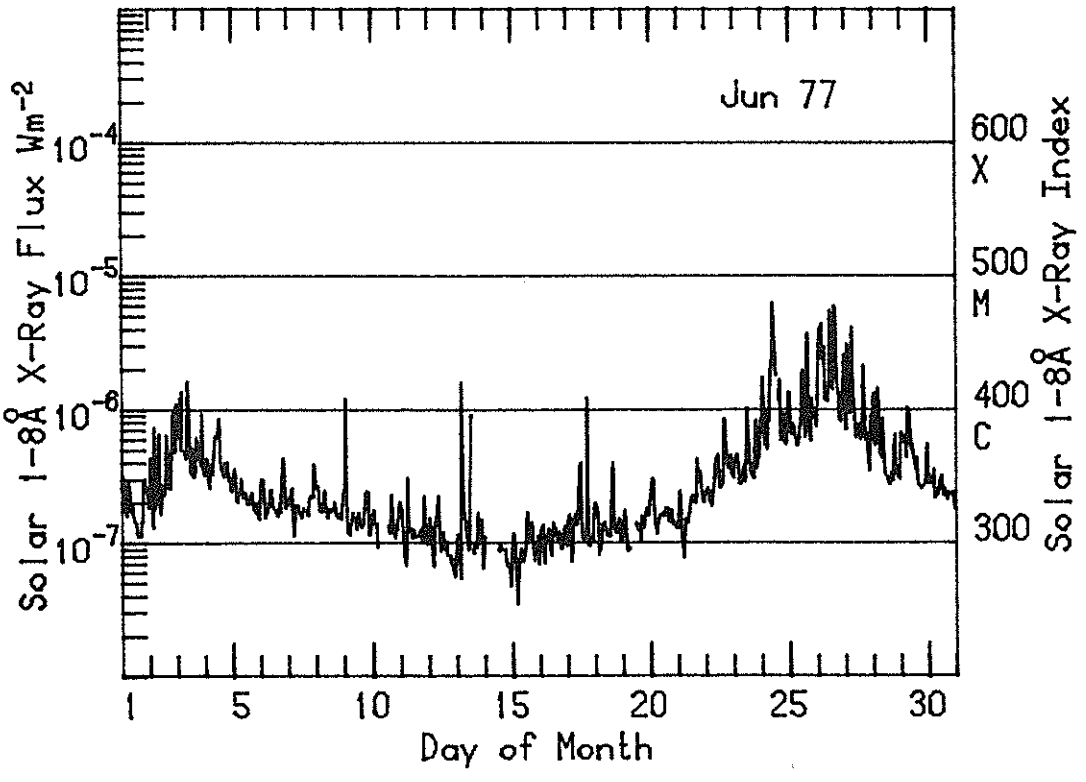
Jun 77
Solar 1-8Å X-Ray Flux Wm-2
10-4
10-5
10-6
10-7
600
X
500
M
400
C
300
Solar 1-8Å X-Ray Index
1
5
10
15
20
25
30
Day of Month

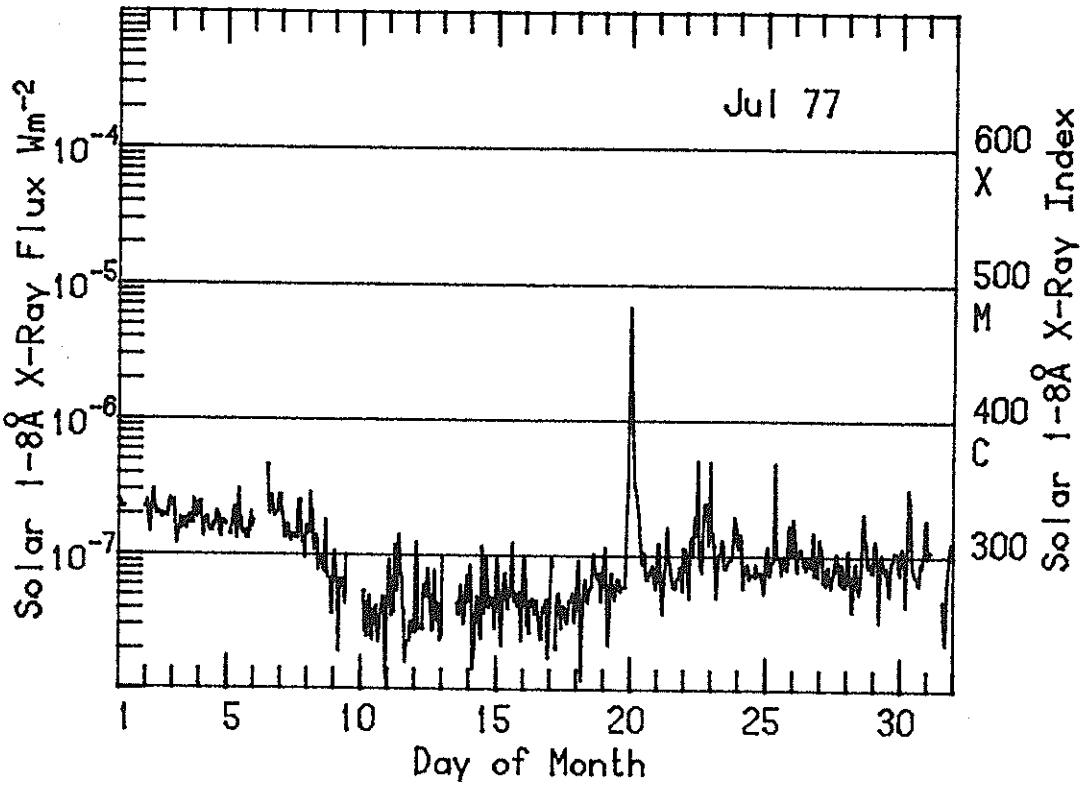
Jul 77
Solar 1-8Å X-Ray Flux Wm⁻²
10⁻⁴
10⁻⁵
10⁻⁶
10⁻⁷
600
X
500
M
400
C
300
Solar 1-8Å X-Ray Index
1
5
10
15
20
25
30
Day of Month

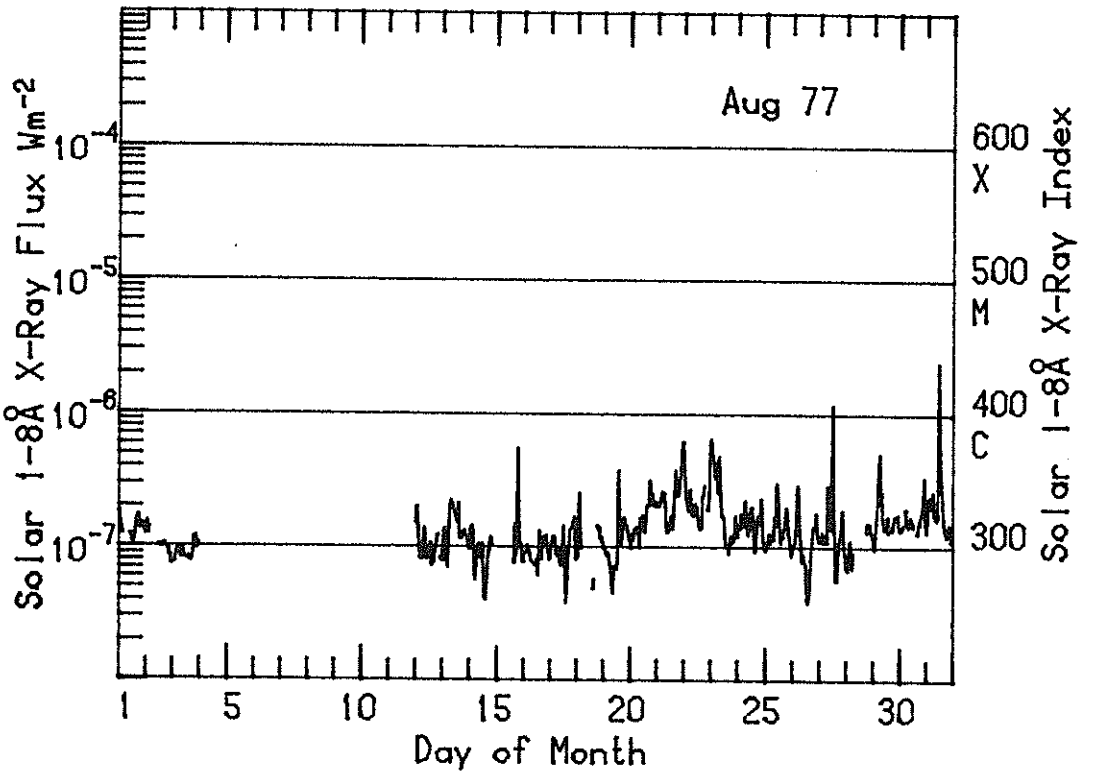
Aug 77
Solar 1-8Å X-Ray Flux Wm⁻²
10⁻⁴
10⁻⁵
10⁻⁶
10⁻⁷
600
X
500
M
400
C
300
Solar 1-8Å X-Ray Index
1
5
10
15
20
25
30
Day of Month

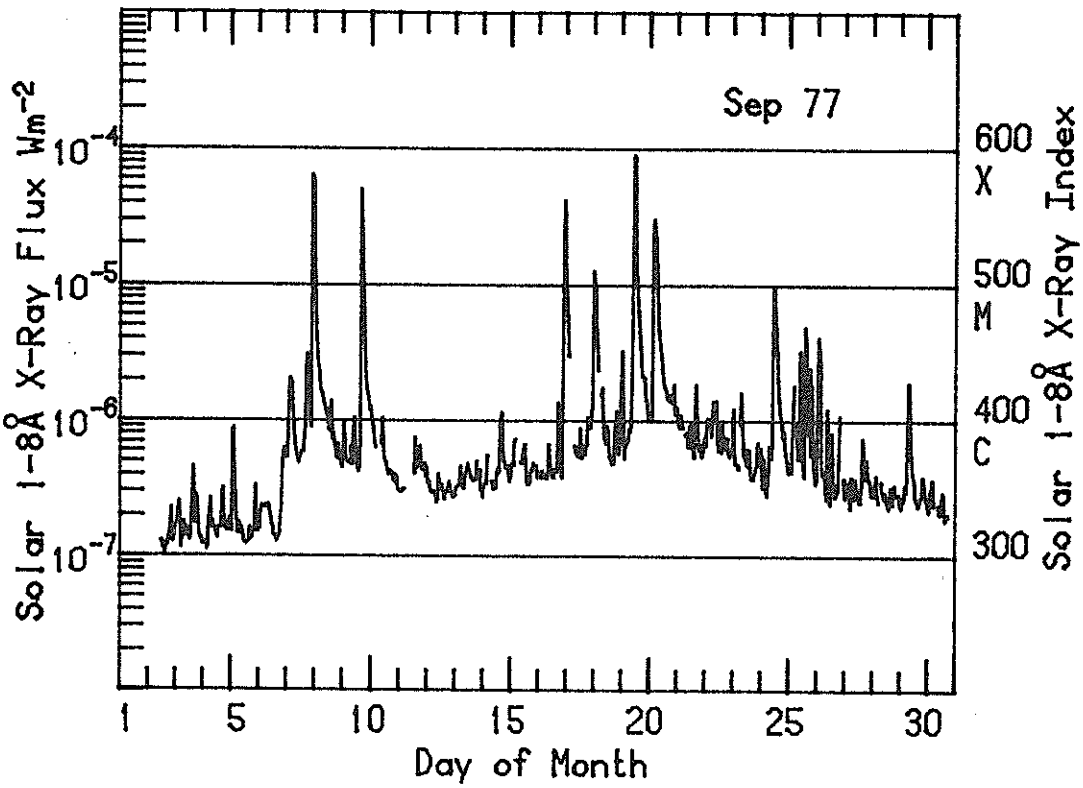
Sep 77
Solar 1-8Å X-Ray Flux Wm-2
10-4
10-5
10-6
10-7
600
X
500
M
400
C
300
Solar 1-8Å X-Ray Index
1
5
10
15
20
25
30
Day of Month

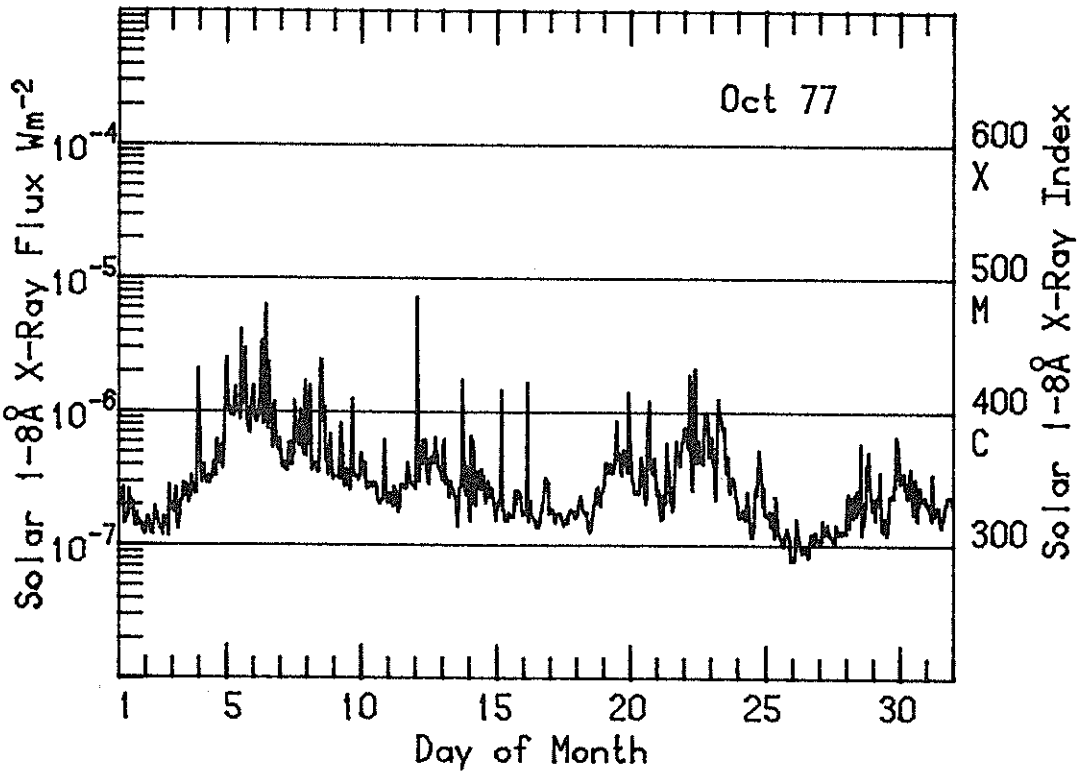
Oct 77
Solar 1-8Å X-Ray Flux Wm-2
10-4
10-5
10-6
10-7
600
X
500
M
400
C
300
Solar 1-8Å X-Ray Index
1
5
10
15
20
25
30
Day of Month

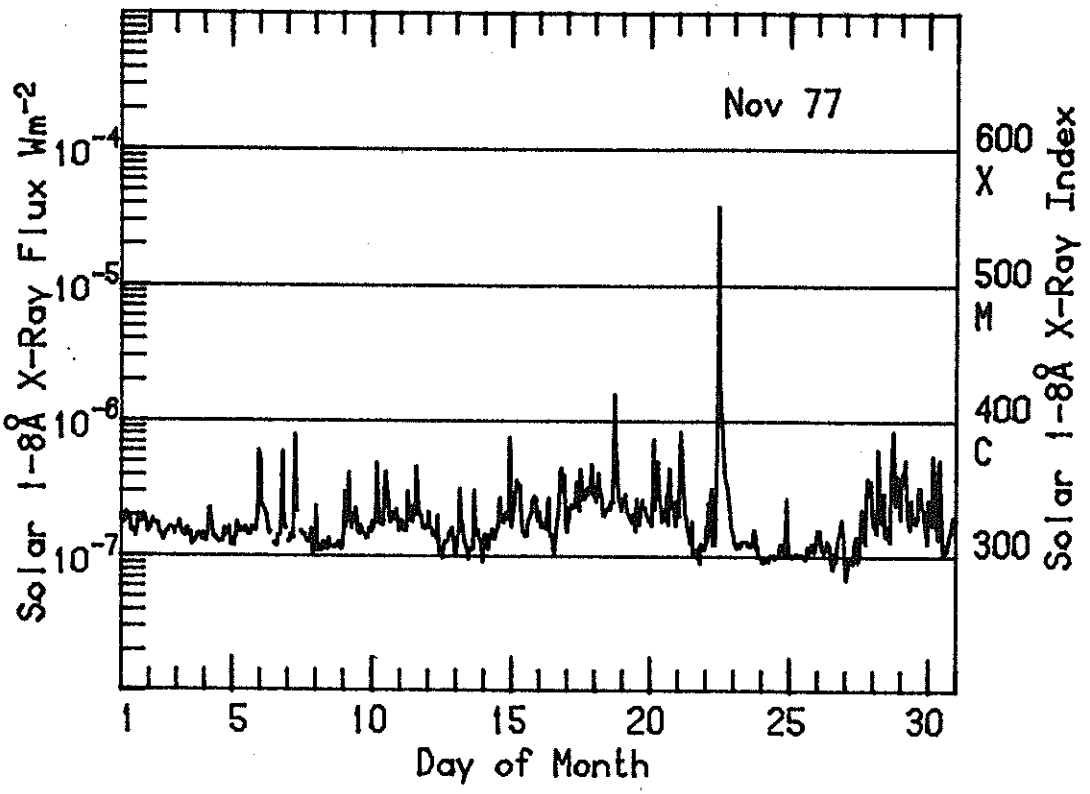
Nov 77
Solar 1-8Å X-Ray Flux Wm⁻²
10⁻⁴
10⁻⁵
10⁻⁶
10⁻⁷
600
X
500
M
400
C
300
Solar 1-8Å X-Ray Index
1
5
10
15
20
25
30
Day of Month

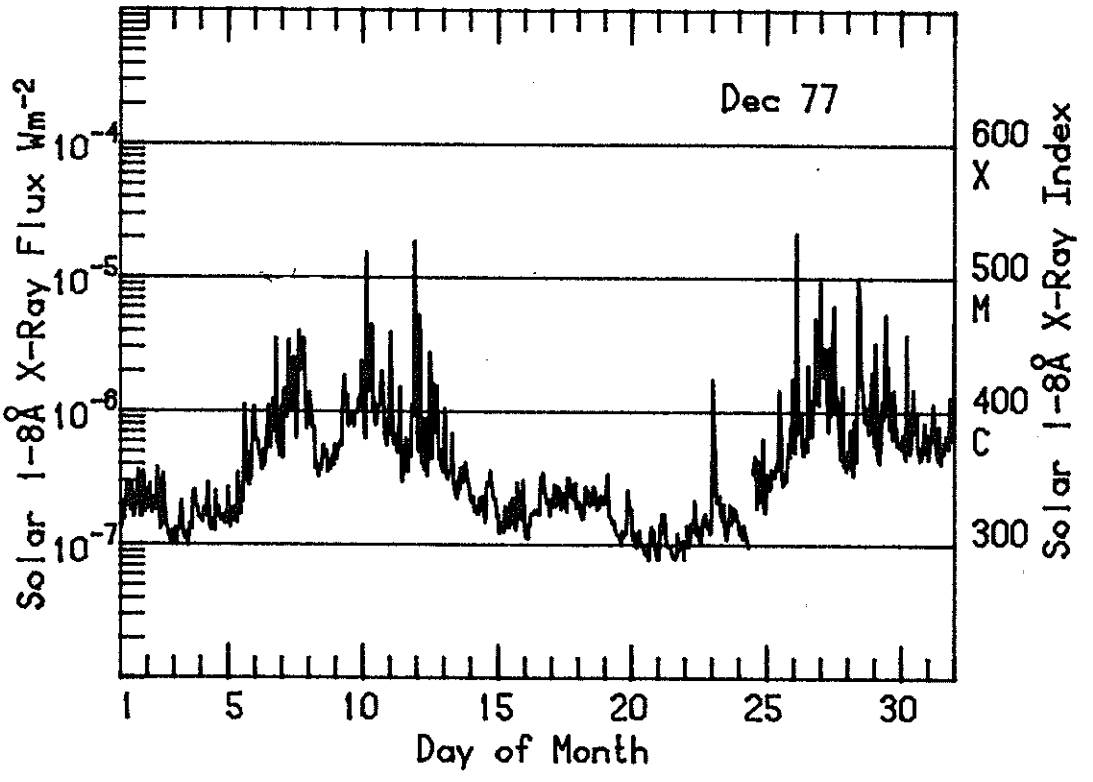
Dec 77
Solar 1-8Å X-Ray Flux Wm⁻²
10⁻⁴
10⁻⁵
10⁻⁶
10⁻⁷
600
X
500
M
400
C
300
Solar 1-8Å X-Ray Index
1
5
10
15
20
25
30
Day of Month

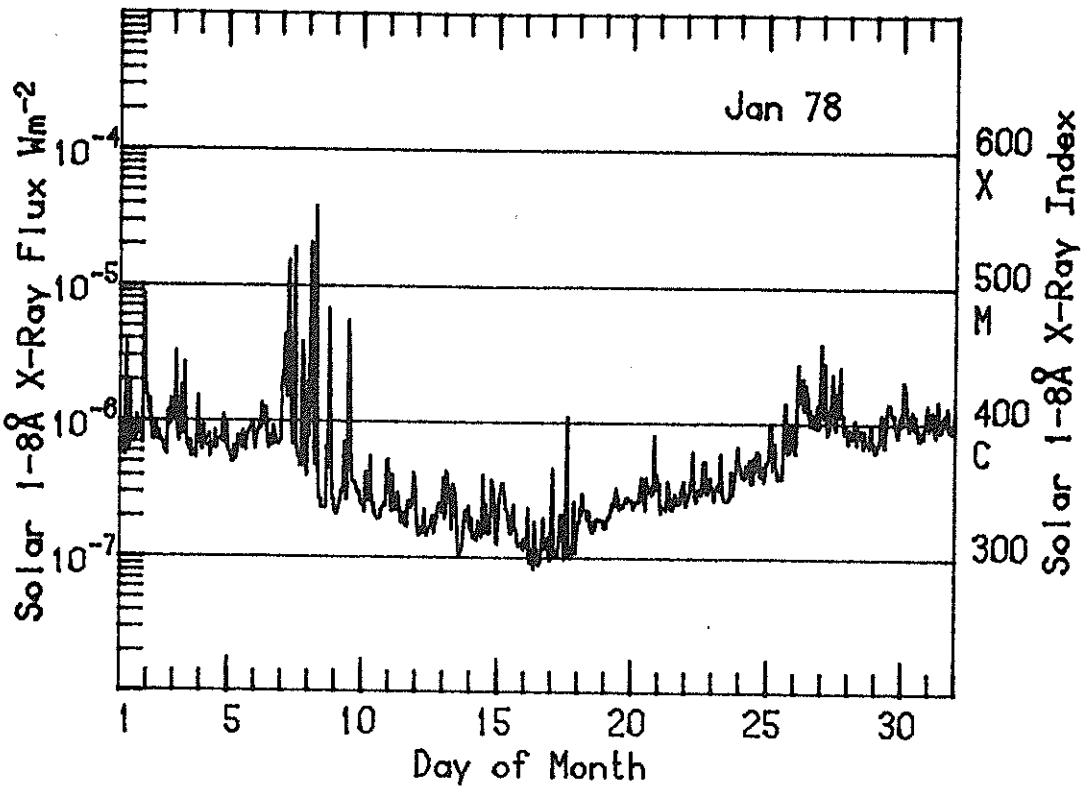
Jan 78
Solar 1-8Å X-Ray Flux Wm-2
10-4
10-5
10-6
10-7
600
X
500
M
400
C
300
Solar 1-8Å X-Ray Index
1
5
10
15
20
25
30
Day of Month

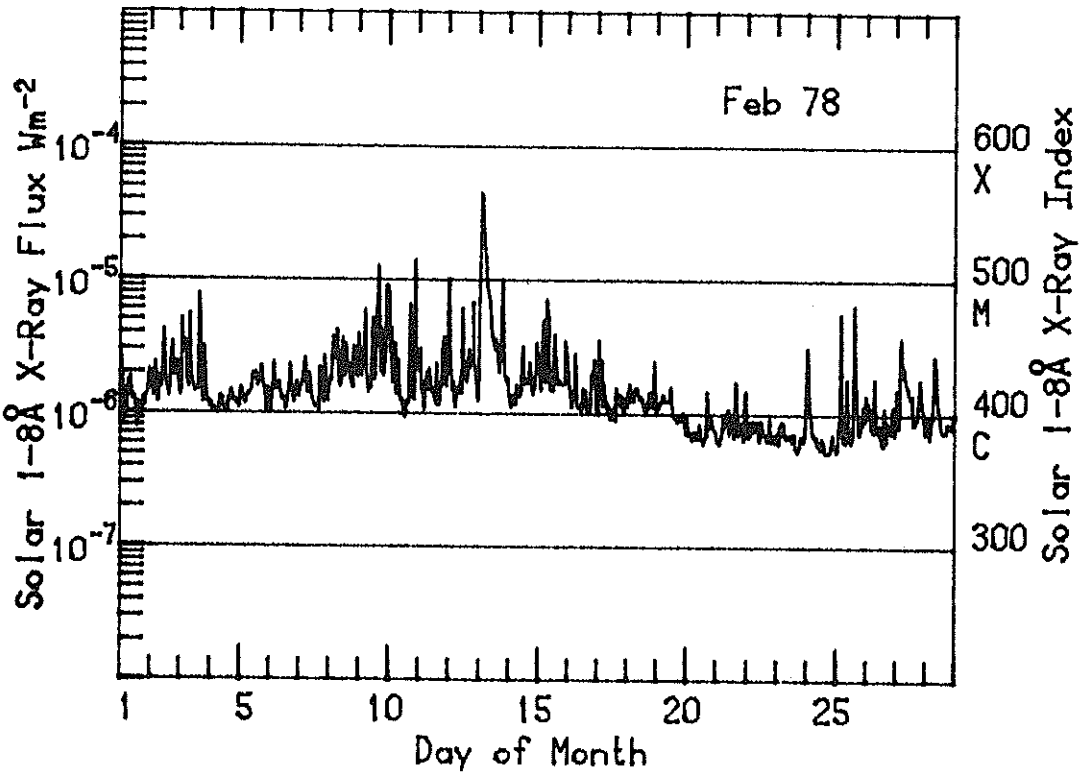
Feb 78
Solar 1-8Å X-Ray Flux Wm-2
10-4
10-5
10-6
10-7
600
X
500
M
400
C
300
Solar 1-8Å X-Ray Index
1
5
10
15
20
25
Day of Month

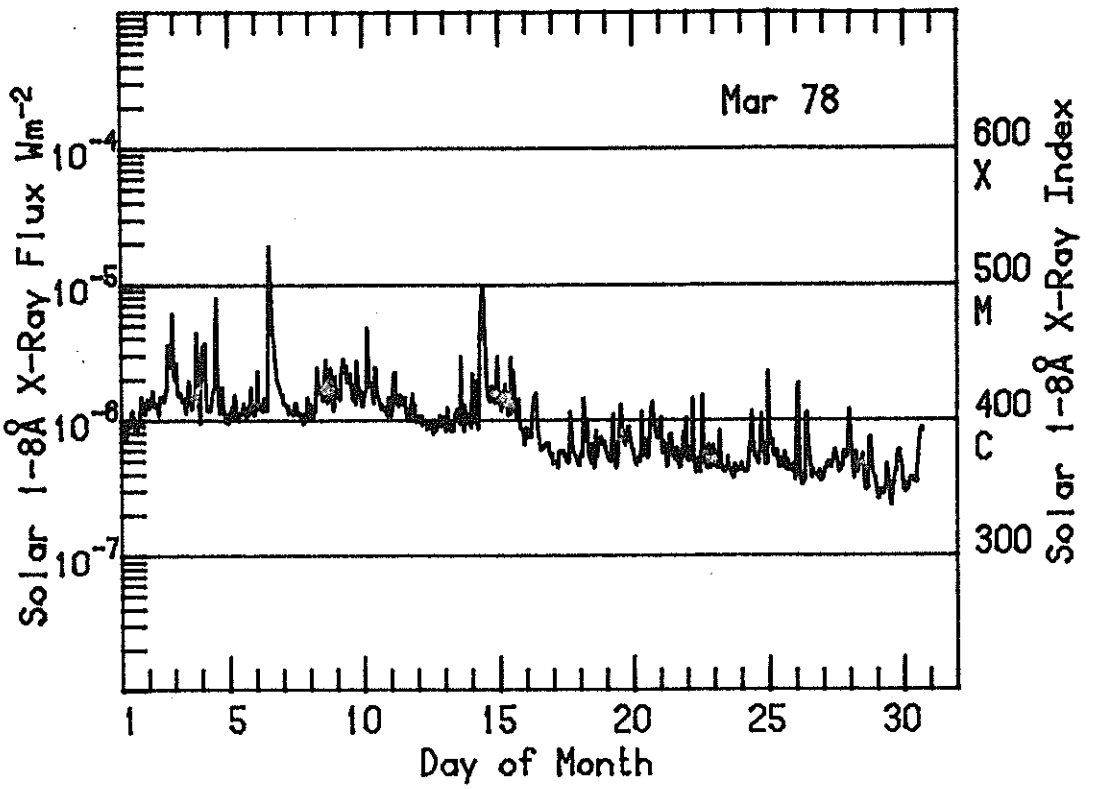
Mar 78
Solar 1-8Å X-Ray Flux Wm⁻²
10⁻⁴
10⁻⁵
10⁻⁶
10⁻⁷
600
X
500
M
400
C
300
Solar 1-8Å X-Ray Index
1
5
10
15
20
25
30
Day of Month

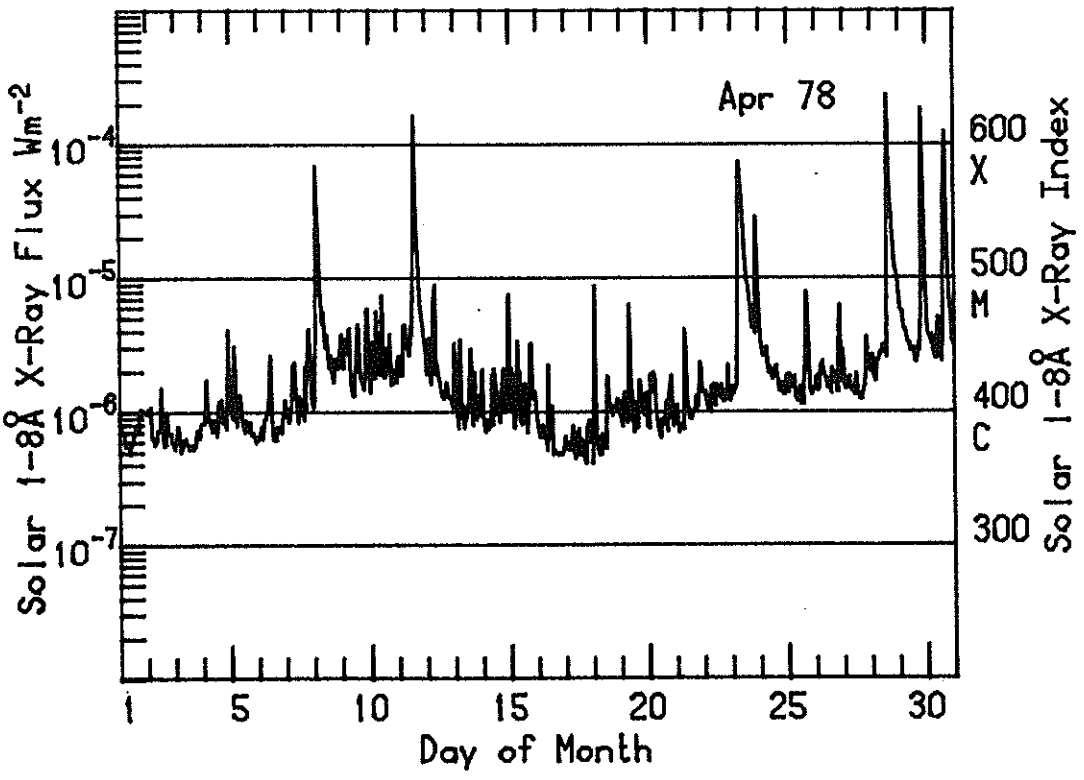
Apr 78
Solar 1-8Å X-Ray Flux Wm⁻²
10⁻⁴
10⁻⁵
10⁻⁶
10⁻⁷
600
X
500
M
400
C
300
Solar 1-8Å X-Ray Index
1
5
10
15
20
25
30
Day of Month

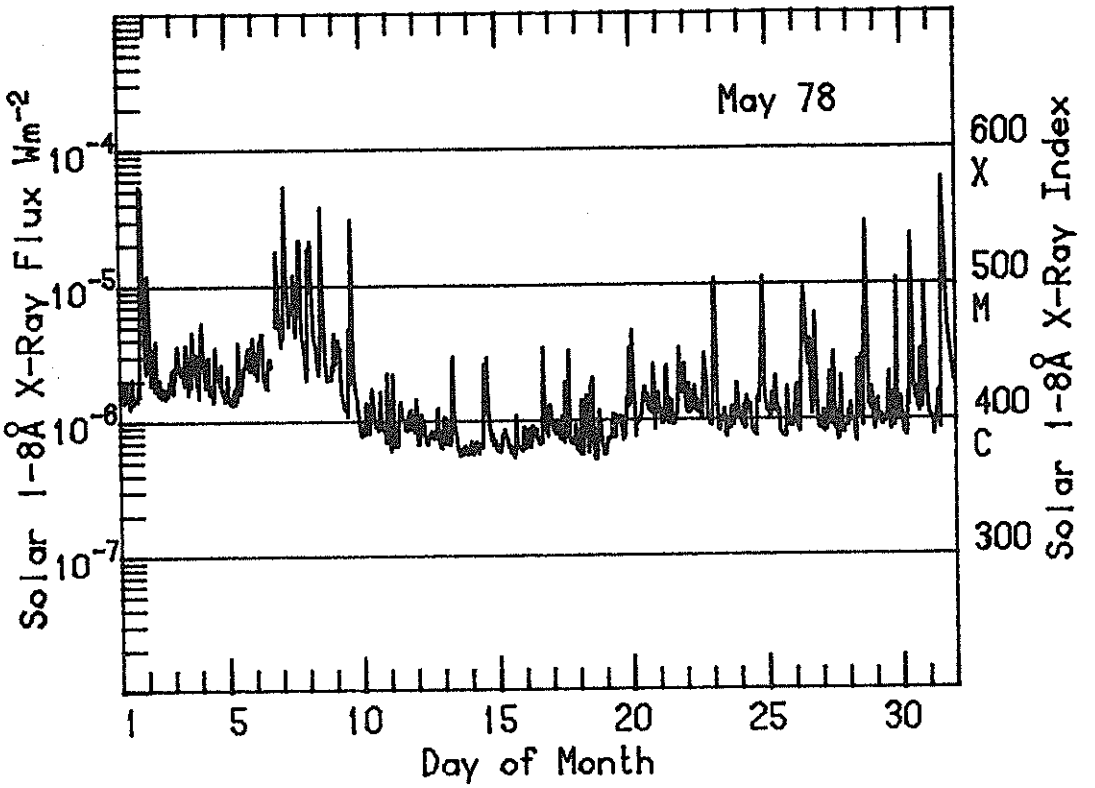
May 78
Solar 1-8Å X-Ray Flux Wm-2
10-4
10-5
10-6
10-7
600
X
500
M
400
C
300
Solar 1-8Å X-Ray Index
1
5
10
15
20
25
30
Day of Month

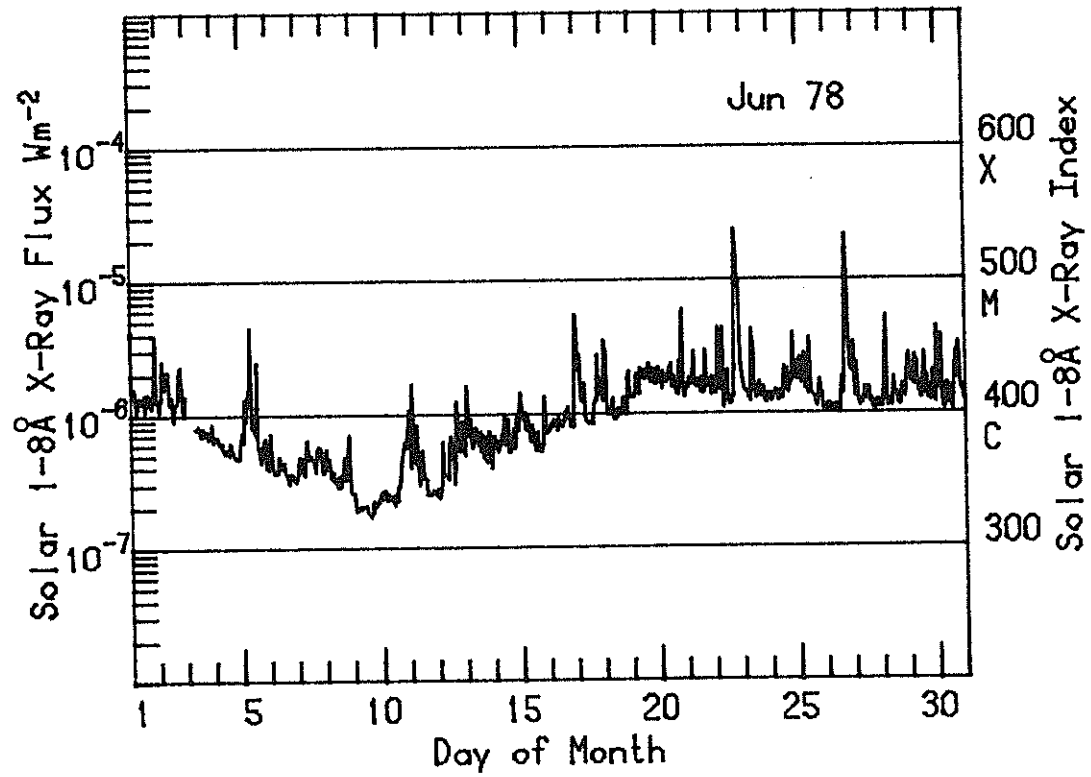
Jun 78
Solar 1-8Å X-Ray Flux Wm-2
10-4
10-5
10-6
10-7
600
X
500
M
400
C
300
Solar 1-8Å X-Ray Index
1
5
10
15
20
25
30
Day of Month

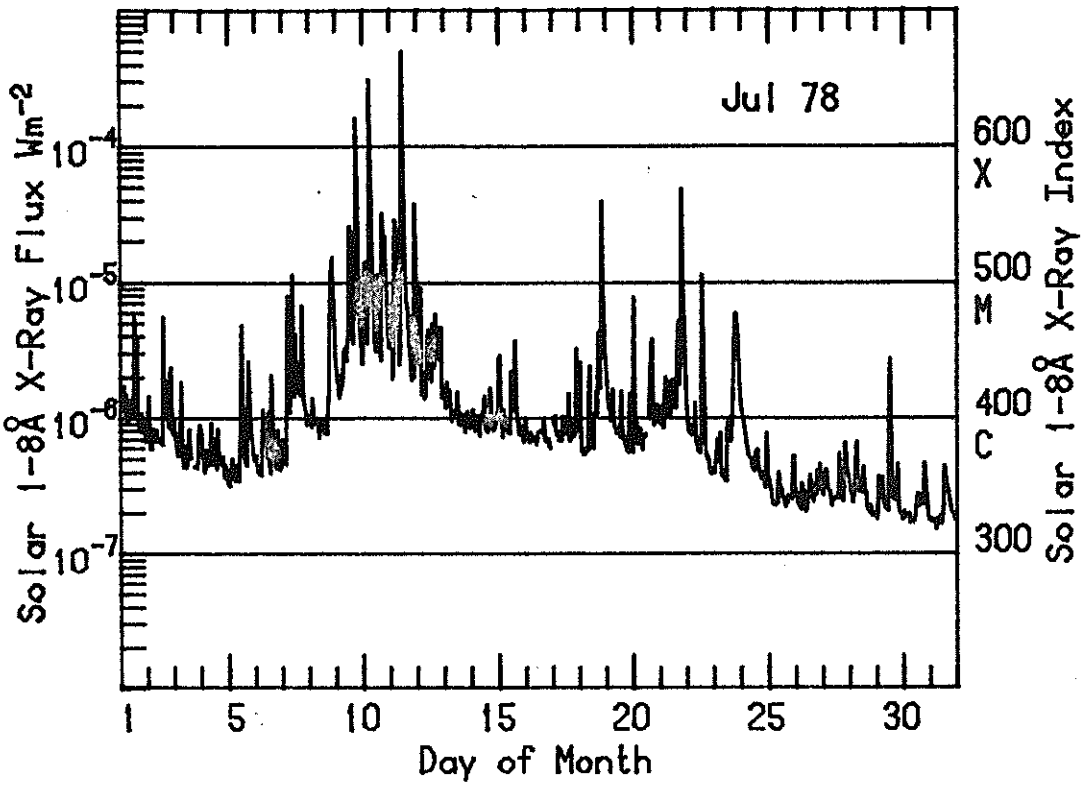
Jul 78
Solar 1-8Å X-Ray Flux Wm-2
10-4
10-5
10-6
10-7
600
X
500
M
400
C
300
Solar 1-8Å X-Ray Index
1
5
10
15
20
25
30
Day of Month

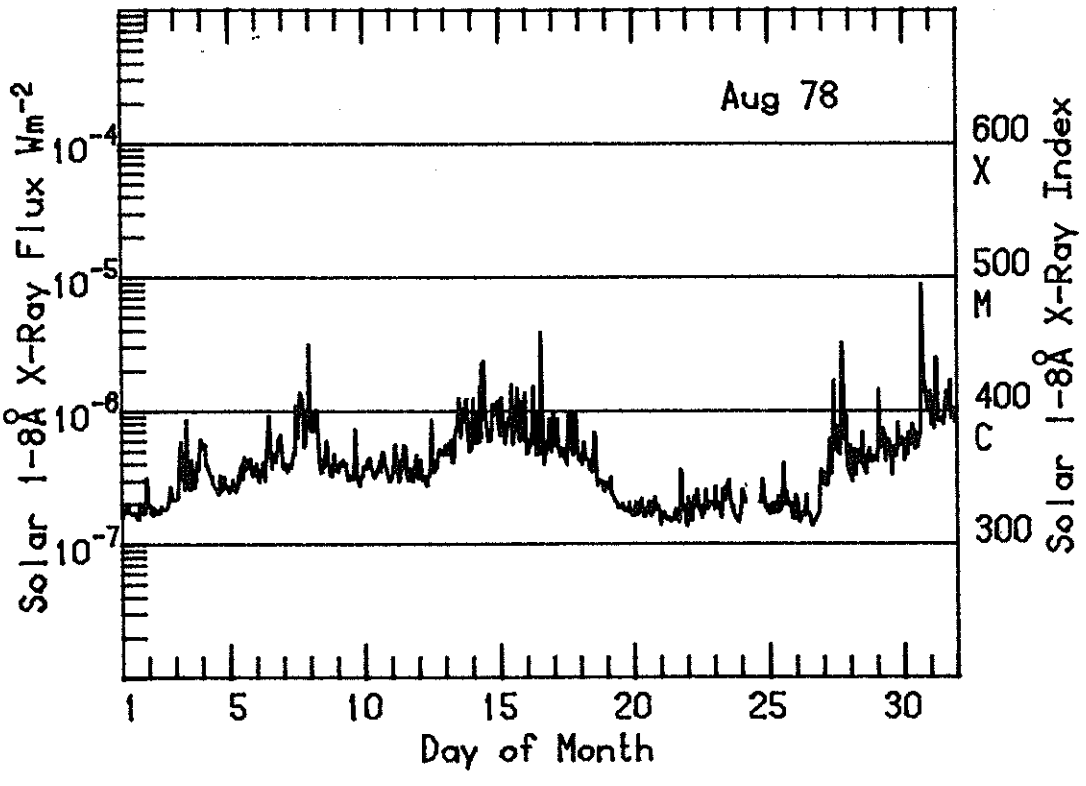
Aug 78
Solar 1-8Å X-Ray Flux Wm-2
10-4
10-5
10-6
10-7
600
X
500
M
400
C
300
Solar 1-8Å X-Ray Index
1
5
10
15
20
25
30
Day of Month

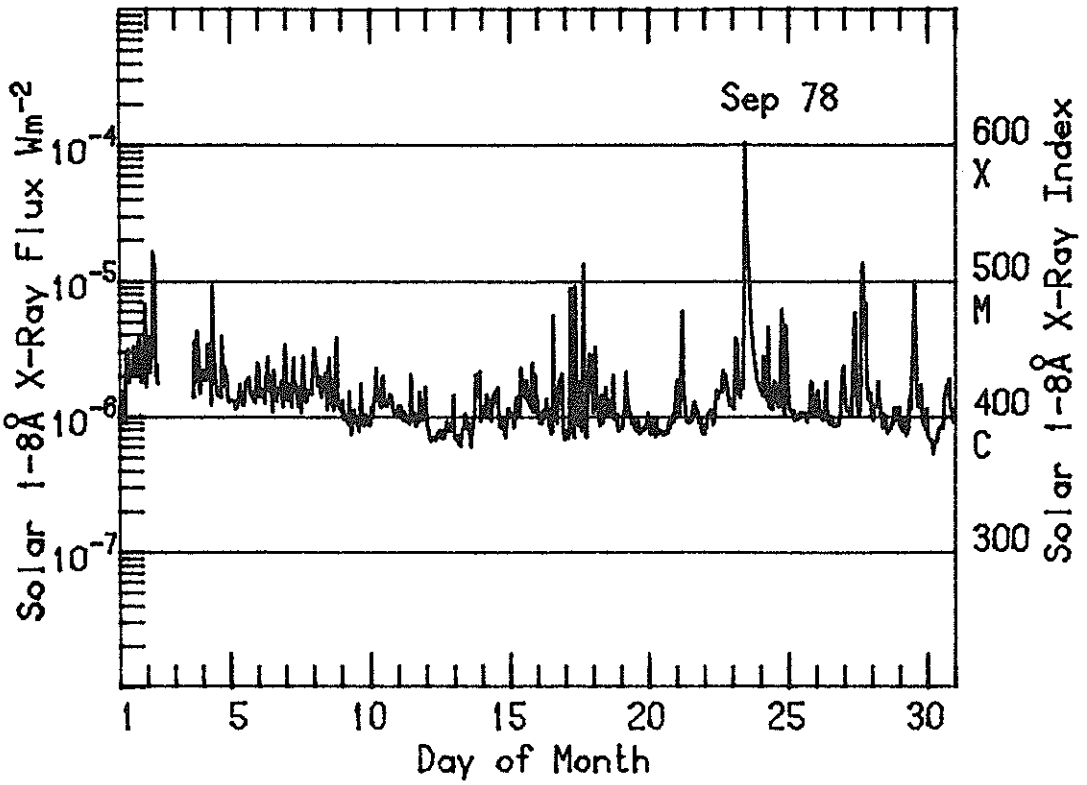
Sep 78
Solar 1-8Å X-Ray Flux Wm-2
10-4
10-5
10-6
10-7
600
X
500
M
400
C
300
Solar 1-8Å X-Ray Index
1
5
10
15
20
25
30
Day of Month

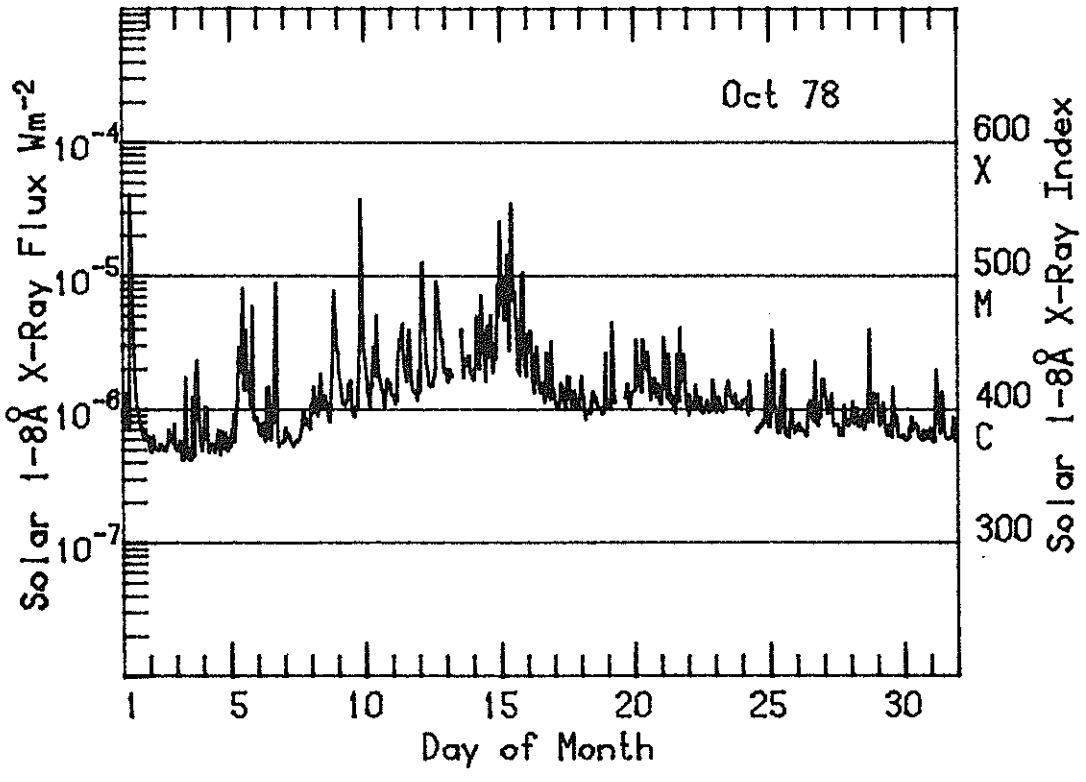
Oct 78
Solar 1-8Å X-Ray Flux Wm-2
10-4
10-5
10-6
10-7
600
X
500
M
400
C
300
Solar 1-8Å X-Ray Index
1
5
10
15
20
25
30
Day of Month

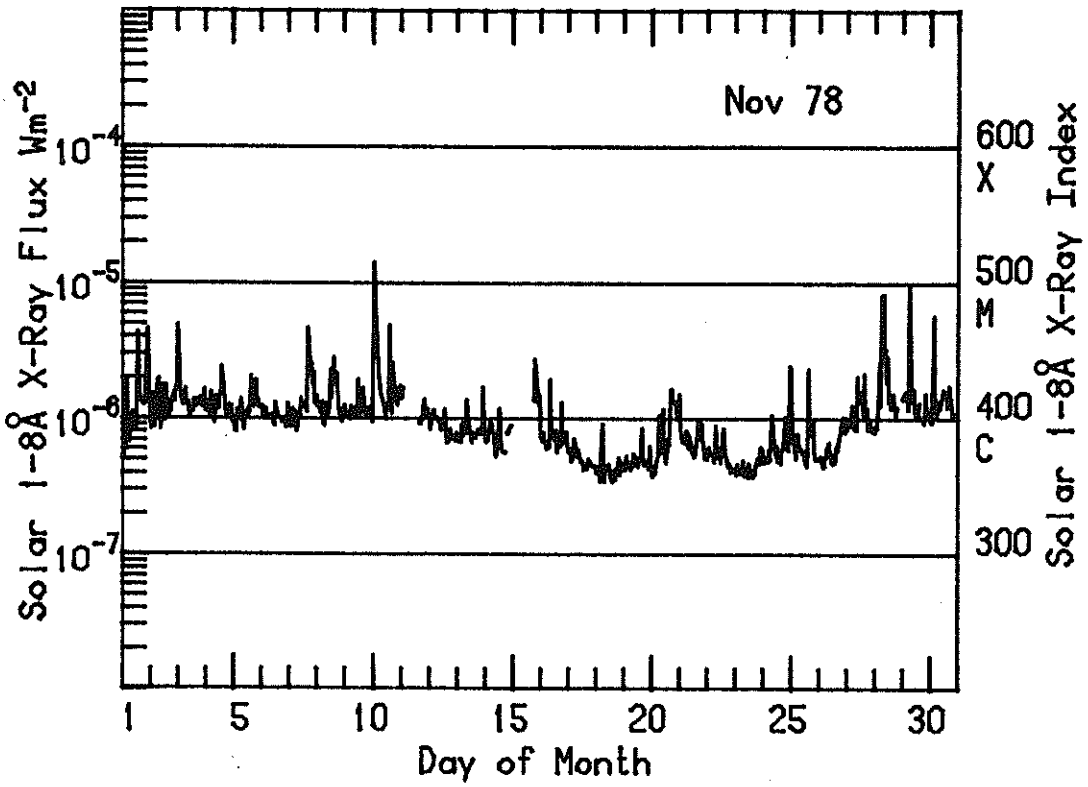
Nov 78
Solar 1-8Å X-Ray Flux Wm-2
10-4
10-5
10-6
10-7
600
X
500
M
400
C
300
Solar 1-8Å X-Ray Index
1
5
10
15
20
25
30
Day of Month

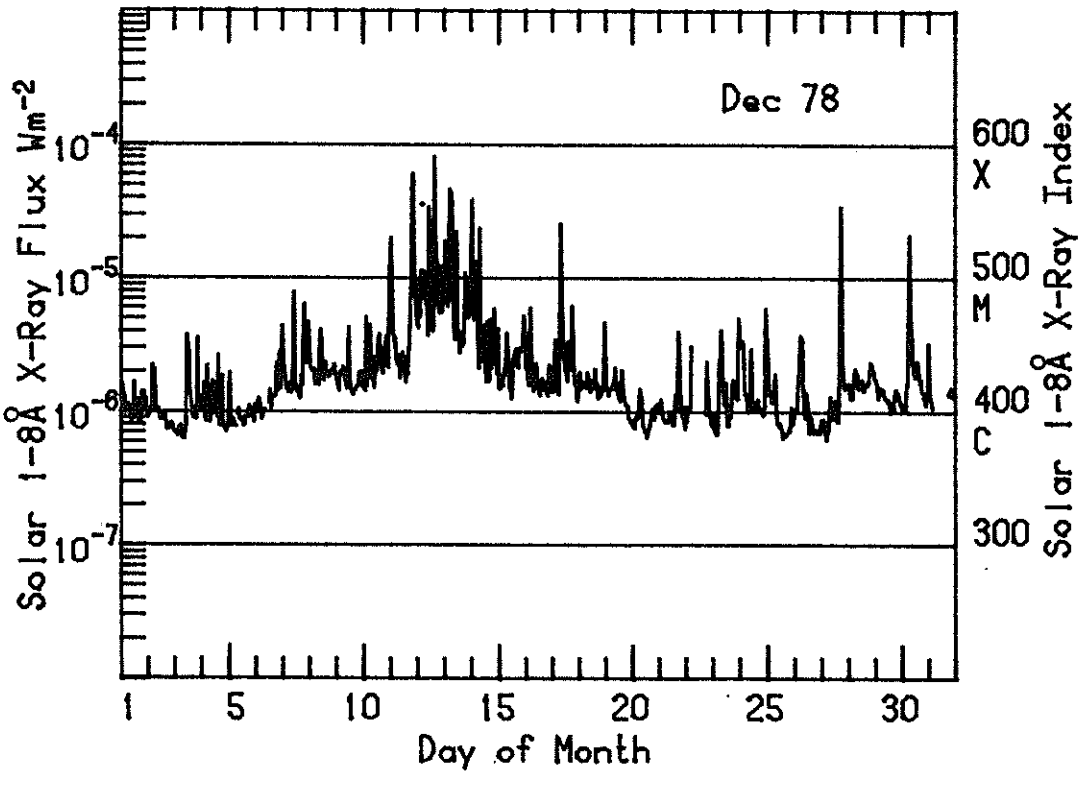
Dec 78
Solar 1-8Å X-Ray Flux Wm-2
10-4
10-5
10-6
10-7
600
X
500
M
400
C
300
Solar 1-8Å X-Ray Index
1
5
10
15
20
25
30
Day of Month

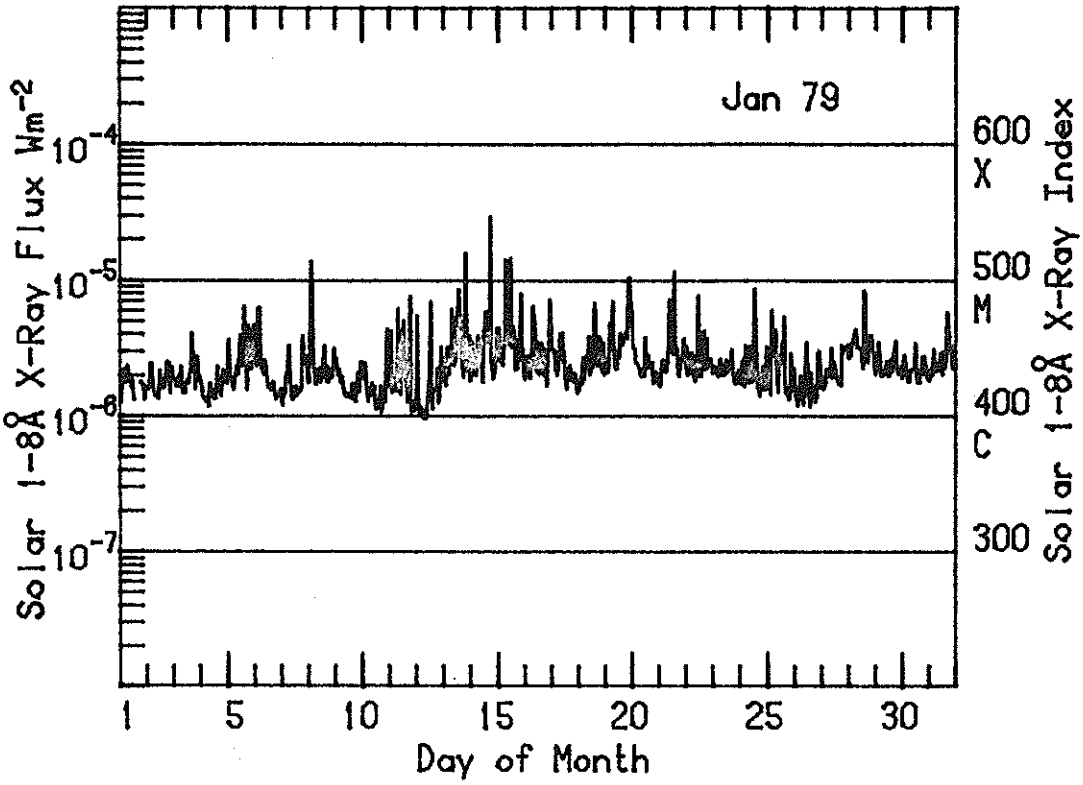
Jan 79
Solar 1-8Å X-Ray Flux Wm-2
10-4
10-5
10-6
10-7
600
X
500
M
400
C
300
Solar 1-8Å X-Ray Index
1
5
10
15
20
25
30
Day of Month

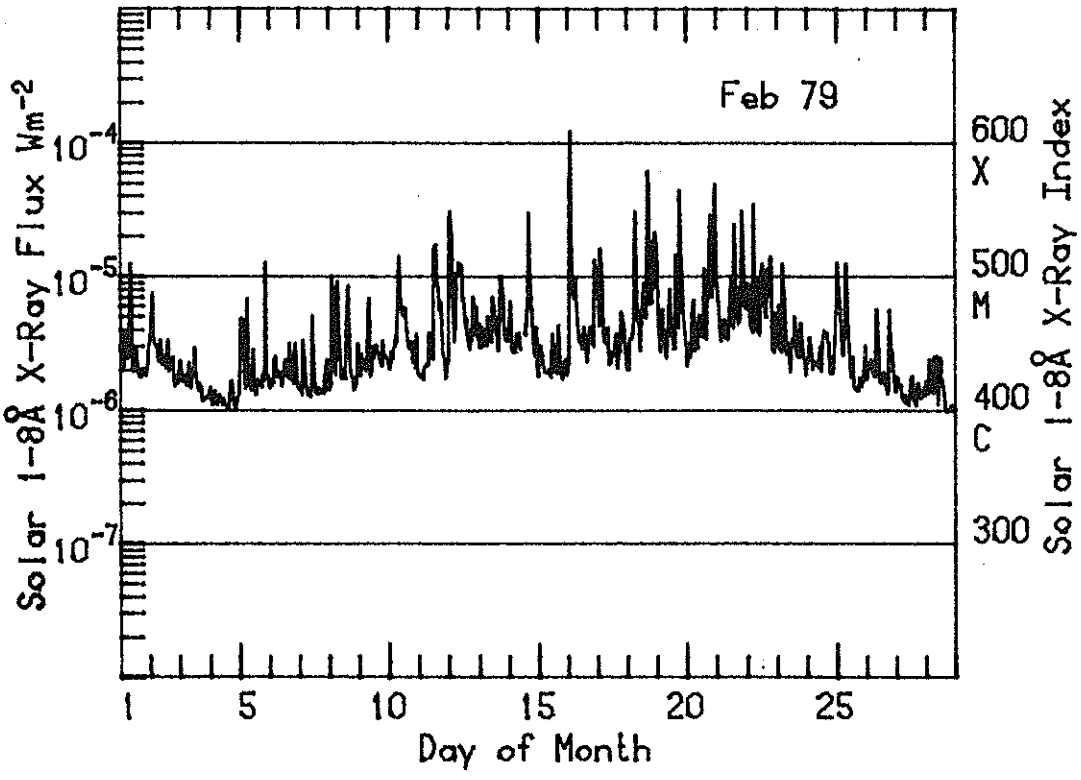
Feb 79
Solar 1-8Å X-Ray Flux Wm-2
10-4
10-5
10-6
10-7
600
X
500
M
400
C
300
Solar 1-8Å X-Ray Index
1
5
10
15
20
25
Day of Month

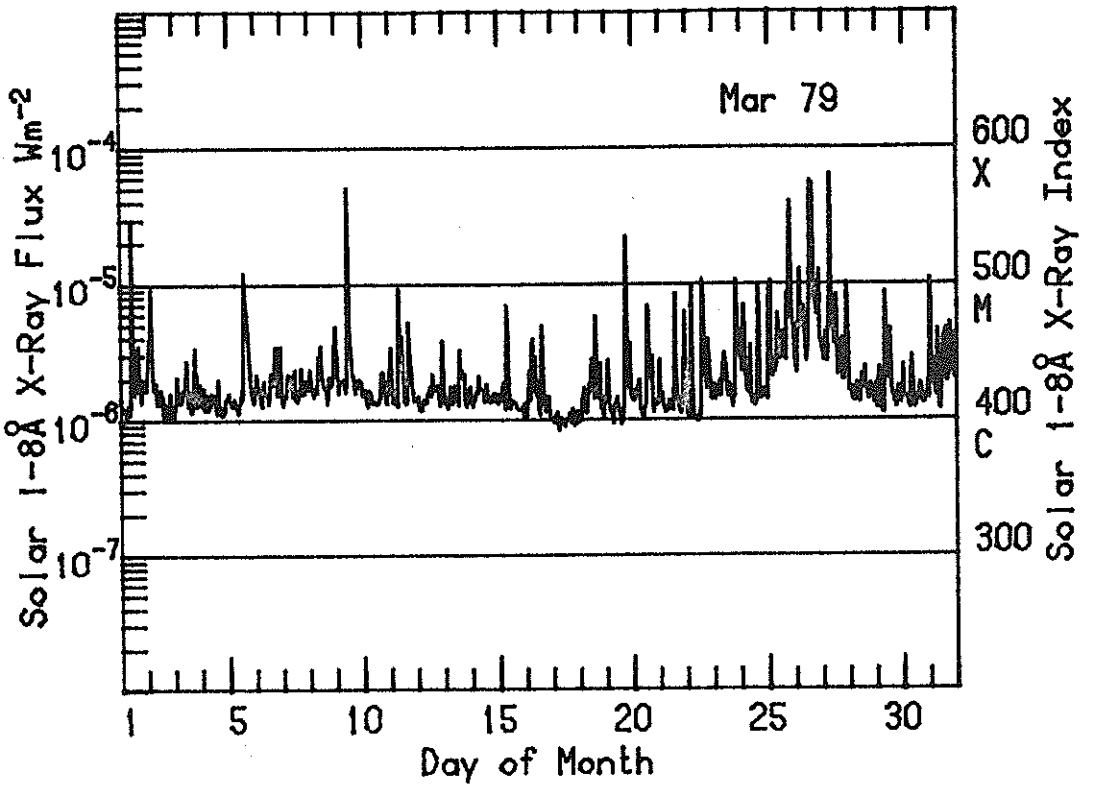
Mar 79
Solar 1-8Å X-Ray Flux Wm-2
10-4
10-5
10-6
10-7
600
X
500
M
400
C
300
Solar 1-8Å X-Ray Index
1
5
10
15
20
25
30
Day of Month

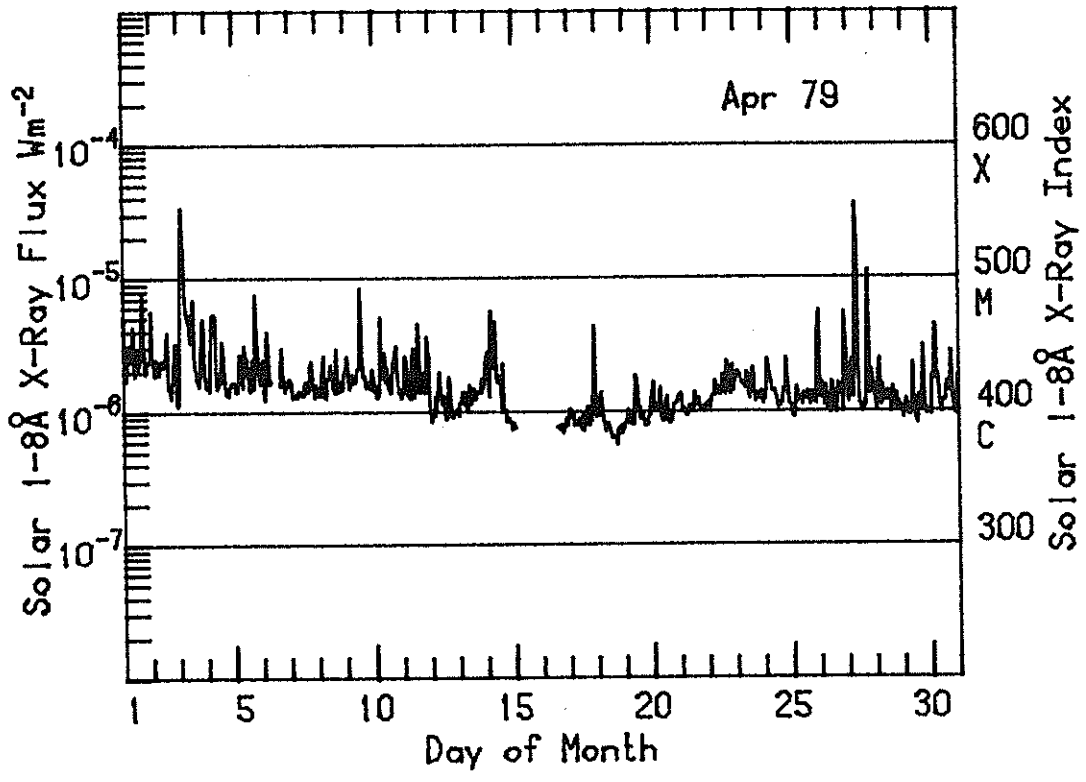
Apr 79
Solar 1-8Å X-Ray Flux Wm-2
10-4
10-5
10-6
10-7
600
X
500
M
400
C
300
Solar 1-8Å X-Ray Index
1
5
10
15
20
25
30
Day of Month

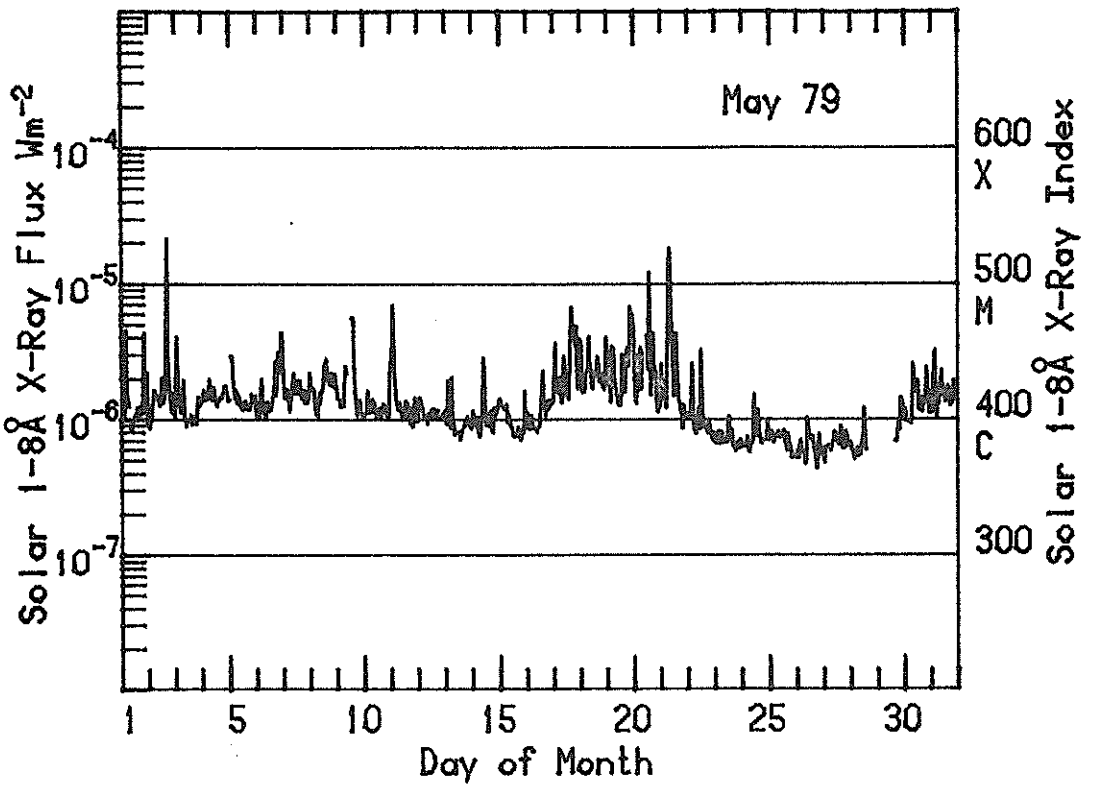
May 79
Solar 1-8Å X-Ray Flux Wm-2
10-4
10-5
10-6
10-7
600
X
500
M
400
C
300
Solar 1-8Å X-Ray Index
1
5
10
15
20
25
30
Day of Month

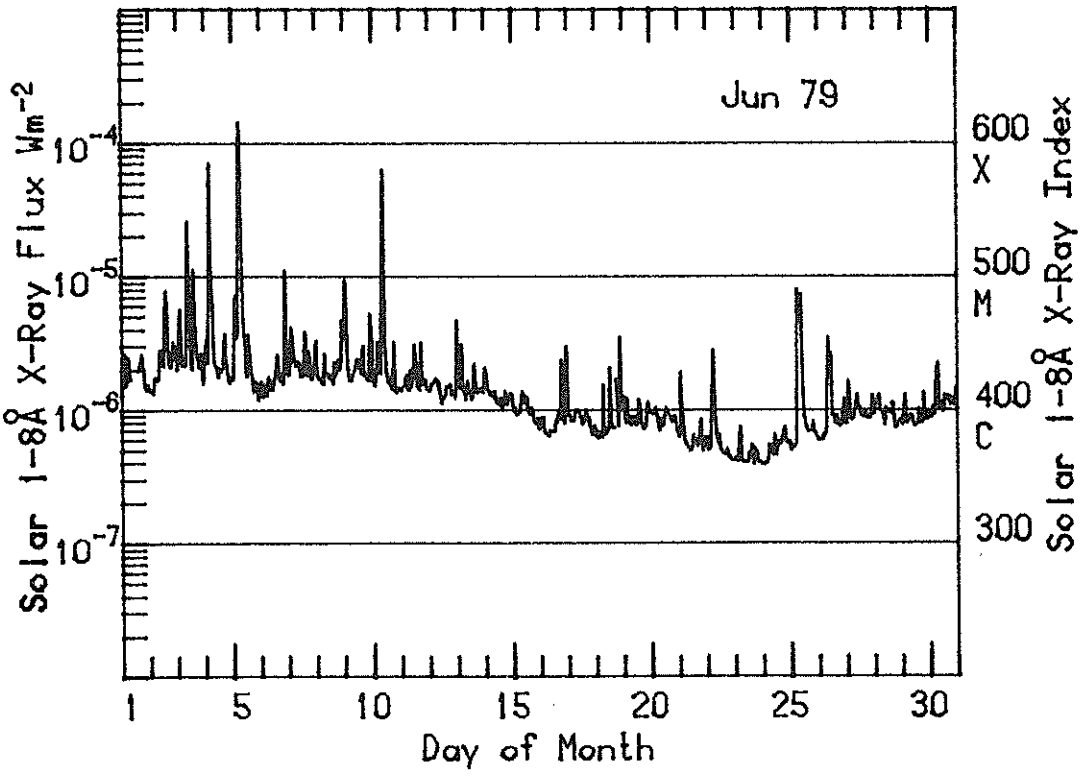
Jun 79
Solar 1-8Å X-Ray Flux Wm-2
10-4
10-5
10-6
10-7
600
X
500
M
400
C
300
Solar 1-8Å X-Ray Index
1
5
10
15
20
25
30
Day of Month

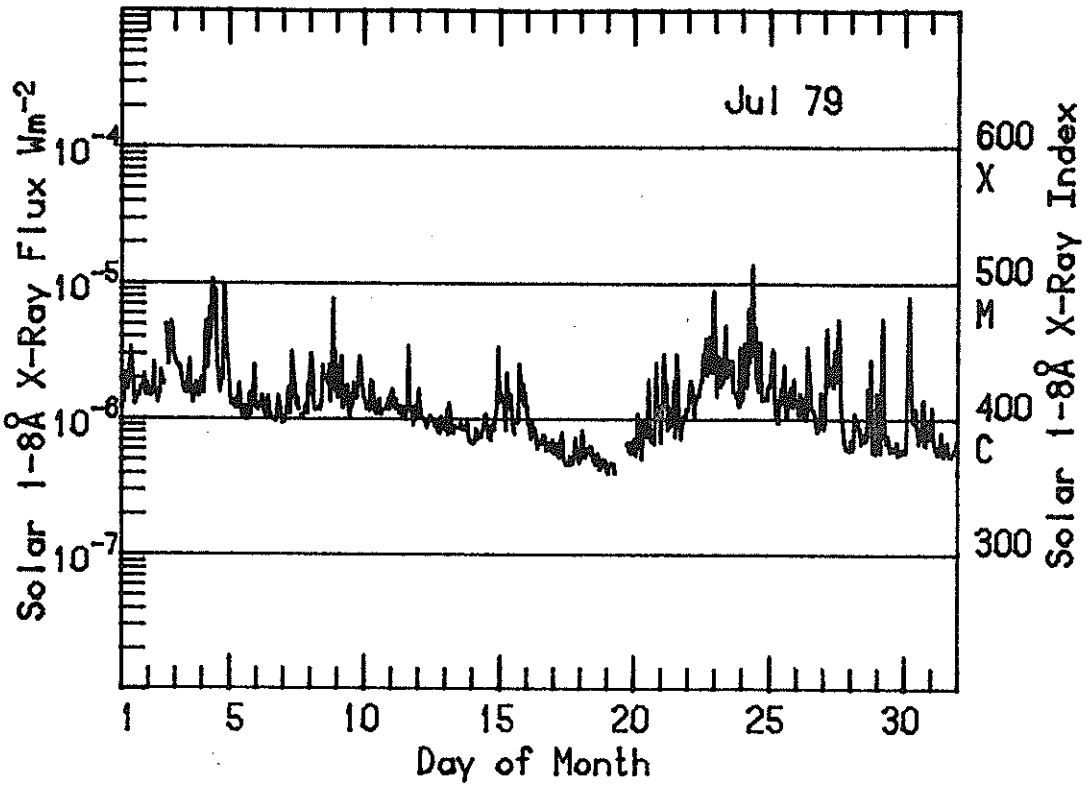
Jul 79
Solar 1-8Å X-Ray Flux Wm⁻²
10⁻⁴
10⁻⁵
10⁻⁶
10⁻⁷
600
X
500
M
400
C
300
Solar 1-8Å X-Ray Index
1
5
10
15
20
25
30
Day of Month

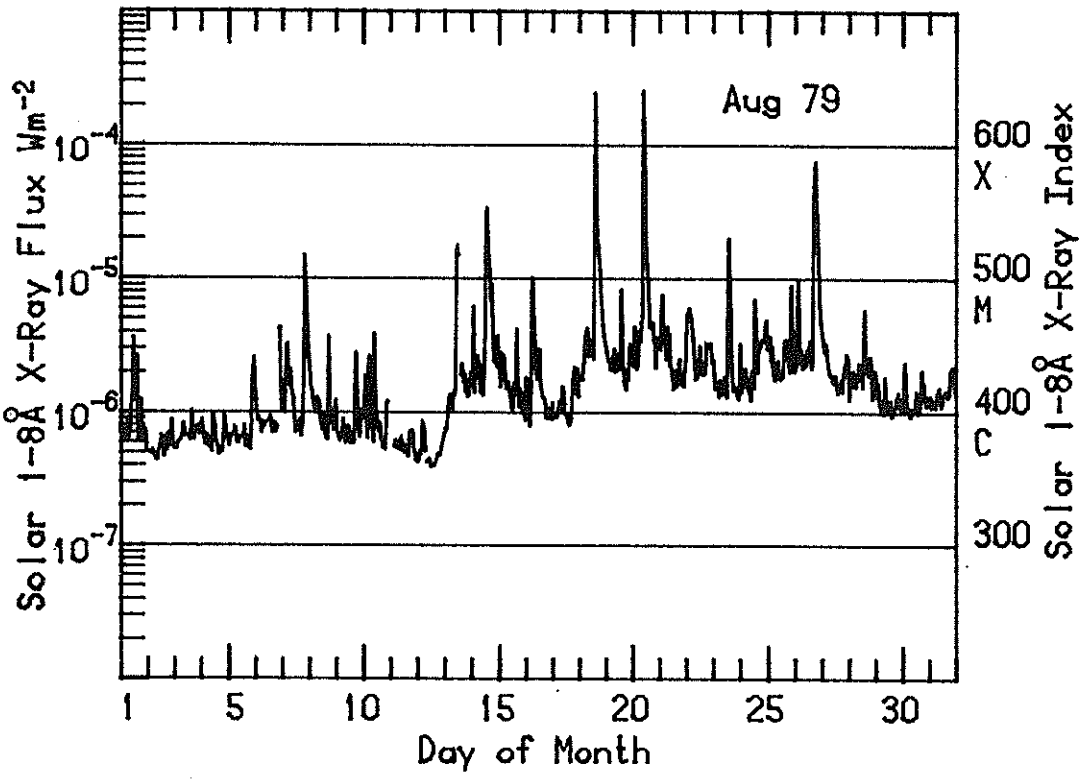
Aug 79
Solar 1-8Å X-Ray Flux Wm⁻²
10⁻⁴
10⁻⁵
10⁻⁶
10⁻⁷
600
X
500
M
400
C
300
Solar 1-8Å X-Ray Index
1
5
10
15
20
25
30
Day of Month

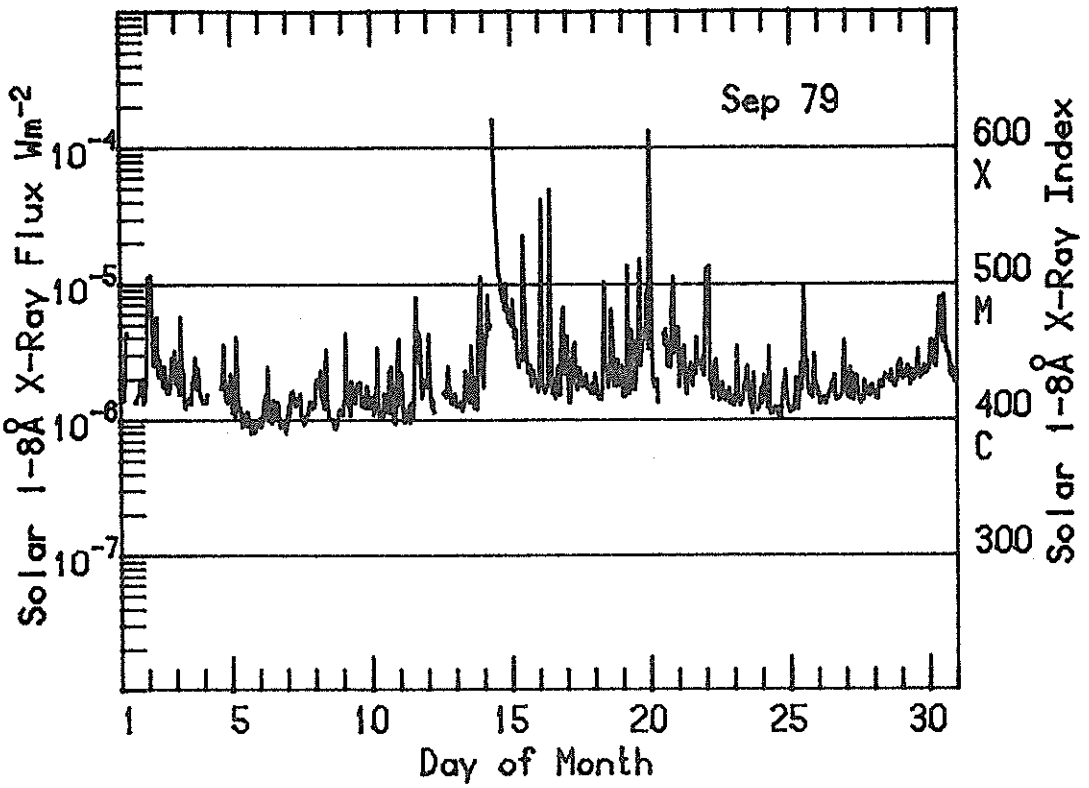
Sep 79
Solar 1-8Å X-Ray Flux Wm-2
10-4
10-5
10-6
10-7
600
X
500
M
400
C
300
Solar 1-8Å X-Ray Index
1
5
10
15
20
25
30
Day of Month

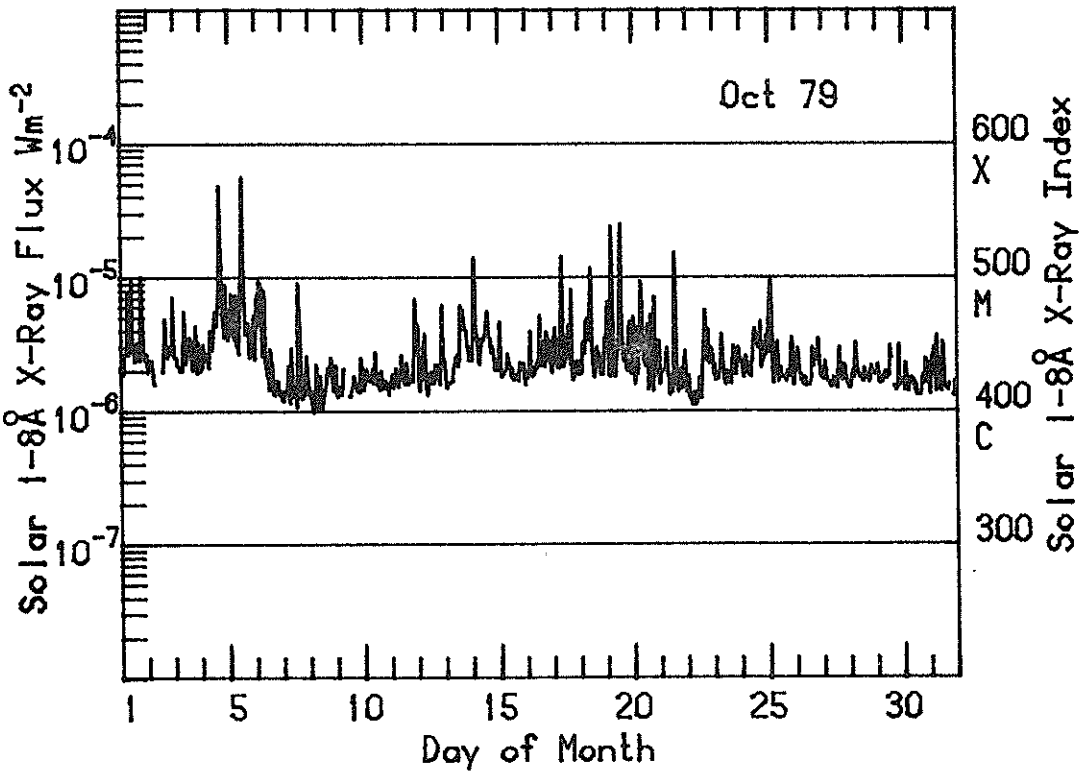
Oct 79
Solar 1-8Å X-Ray Flux Wm-2
10-4
10-5
10-6
10-7
600
X
500
M
400
C
300
Solar 1-8Å X-Ray Index
1
5
10
15
20
25
30
Day of Month

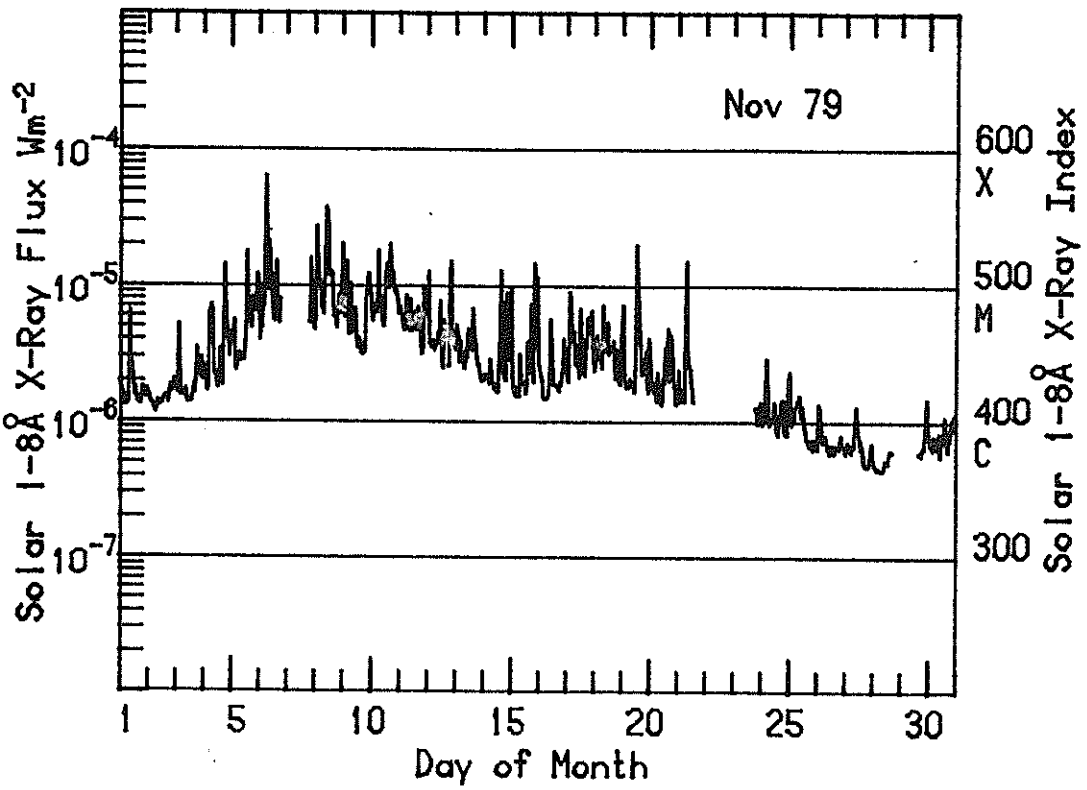
Nov 79
Solar 1-8Å X-Ray Flux Wm-2
10-4
10-5
10-6
10-7
600
X
500
M
400
C
300
Solar 1-8Å X-Ray Index
1
5
10
15
20
25
30
Day of Month

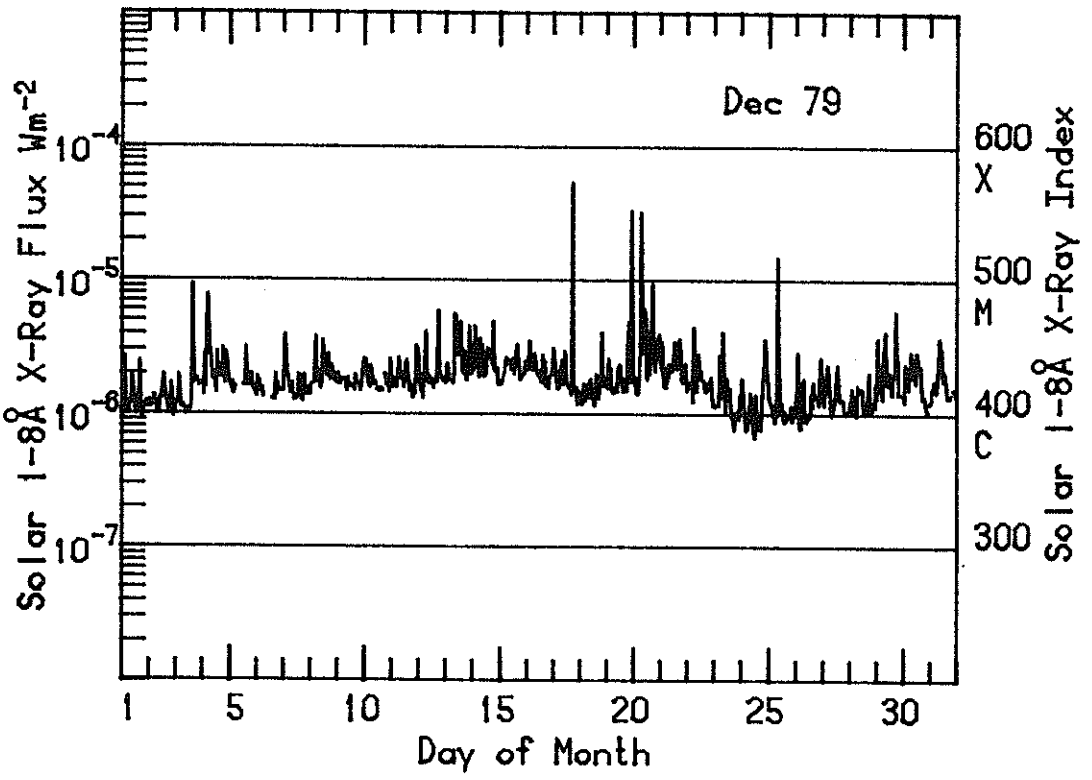
Dec 79
Solar 1-8Å X-Ray Flux Wm-2
10-4
10-5
10-6
10-7
600
X
500
M
400
C
300
Solar 1-8Å X-Ray Index
1
5
10
15
20
25
30
Day of Month

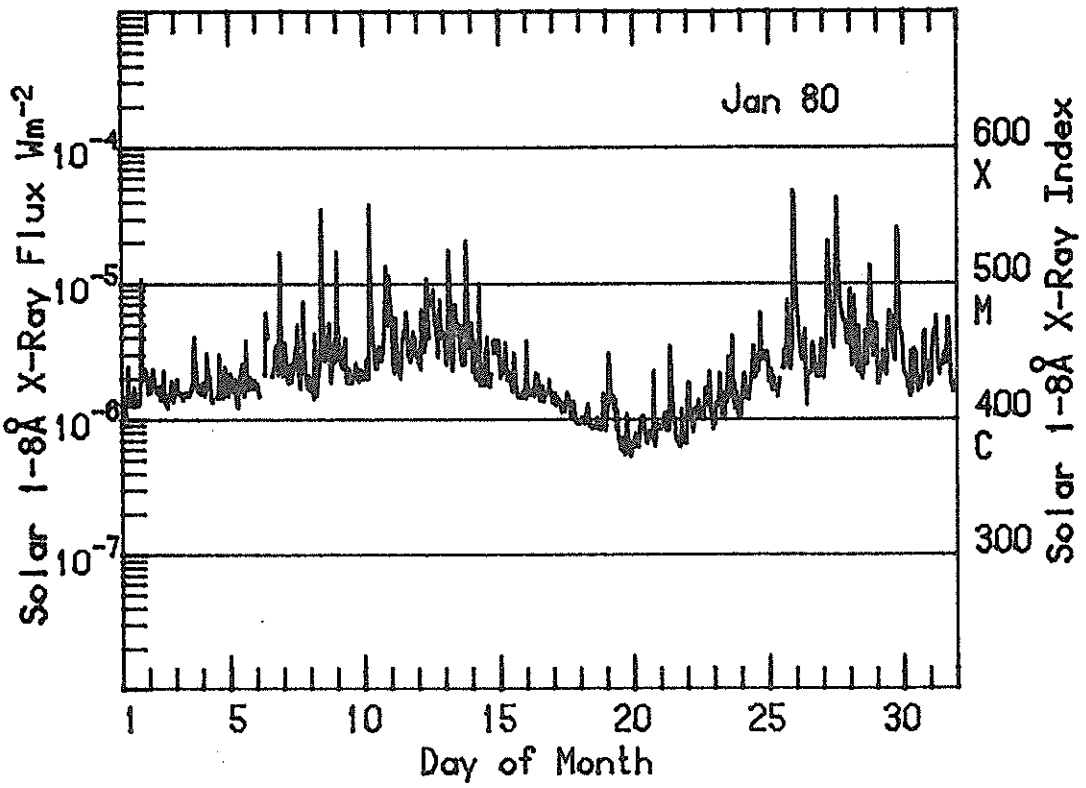
Jan 80
Solar 1-8Å X-Ray Flux Wm-2
10-4
10-5
10-6
10-7
600
X
500
M
400
C
300
Solar 1-8Å X-Ray Index
1
5
10
15
20
25
30
Day of Month

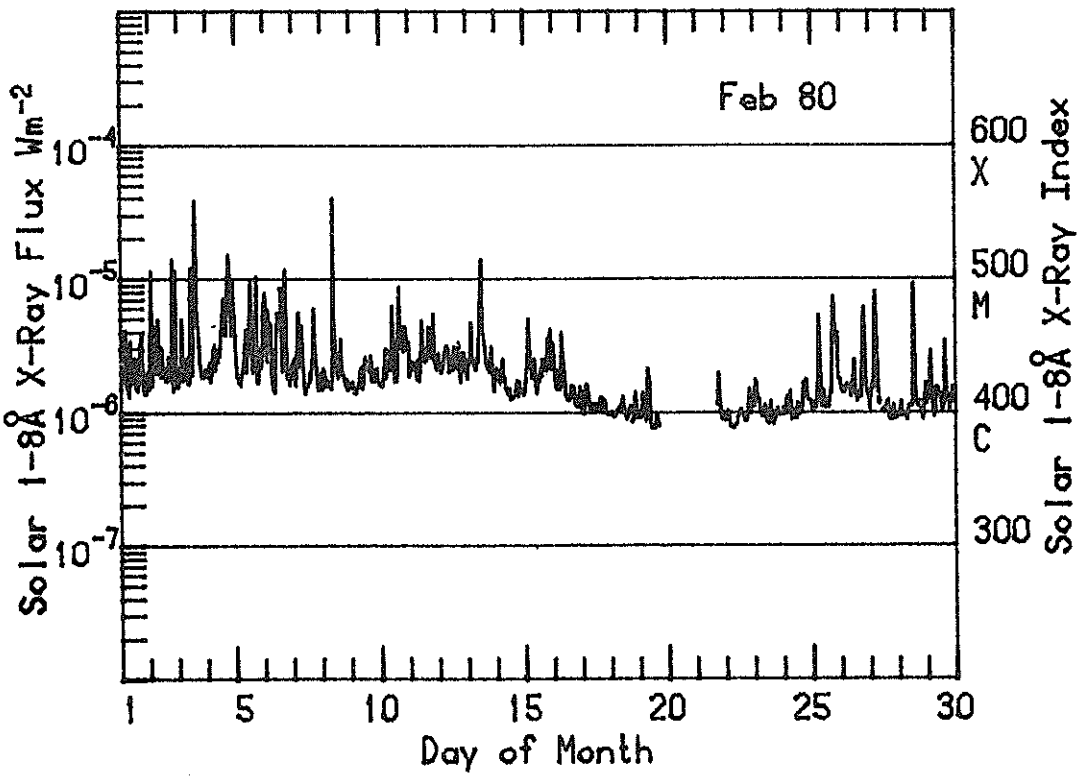
Feb 80
Solar 1-8Å X-Ray Flux Wm-2
10-4
10-5
10-6
10-7
600
X
500
M
400
C
300
Solar 1-8Å X-Ray Index
1
5
10
15
20
25
30
Day of Month

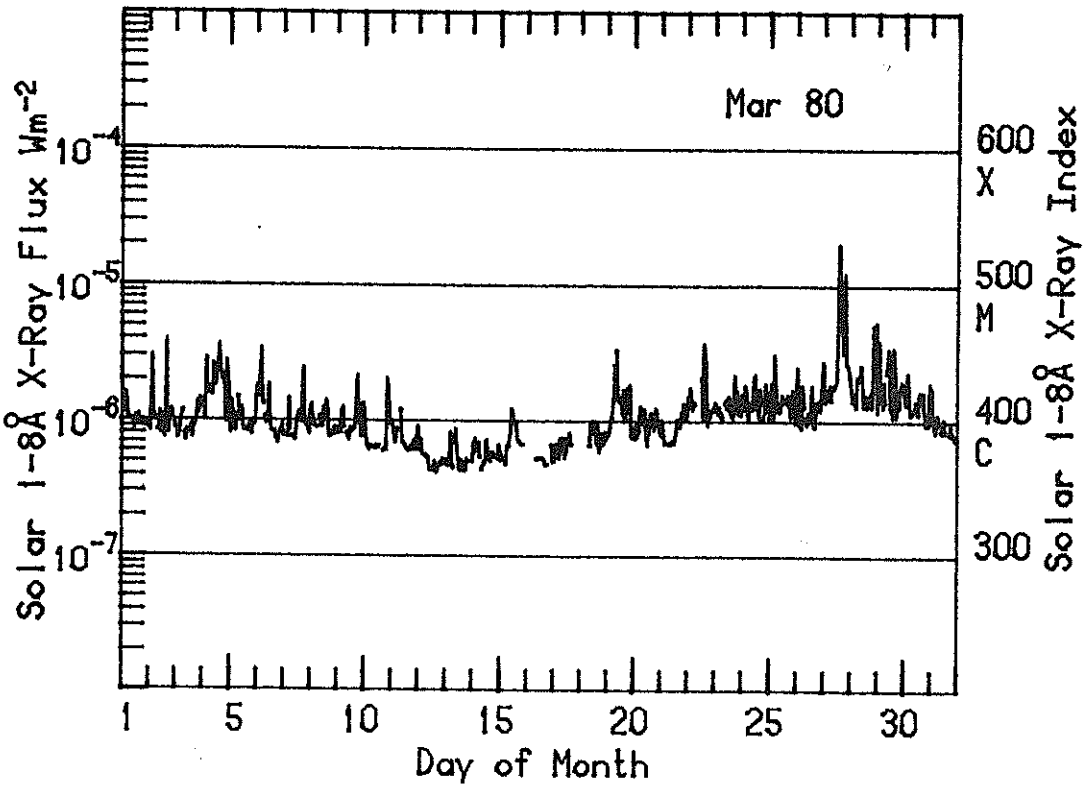
Mar 80
Solar 1-8Å X-Ray Flux Wm-2
10-4
10-5
10-6
10-7
600
X
500
M
400
C
300
Solar 1-8Å X-Ray Index
1
5
10
15
20
25
30
Day of Month

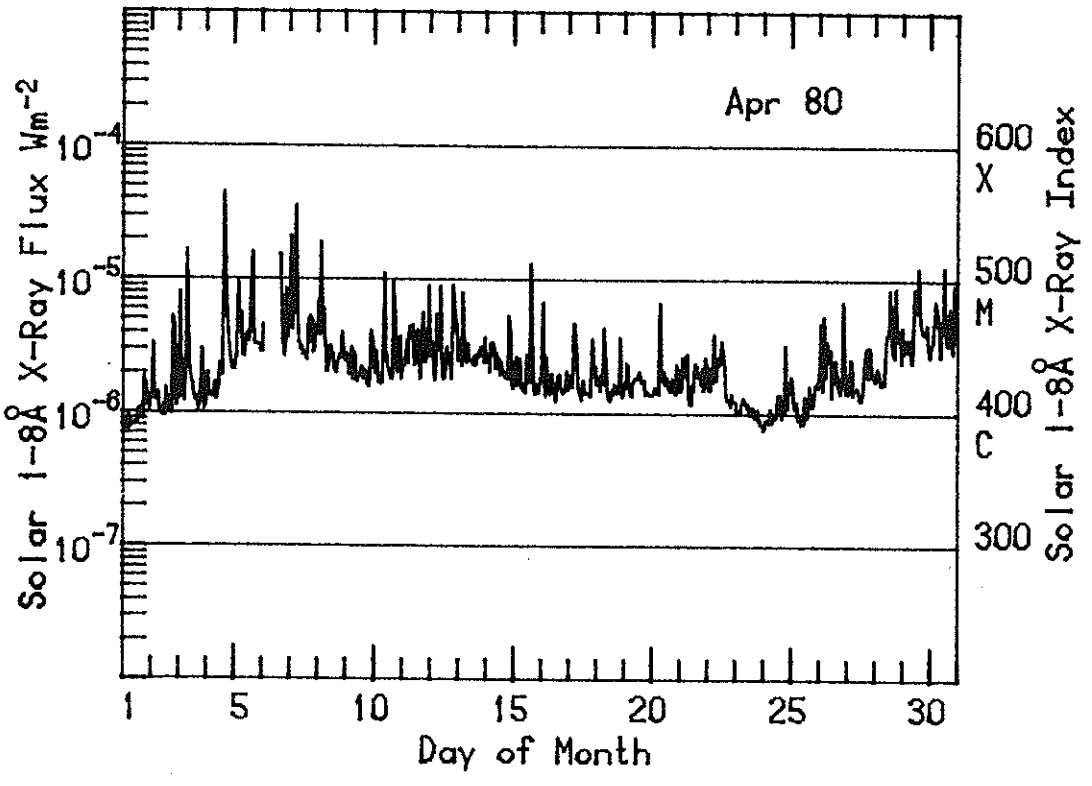
Apr 80
Solar 1-8Å X-Ray Flux Wm-2
10-4
10-5
10-6
10-7
600
X
500
M
400
C
300
Solar 1-8Å X-Ray Index
1
5
10
15
20
25
30
Day of Month

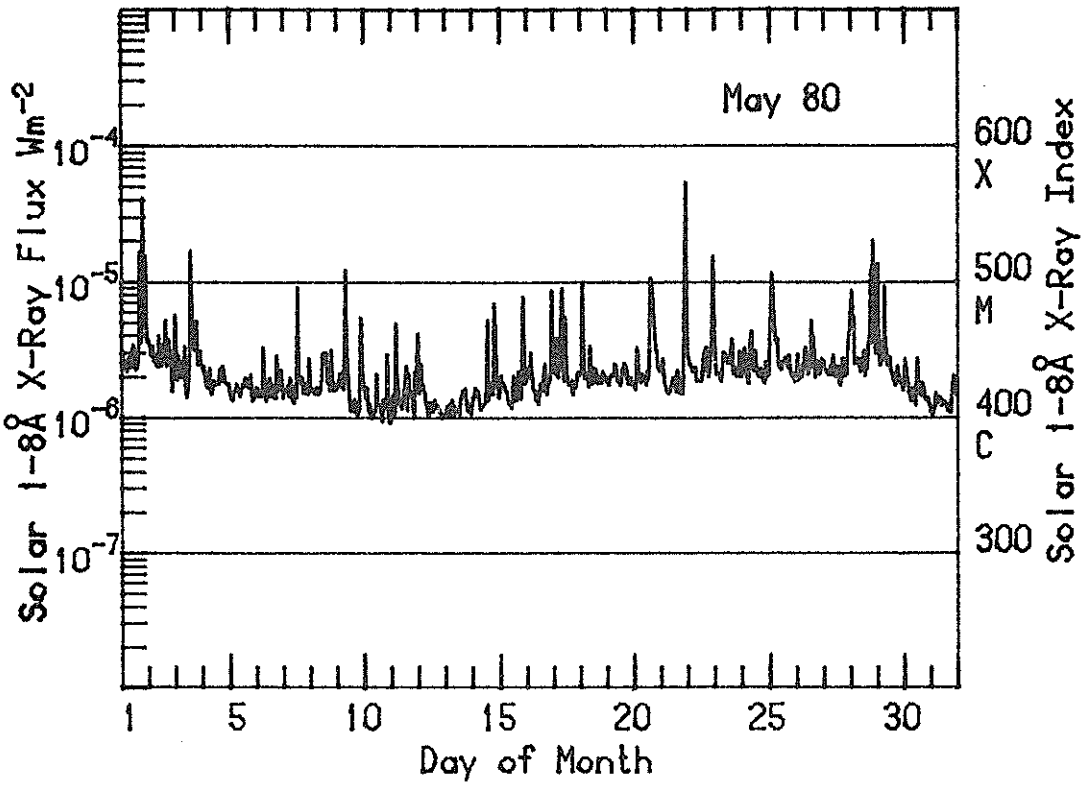
May 80
Solar 1-8Å X-Ray Flux Wm⁻²
10⁻⁴
10⁻⁵
10⁻⁶
10⁻⁷
600
X
500
M
400
C
300
Solar 1-8Å X-Ray Index
1
5
10
15
20
25
30
Day of Month

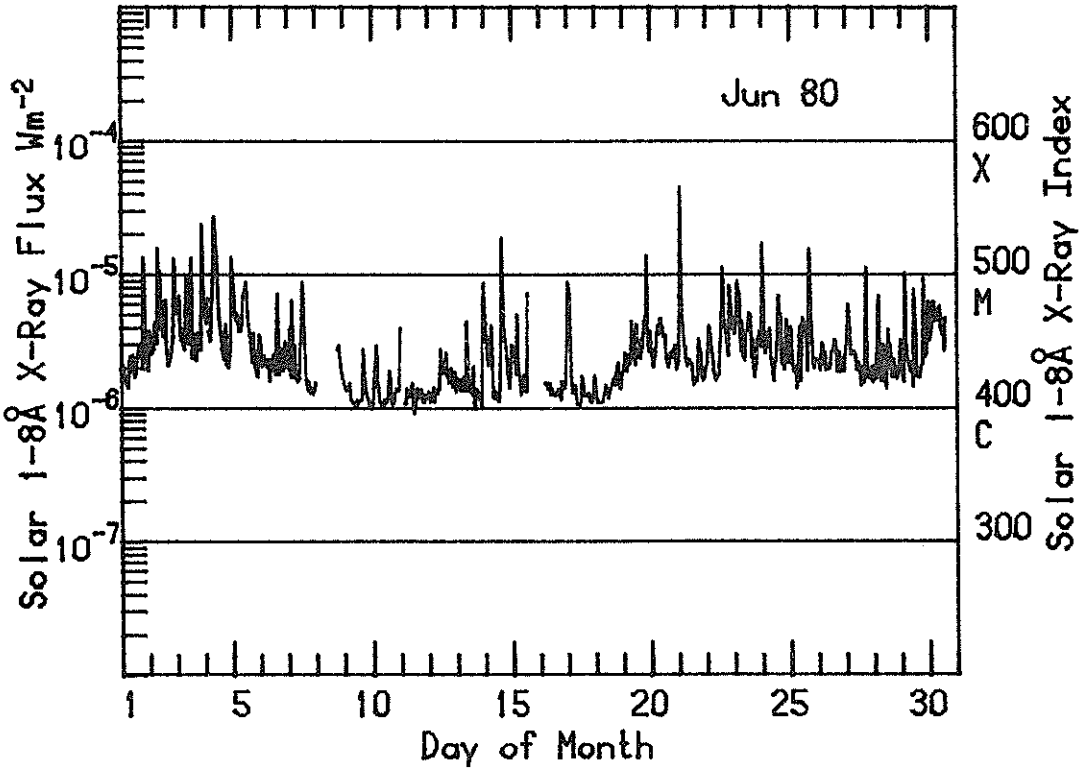
Jun 80
Solar 1-8Å X-Ray Flux Wm⁻²
10⁻⁴
10⁻⁵
10⁻⁶
10⁻⁷
600
X
500
M
400
C
300
Solar 1-8Å X-Ray Index
1
5
10
15
20
25
30
Day of Month

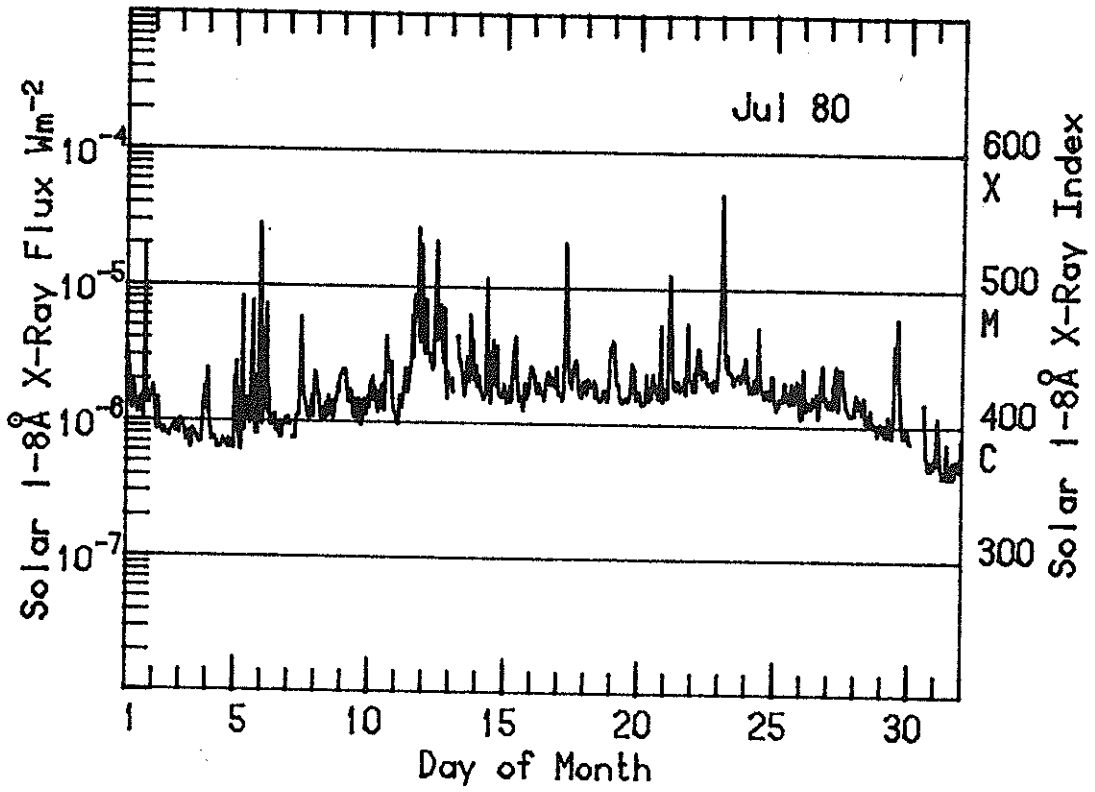
Jul 80
Solar 1-8Å X-Ray Flux Wm-2
10-4
10-5
10-6
10-7
600
X
500
M
400
C
300
Solar 1-8Å X-Ray Index
1
5
10
15
20
25
30
Day of Month

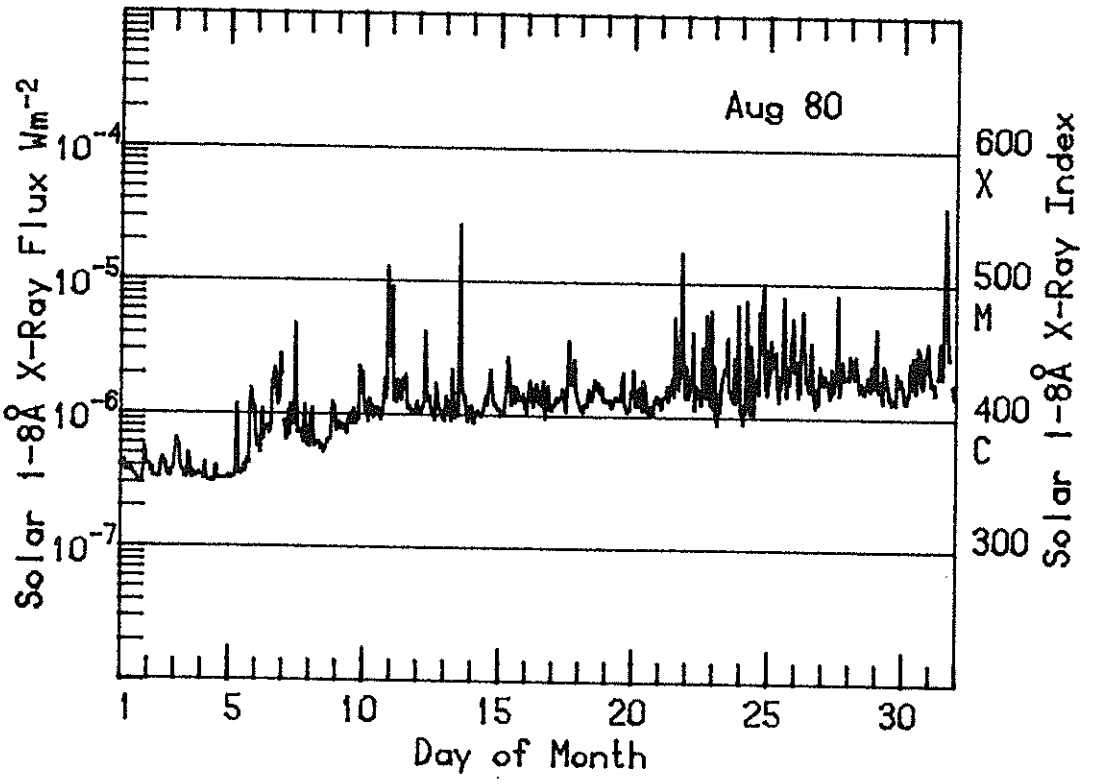
Aug 80
Solar 1-8Å X-Ray Flux Wm-2
10-4
10-5
10-6
10-7
600
X
500
M
400
C
300
Solar 1-8Å X-Ray Index
1
5
10
15
20
25
30
Day of Month

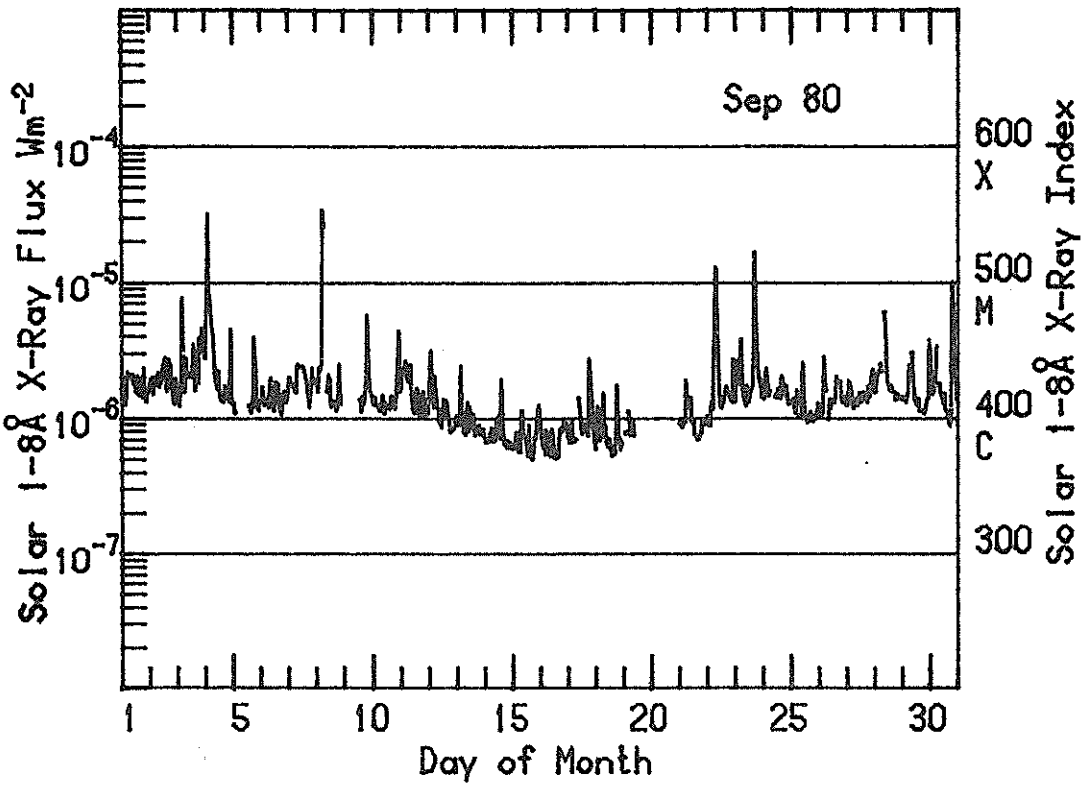
Sep 80
Solar 1-8Å X-Ray Flux Wm-2
10-4
10-5
10-6
10-7
600
X
500
M
400
C
300
Solar 1-8Å X-Ray Index
1
5
10
15
20
25
30
Day of Month

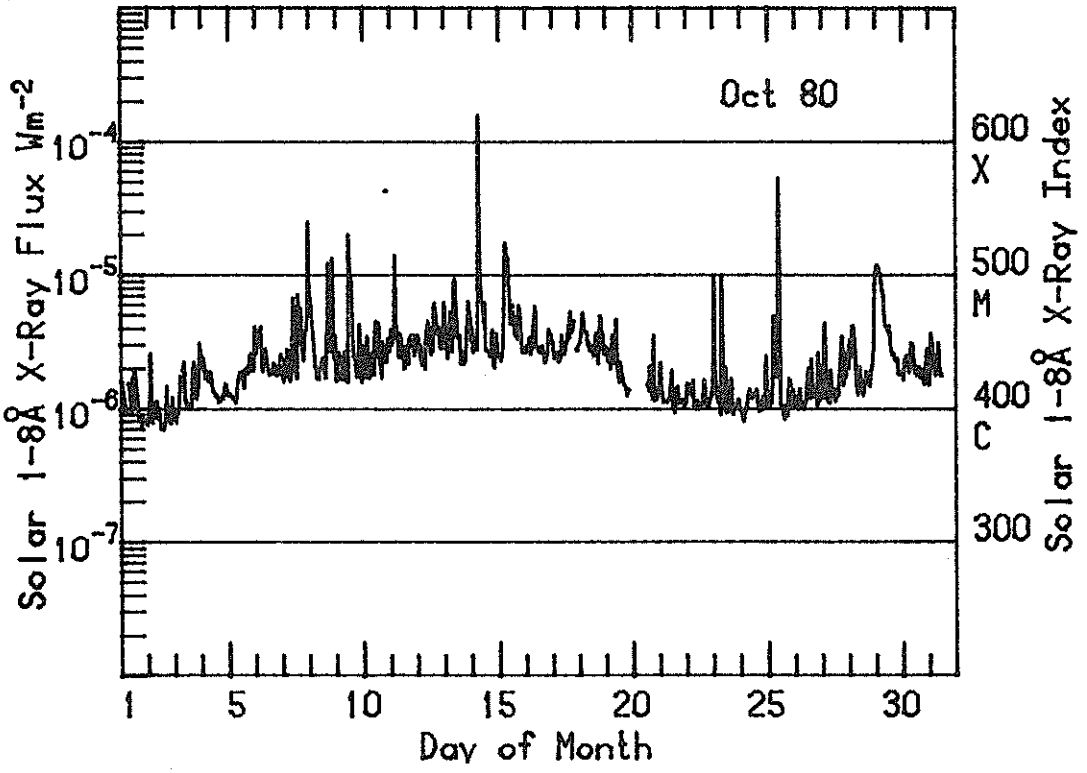
Oct 80
Solar 1-8Å X-Ray Flux Wm-2
10-4
10-5
10-6
10-7
600
X
500
M
400
C
300
Solar 1-8Å X-Ray Index
1
5
10
15
20
25
30
Day of Month

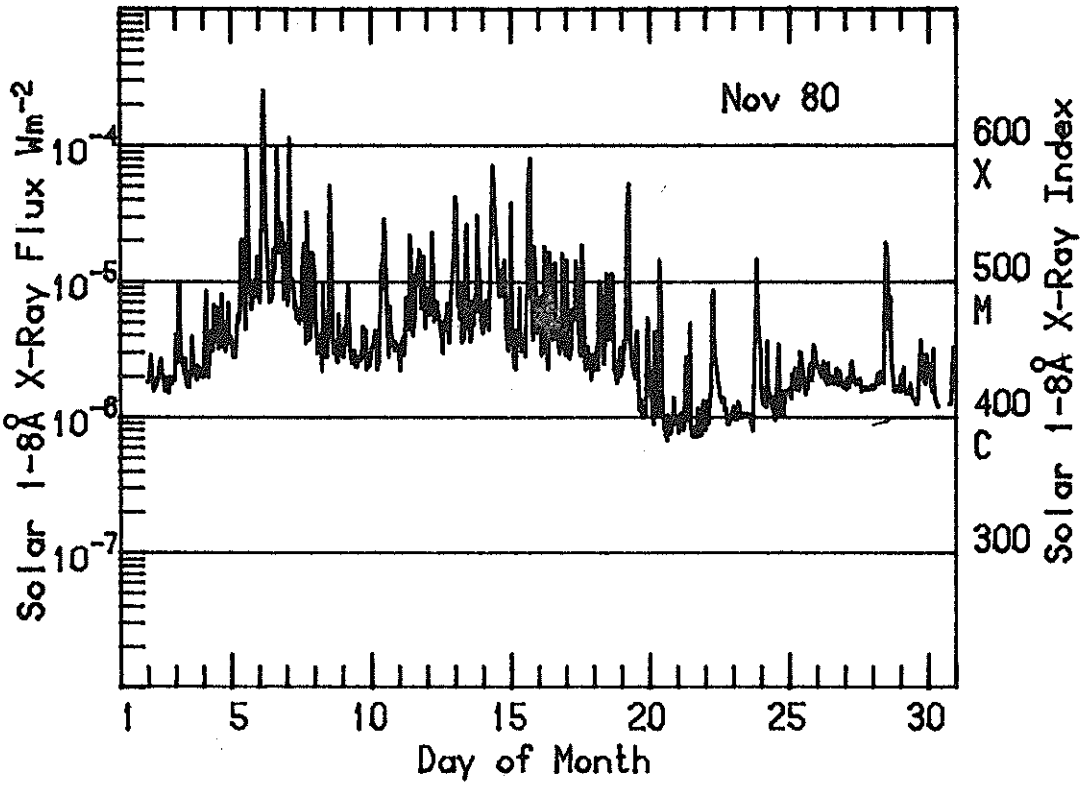
Nov 80
Solar 1-8Å X-Ray Flux Wm⁻²
10⁻⁴
10⁻⁵
10⁻⁶
10⁻⁷
600
X
500
M
400
C
300
Solar 1-8Å X-Ray Index
1
5
10
15
20
25
30
Day of Month

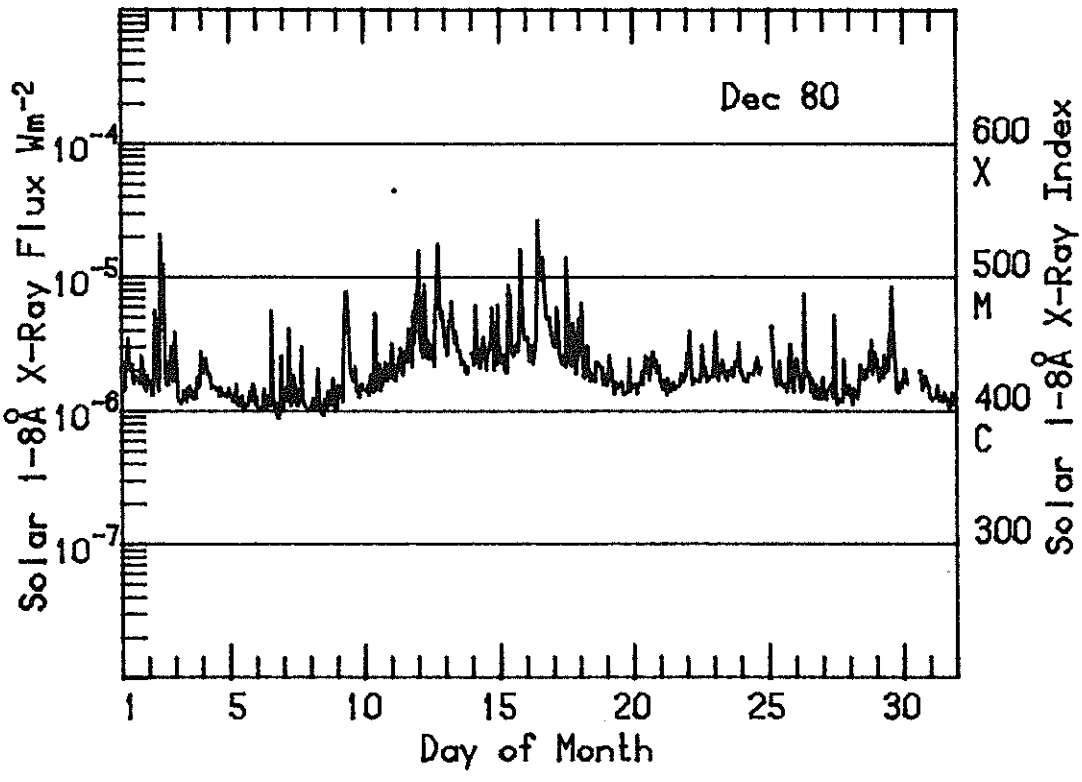
Dec 80
Solar 1-8Å X-Ray Flux Wm⁻²
10⁻⁴
10⁻⁵
10⁻⁶
10⁻⁷
600
X
500
M
400
C
300
Solar 1-8Å X-Ray Index
1
5
10
15
20
25
30
Day of Month

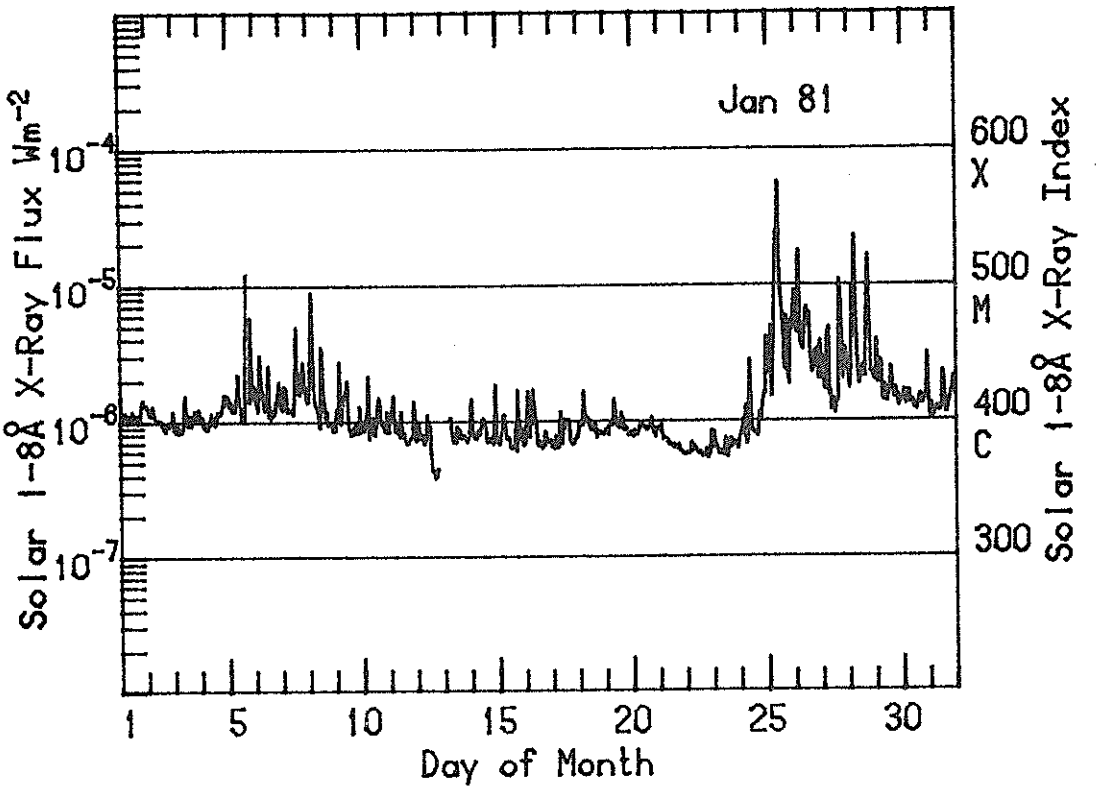
Jan 81
Solar 1-8Å X-Ray Flux Wm-2
10-4
10-5
10-6
10-7
600
X
500
M
400
C
300
Solar 1-8Å X-Ray Index
1
5
10
15
20
25
30
Day of Month

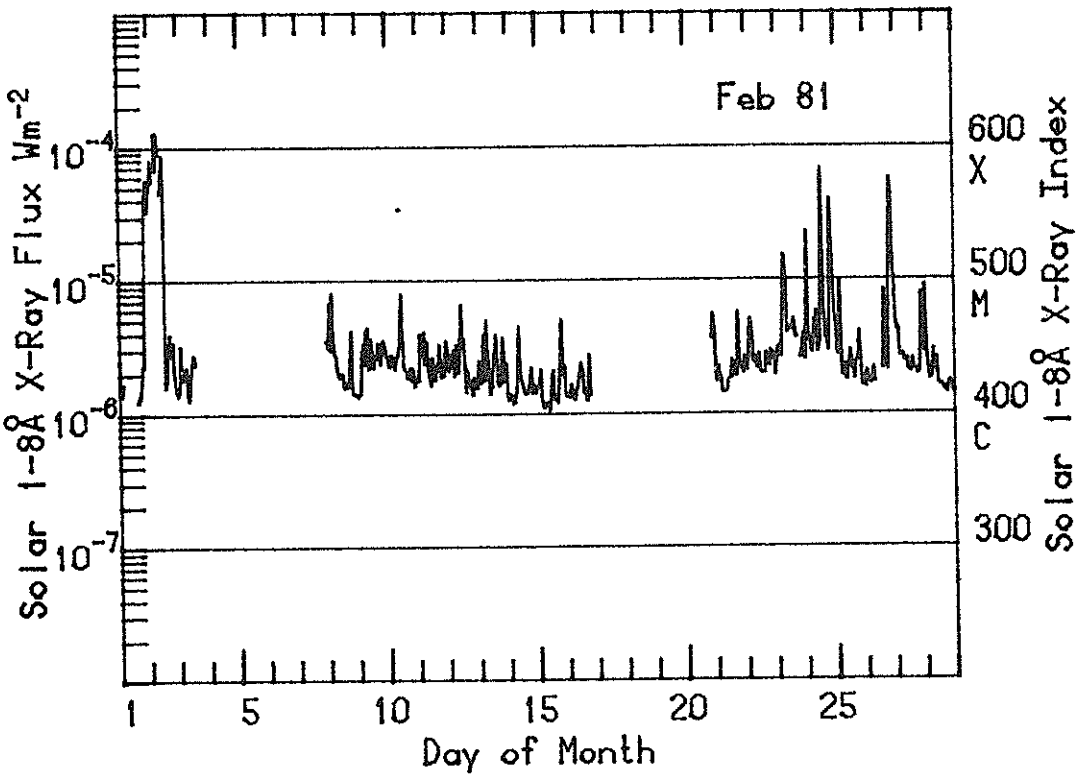
Feb 81
Solar 1-8Å X-Ray Flux Wm-2
10-4
10-5
10-6
10-7
600
X
500
M
400
C
300
Solar 1-8Å X-Ray Index
1
5
10
15
20
25
Day of Month

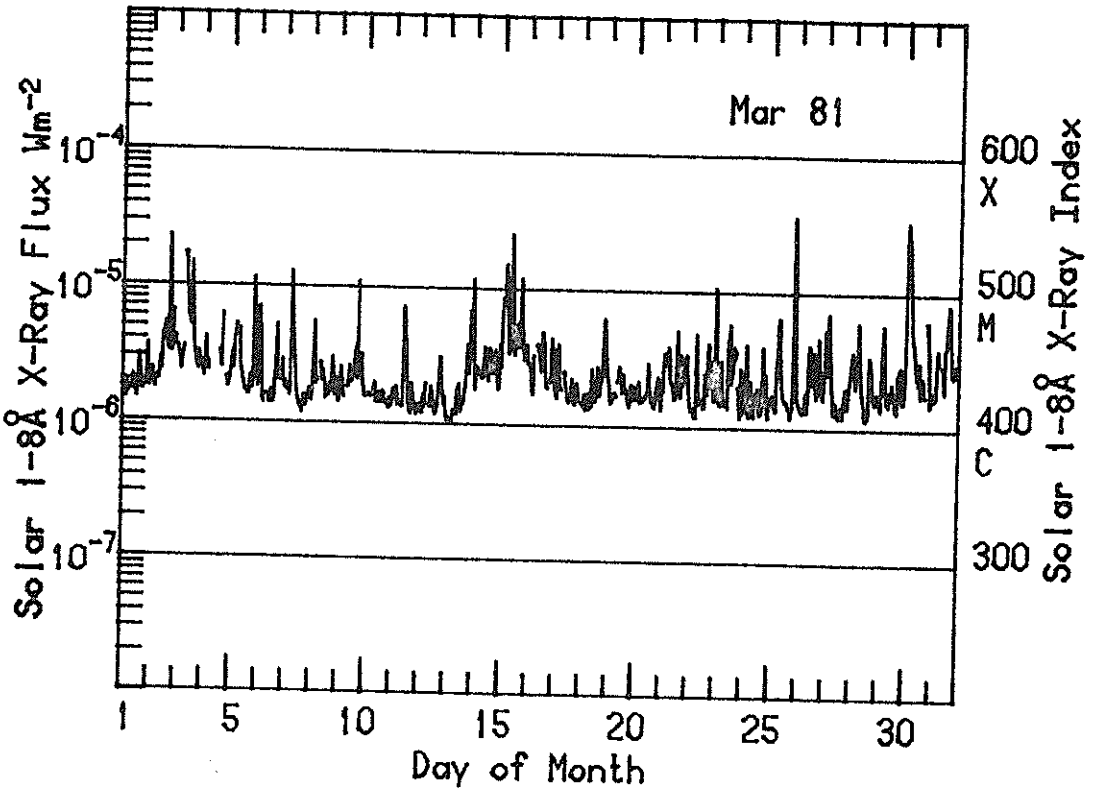
Mar 81
Solar 1-8Å X-Ray Flux Wm-2
10-4
10-5
10-6
10-7
600
X
500
M
400
C
300
Solar 1-8Å X-Ray Index
1
5
10
15
20
25
30
Day of Month

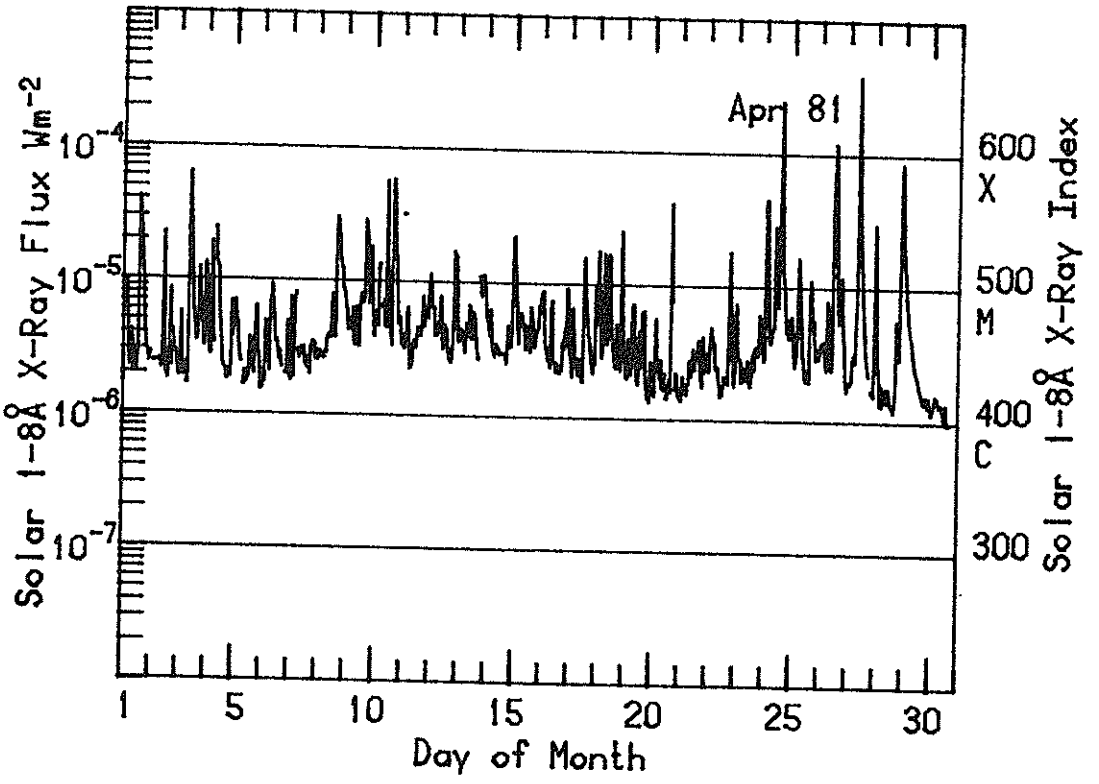
Apr 81
Solar 1-8Å X-Ray Flux Wm-2
10-4
10-5
10-6
10-7
600
X
500
M
400
C
300
Solar 1-8Å X-Ray Index
1
5
10
15
20
25
30
Day of Month

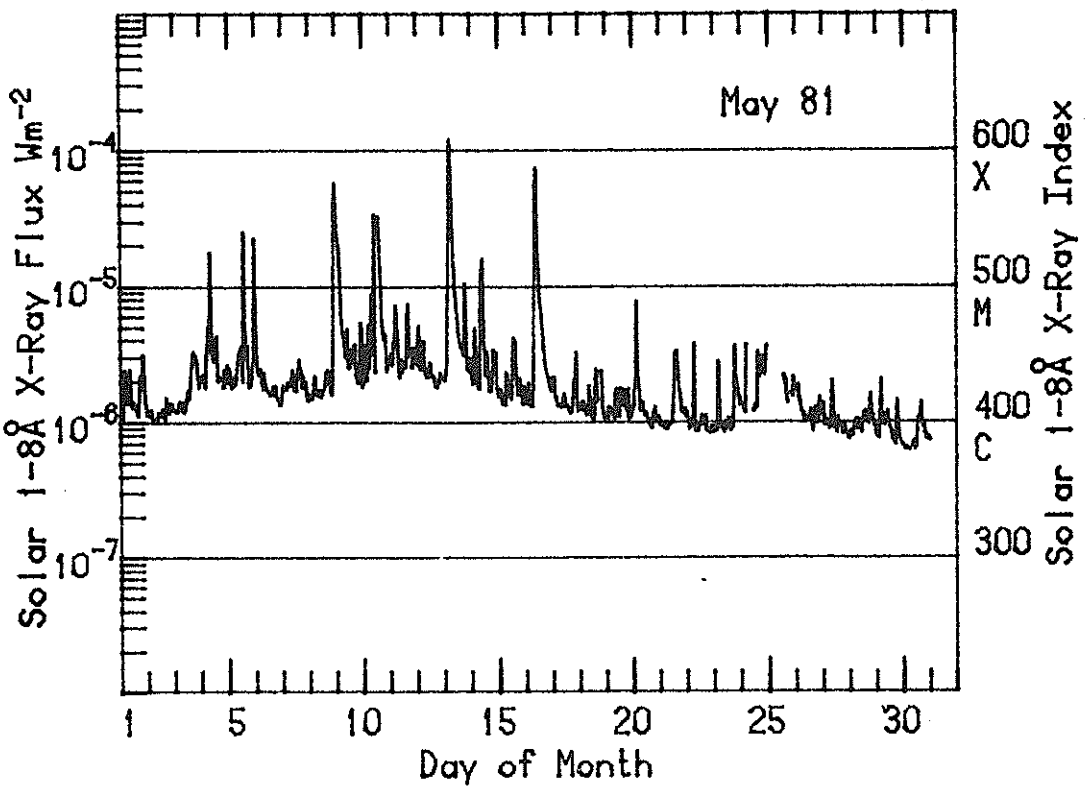
May 81
Solar 1-8Å X-Ray Flux Wm-2
10-4
10-5
10-6
10-7
600
X
500
M
400
C
300
Solar 1-8Å X-Ray Index
1
5
10
15
20
25
30
Day of Month

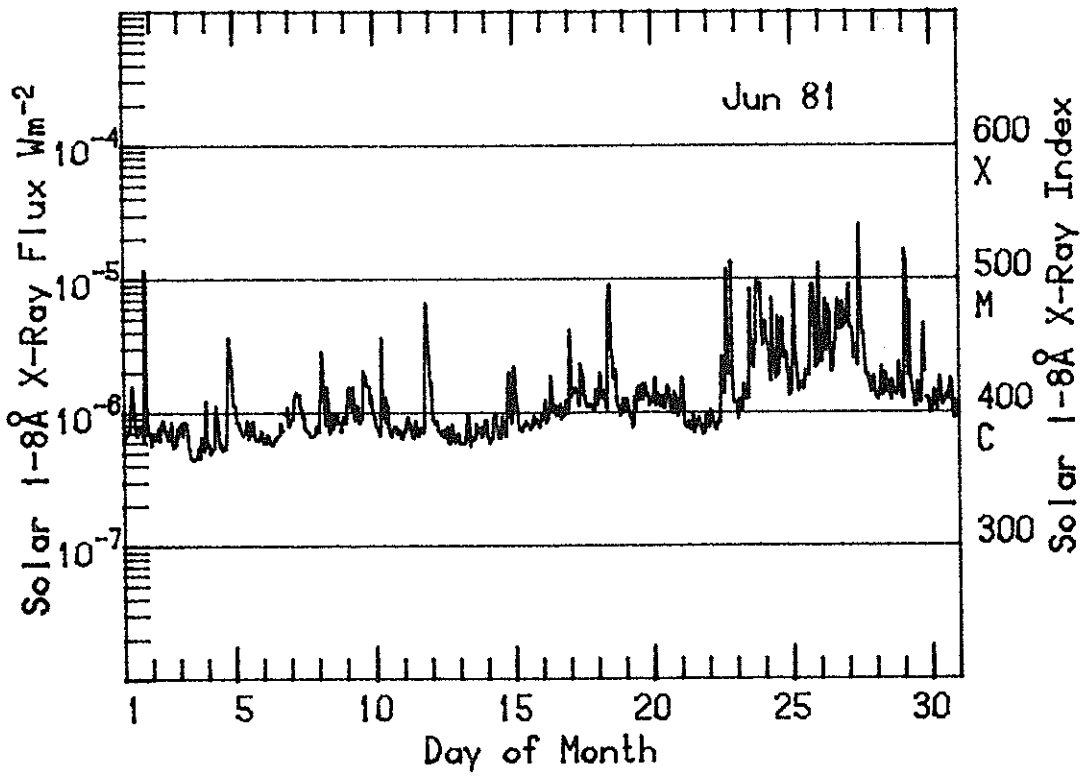
Jun 81
Solar 1-8Å X-Ray Flux Wm-2
10-4
10-5
10-6
10-7
600
X
500
M
400
C
300
Solar 1-8Å X-Ray Index
1
5
10
15
20
25
30
Day of Month

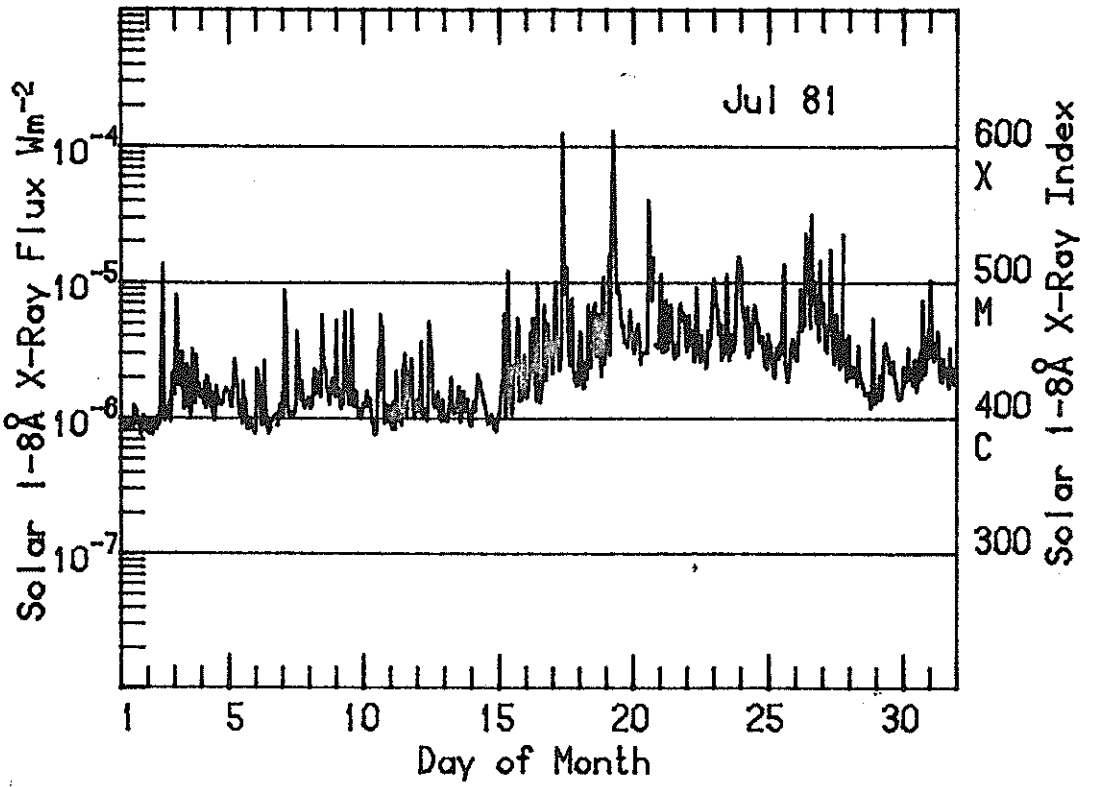
Jul 81
Solar 1-8Å X-Ray Flux Wm-2
10-4
10-5
10-6
10-7
600
X
500
M
400
C
300
Solar 1-8Å X-Ray Index
1
5
10
15
20
25
30
Day of Month

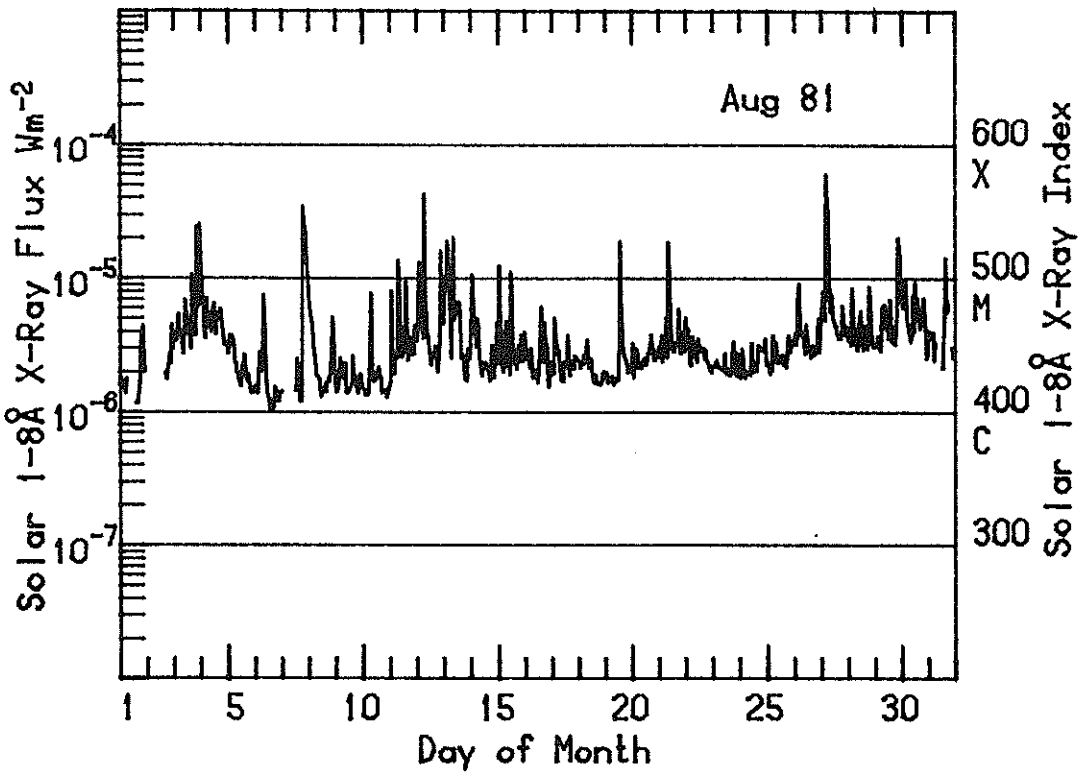
Aug 81
Solar 1-8Å X-Ray Flux Wm-2
10-4
10-5
10-6
10-7
600
X
500
M
400
C
300
Solar 1-8Å X-Ray Index
1
5
10
15
20
25
30
Day of Month

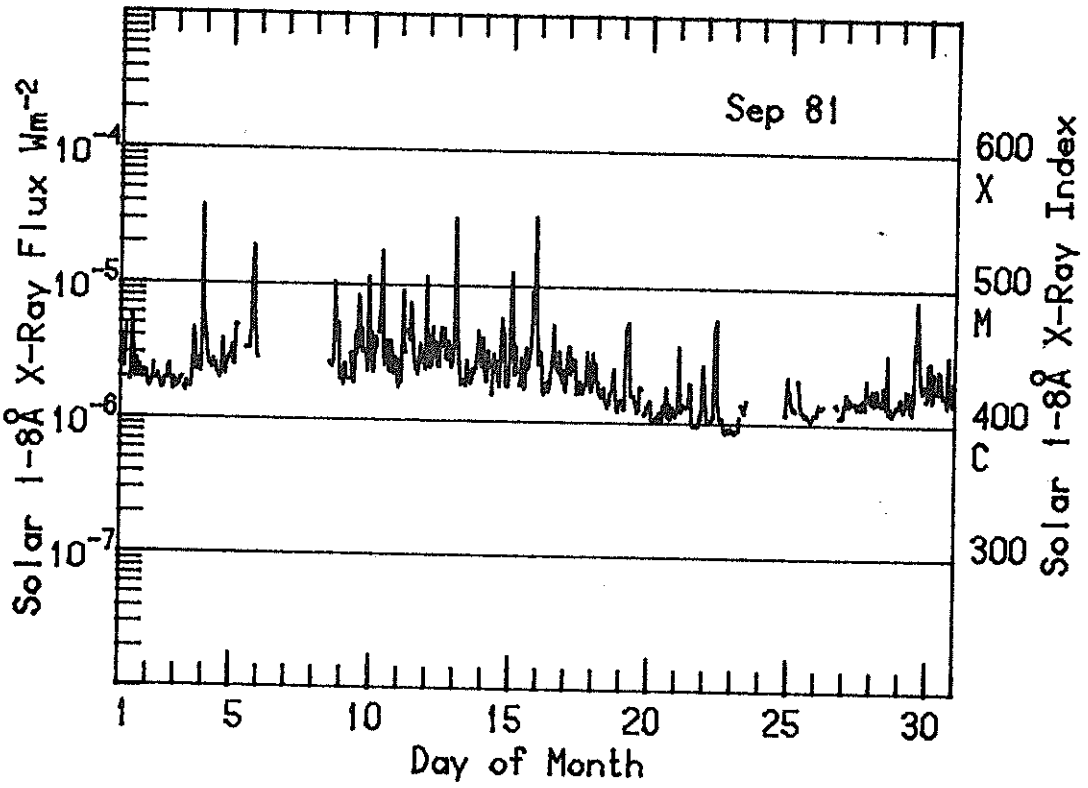
Sep 81
Solar 1-8Å X-Ray Flux Wm⁻²
10⁻⁴
10⁻⁵
10⁻⁶
10⁻⁷
600
X
500
M
400
C
300
Solar 1-8Å X-Ray Index
1
5
10
15
20
25
30
Day of Month

7.2 Tables of the Daily Background X-ray Index

Daily Background Solar X-Ray Index, 1977

Date	JAN	FEB	MAR	APR	MAY	JUN	JUL	AUG	SEP	OCT	NOV	DEC
1	228	324	240	223	275	304	333	301	---	311	314	316
2	262	301	243	258	245	321	322	299	301	307	311	311
3	267	286	238	246	313	349	315	288	307	326	308	299
4	275	272	254	244	292	340	312	---	312	346	309	310
5	271	268	269	224	273	324	311	---	308	390	313	316
6	255	249	259	209	268	319	326	---	311	382	307	358
7	212	242	255	217	268	313	304	323	368	359	305	376
8	210	292	281	205	287	318	286	---	385	352	304	350
9	204	298	256	225	312	305	263	---	361	341	316	378
10	220	299	205	301	293	300	226	483	359	332	319	377
11	204	281	209	313	279	291	219	310	353	324	319	346
12	271	327	203	325	277	278	240	285	339	345	298	350
13	281	323	204	321	288	276	255	291	347	313	297	334
14	254	300	247	320	302	289	232	259	349	318	312	316
15	280	293	216	315	305	271	234	289	352	317	314	311
16	300	305	224	302	302	290	233	278	357	312	301	313
17	287	318	205	282	286	292	241	257	371	314	333	324
18	324	295	210	261	281	295	245	269	368	309	330	323
19	311	288	211	219	278	301	260	264	388	349	318	301
20	283	285	202	271	265	308	281	299	402	330	322	289
21	240	279	201	270	259	313	266	310	372	325	299	289
22	242	238	205	281	265	339	286	313	376	351	312	301
23	265	210	254	267	275	345	284	295	356	332	302	304
24	258	213	241	274	243	371	273	296	353	305	298	313
25	240	206	218	275	218	374	286	295	357	297	298	344
26	254	211	207	258	217	395	286	258	338	290	290	367
27	222	209	231	232	229	371	276	274	339	300	296	373
28	251	220	204	225	234	343	271	305	335	307	311	364
29	241		205	201	263	343	270	306	336	307	315	367
30	211		213	281	305	329	271	311	326	318	300	364
31	308		213		319		234	311		314		360

Daily Background Solar X-Ray Index, 1978

Date	JAN	FEB	MAR	APR	MAY	JUN	JUL	AUG	SEP	OCT	NOV	DEC
1	379	388	390	368	409	401	390	318	411	380	390	391
2	380	412	403	374	417	395	380	323	424	368	391	390
3	378	410	405	371	418	383	363	338	415	361	400	379
4	373	399	402	382	413	369	357	337	409	365	396	388
5	371	403	399	382	415	370	353	345	408	382	391	389
6	380	402	406	378	423	352	359	347	403	373	394	401
7	372	403	401	391	443	355	382	361	402	371	400	409
8	336	417	404	415	433	345	385	353	404	392	396	419
9	335	418	413	411	401	322	438	347	385	394	398	412
10	327	396	408	416	386	331	441	349	393	401	399	417
11	322	405	400	438	385	339	428	347	392	405	396	421
12	315	407	390	409	380	347	414	350	384	416	381	456
13	300	425	391	387	374	367	393	364	377	420	381	443
14	311	408	404	389	376	370	388	377	390	420	371	421
15	307	416	395	383	372	372	383	374	397	428	409	409
16	291	401	378	367	383	388	379	359	387	404	374	411
17	298	394	366	364	382	391	382	359	384	399	362	410
18	318	400	364	372	370	395	377	343	391	394	353	413
19	331	395	364	384	380	416	384	325	387	401	363	402
20	336	377	372	380	390	413	376	318	386	406	367	380
21	336	379	365	394	396	414	403	316	394	396	371	389
22	341	379	361	403	400	406	374	319	397	396	364	389
23	342	374	358	441	386	408	353	318	412	399	356	388
24	355	370	364	421	387	410	360	328	404	383	366	398
25	359	378	363	405	386	404	334	321	396	379	365	380
26	388	376	353	413	392	399	331	313	393	380	366	383
27	388	388	362	408	384	402	337	348	401	380	391	392
28	382	386	348	440	388	405	332	352	388	384	398	414
29	383		337	436	391	409	327	351	387	378	400	399
30	388		354	437	396	401	323	370	386	376	399	403
31	392		---		392		321	389		376		411

Daily Background Solar X-Ray Index, 1979

Date	JAN	FEB	MAR	APR	MAY	JUN	JUL	AUG	SEP	OCT	NOV	DEC
1	411	424	404	425	393	412	410	375	412	432	412	398
2	412	427	401	416	399	422	412	364	424	430	410	399
3	416	412	405	416	395	424	417	376	403	429	413	399
4	411	400	404	413	409	424	419	368	412	443	424	415
5	419	410	404	415	406	415	399	373	394	442	445	414
6	418	415	411	411	402	414	400	384	392	415	466	411
7	411	409	413	410	403	424	400	384	395	402	467	409
8	423	414	414	411	411	419	406	379	400	400	473	418
9	412	424	419	416	405	422	402	376	405	411	450	417
10	404	428	410	410	401	415	403	376	399	414	470	416
11	410	423	411	407	399	414	399	366	397	419	459	415
12	397	448	408	393	397	405	391	359	408	411	439	418
13	424	444	409	404	385	407	385	400	407	428	434	424
14	424	436	410	399	389	400	384	412	453	432	421	424
15	433	423	405	387	387	391	389	401	430	422	420	423
16	424	436	401	386	390	383	378	392	415	427	419	423
17	419	434	394	385	415	386	366	390	415	427	432	412
18	425	444	400	379	420	381	366	440	420	424	432	406
19	434	441	396	389	410	387	374	425	421	426	422	416
20	427	446	402	390	408	382	376	433	427	415	412	423
21	425	452	405	398	401	368	386	417	424	411	414	418
22	425	451	398	407	387	366	417	424	413	404	---	407
23	426	428	412	409	379	360	413	411	405	419	398	397
24	418	428	410	402	379	365	414	409	400	428	390	382
25	414	414	440	400	377	373	400	424	411	419	386	393
26	406	416	442	398	365	382	395	433	413	418	377	394
27	420	402	432	399	373	393	388	414	412	416	359	399
28	435	401	412	393	374	389	376	414	420	421	366	400
29	428		407	390	384	387	374	396	428	418	377	413
30	424		403	393	400	399	378	399	433	411	374	406
31	430		407		405		372	404		413		411

Daily Background Solar X-Ray Index, 1980

Date	JAN	FEB	MAR	APR	MAY	JUN	JUL	AUG	SEP	OCT	NOV	DEC
1	407	412	393	390	435	422	402	349	410	392	---	414
2	411	416	386	397	428	436	388	351	414	383	418	414
3	416	421	385	405	415	436	380	351	418	398	421	406
4	412	437	400	409	416	440	380	348	411	405	440	411
5	408	420	390	439	412	443	384	354	404	415	464	399
6	425	414	391	441	411	419	392	385	405	424	484	397
7	422	413	385	439	410	415	395	378	413	422	468	400
8	420	417	391	430	418	417	402	371	408	421	437	396
9	426	417	385	422	404	400	400	385	404	419	436	405
10	436	422	378	423	397	400	406	395	403	423	442	414
11	430	423	377	428	400	395	421	404	403	429	452	426
12	441	426	362	425	400	407	433	396	393	438	446	433
13	438	420	363	435	402	403	419	395	387	433	455	435
14	423	409	364	424	407	404	414	398	379	436	455	430
15	420	414	375	415	406	411	412	403	371	438	444	437
16	412	408	370	408	409	408	417	399	370	437	435	446
17	400	398	372	410	423	401	418	402	382	440	435	431
18	392	394	382	409	424	406	416	406	372	439	430	421
19	376	387	388	413	423	431	415	405	387	419	404	411
20	379	---	382	414	423	429	415	400	---	413	383	418
21	383	394	383	406	417	417	421	409	384	397	385	414
22	391	390	401	411	426	420	425	406	403	399	394	420
23	399	390	402	393	428	432	429	398	409	395	394	422
24	429	395	400	394	425	420	420	401	412	394	398	425
25	423	403	399	392	433	419	408	411	396	391	416	416
26	410	407	395	412	428	427	406	411	404	400	423	411
27	445	400	422	410	423	417	411	416	410	405	419	404
28	430	395	408	430	430	414	402	418	416	409	420	417
29	432	399	402	441	423	415	392	411	405	440	409	418
30	420		401	442	408	442	375	417	396	419	410	415
31	424		389		403		361	417		424		404

Daily Background Solar X-Ray Index, 1981

Date	JAN	FEB	MAR	APR	MAY	JUN	JUL	AUG	SEP
1	399	410	417	429	403	380	391	407	427
2	394	419	430	425	400	374	391	425	421
3	395	409	437	430	407	364	401	443	419
4	397	---	429	433	426	370	398	452	429
5	399	---	420	422	425	380	395	419	442
6	403	---	413	425	418	375	388	401	---
7	405	454	407	427	418	385	402	411	---
8	395	418	417	456	418	383	408	411	438
9	390	426	417	450	439	391	403	413	426
10	389	426	414	451	431	381	387	412	429
11	383	420	410	439	432	380	394	431	431
12	363	415	406	449	430	377	397	435	438
13	384	413	407	444	434	374	396	432	425
14	384	411	425	442	422	379	395	426	422
15	379	401	444	448	412	386	402	428	423
16	379	409	425	433	417	393	411	421	421
17	381	---	416	426	406	403	428	422	420
18	392	---	415	438	400	400	426	421	410
19	390	---	415	422	401	397	449	423	408
20	388	439	415	416	397	400	445	432	401
21	379	417	420	419	399	384	444	440	397
22	373	429	413	417	392	392	439	432	396
23	373	441	412	425	392	409	442	427	407
24	388	445	408	454	408	418	440	427	407
25	422	423	410	429	430	416	428	431	405
26	435	426	416	431	393	429	450	440	405
27	405	430	408	423	391	424	436	454	411
28	426	416	406	407	389	408	416	446	408
29	412		412	419	385	403	413	448	408
30	407		423	398	380	398	419	446	416
31	405		427		---		427	433	

7.3 Tables of the Daily Mean Index

Daily Mean Solar X-Ray Index, 1977

Date	JAN	FEB	MAR	APR	MAY	JUN	JUL	AUG	SEP	OCT	NOV	DEC
1	293	362	271	246	288	329	337	314	---	325	324	333
2	286	368	297	259	280	359	332	302	312	319	320	329
3	290	331	268	277	359	379	326	295	327	350	316	318
4	324	324	265	302	336	361	324	---	323	366	316	323
5	290	297	283	256	303	335	323	---	335	413	324	354
6	281	270	265	255	298	333	338	---	339	414	331	388
7	270	279	264	303	283	329	322	323	478	378	327	423
8	230	327	337	262	300	327	306	---	427	385	309	373
9	225	339	324	283	352	330	282	---	466	360	326	400
10	236	321	279	337	303	316	254	483	377	347	335	429
11	259	362	303	373	295	311	275	310	364	341	331	422
12	362	352	301	416	294	302	270	302	349	388	314	405
13	338	386	264	408	299	334	269	315	357	355	316	357
14	285	323	292	393	314	290	269	296	366	345	331	334
15	302	306	247	358	312	297	272	318	368	339	335	323
16	314	324	249	383	311	304	262	296	453	340	333	329
17	312	375	233	391	306	328	264	301	423	322	345	337
18	320	319	293	281	296	314	278	307	431	329	354	333
19	375	302	232	330	313	315	356	305	501	366	332	322
20	310	311	224	320	278	322	360	323	473	356	345	301
21	265	293	223	295	273	332	291	341	393	355	331	303
22	265	261	269	310	293	356	322	337	392	387	434	314
23	287	246	304	288	289	365	304	337	378	359	308	343
24	279	272	278	293	279	417	290	318	423	333	304	337
25	277	249	274	286	255	402	306	314	411	312	303	370
26	274	251	255	279	250	438	302	306	391	301	308	438
27	255	238	257	253	257	405	289	323	354	310	322	420
28	311	369	244	260	263	373	295	305	346	338	345	419
29	271		270	261	291	367	294	327	365	339	339	409
30	280		233	306	339	340	304	322	342	340	332	389
31	354		269		339		289	351		329		390

Daily Mean Solar X-Ray Index, 1978

Date	JAN	FEB	MAR	APR	MAY	JUN	JUL	AUG	SEP	OCT	NOV	DEC
1	419	412	400	388	481	418	417	326	437	453	420	404
2	397	429	427	388	443	417	408	328	470	374	410	400
3	402	438	422	379	440	386	380	357	437	387	418	407
4	387	406	433	404	436	374	372	351	437	378	411	406
5	384	418	407	399	434	400	394	352	417	429	407	399
6	392	416	453	395	461	359	380	367	423	411	402	412
7	451	419	407	419	497	366	438	388	421	383	419	441
8	456	436	419	490	485	358	440	374	426	425	414	434
9	378	459	426	443	456	331	512	356	400	455	407	425
10	345	444	423	442	403	357	536	357	412	425	441	446
11	341	428	413	518	399	364	559	358	403	432	408	497
12	327	442	398	433	390	370	454	361	390	459	394	509
13	334	496	403	416	394	384	405	384	399	432	393	508
14	328	423	442	422	395	385	399	399	406	464	387	479
15	329	439	412	415	383	388	411	393	414	493	425	438
16	309	416	391	382	399	405	386	389	411	430	388	428
17	331	413	375	374	398	417	398	377	439	403	370	455
18	329	412	383	409	394	412	454	358	409	406	363	423
19	339	403	384	415	407	426	398	331	399	416	370	413
20	351	388	386	405	413	428	416	326	394	426	394	396
21	344	395	379	412	417	424	464	324	410	423	383	407
22	354	387	377	413	415	460	410	328	412	404	373	410
23	356	383	366	521	427	420	417	331	500	405	364	421
24	366	391	381	430	426	423	373	334	428	400	388	425
25	383	413	370	432	403	421	346	330	404	403	385	401
26	416	394	376	433	444	448	345	327	407	398	381	408
27	412	416	373	423	406	410	353	386	447	394	405	447
28	391	400	366	538	446	422	346	363	402	402	435	422
29	400		356	515	420	427	364	377	422	339	422	410
30	403		368	510	448	423	335	413	399	382	417	447
31	401		---		488		333	405		390		413

Daily Mean Solar X-Ray Index, 1979

Date	JAN	FEB	MAR	APR	MAY	JUN	JUL	AUG	SEP	OCT	NOV	DEC
1	423	447	447	444	423	427	425	401	431	454	426	413
2	426	444	431	435	440	441	439	374	456	446	417	410
3	430	421	421	480	412	463	428	384	427	443	431	424
4	420	408	412	436	418	477	466	381	424	480	459	439
5	446	444	440	435	418	516	412	391	405	486	477	423
6	437	429	427	428	424	432	407	402	405	454	509	418
7	428	424	423	417	420	437	414	436	410	429	490	423
8	446	452	432	423	425	432	431	406	414	419	511	432
9	424	443	468	432	427	445	424	394	420	420	484	423
10	423	461	418	428	409	474	411	407	420	423	496	425
11	436	465	439	429	422	424	412	375	431	436	477	428
12	427	493	420	405	405	416	399	370	423	433	472	431
13	460	465	421	413	399	423	394	444	436	444	453	443
14	462	473	417	428	406	411	400	479	525	460	448	442
15	464	435	423	388	399	400	414	423	461	432	459	435
16	449	508	426	389	405	401	387	435	480	440	434	434
17	438	464	400	403	444	393	373	409	431	452	463	460
18	445	508	424	390	435	401	373	528	442	452	451	420
19	452	485	439	399	443	395	373	443	499	471	458	451
20	437	493	430	404	445	393	399	524	458	452	435	465
21	451	488	428	403	454	382	413	445	446	443	451	435
22	444	491	442	419	404	383	443	449	443	431	---	426
23	434	458	439	418	385	365	434	444	420	434	407	414
24	438	445	441	416	388	373	449	443	417	443	410	412
25	439	456	480	418	384	423	421	445	433	443	398	423
26	424	435	504	419	380	403	412	502	422	432	386	413
27	437	414	482	463	383	400	428	431	421	426	382	414
28	455	418	422	410	381	398	396	431	429	428	370	411
29	437		433	407	400	395	395	407	436	427	392	435
30	434		428	423	414	408	416	411	457	421	390	426
31	445		445		420		380	415		429		425

Daily Mean Solar X-Ray Index, 1980

Date	JAN	FEB	MAR	APR	MAY	JUN	JUL	AUG	SEP	OCT	NOV	DEC
1	429	432	406	399	476	443	438	357	424	406	---	428
2	422	455	408	419	448	471	397	357	429	399	428	457
3	425	473	398	443	456	474	395	360	442	416	447	418
4	427	467	430	470	428	484	390	352	462	418	463	421
5	426	450	399	466	420	465	456	378	417	425	516	408
6	457	459	408	475	425	439	414	406	415	436	559	413
7	443	439	400	481	429	442	418	400	429	460	514	415
8	465	455	399	458	428	434	416	385	465	458	481	406
9	448	427	399	434	437	410	417	401	430	454	453	438
10	478	448	392	448	411	415	426	427	416	442	481	429
11	455	443	387	453	424	413	468	424	420	455	491	449
12	472	438	371	455	411	421	468	411	410	455	487	471
13	476	453	371	447	409	431	445	440	399	458	507	448
14	448	420	376	440	430	449	438	408	389	502	516	448
15	430	438	386	436	428	439	429	414	387	475	508	460
16	424	422	372	427	435	416	430	413	385	449	481	483
17	408	405	380	430	441	429	449	421	400	449	473	455
18	399	401	389	426	439	414	428	415	390	453	468	434
19	402	402	413	422	430	454	429	413	393	433	476	421
20	393	---	398	429	451	445	427	412	---	420	431	429
21	402	405	396	428	464	465	445	443	400	409	409	421
22	410	398	417	428	449	458	439	433	437	409	430	430
23	420	402	411	401	438	465	470	430	444	429	435	433
24	440	406	416	407	438	452	431	444	420	406	419	428
25	434	433	416	408	453	454	421	445	408	463	432	430
26	448	427	412	440	442	438	420	435	417	414	430	428
27	495	422	462	427	440	443	421	435	418	426	425	418
28	464	416	428	453	470	438	408	432	431	442	458	428
29	473	417	426	465	443	453	418	426	422	469	426	438
30	437		413	468	421	466	380	433	436	432	428	423
31	449		396		413		373	471		435		409

Daily Mean Solar X-Ray Index, 1981

Date	JAN	FEB	MAR	APR	MAY	JUN	JUL	AUG	SEP
1	406	505	428	486	421	423	397	429	441
2	401	560	460	457	407	383	422	442	428
3	402	431	470	492	426	379	434	482	457
4	404	---	446	479	456	400	416	470	445
5	432	---	448	451	463	386	411	434	459
6	418	---	437	456	433	384	409	428	---
7	424	454	438	453	428	396	429	499	---
8	428	440	433	491	476	402	429	443	456
9	406	444	441	491	483	410	430	424	455
10	401	441	419	512	488	396	421	428	459
11	396	440	430	465	454	413	414	462	460
12	384	439	419	477	439	388	420	482	453
13	391	437	439	474	518	384	403	479	462
14	394	421	442	463	453	396	408	453	443
15	391	422	481	476	428	395	440	458	473
16	393	421	447	462	499	403	448	441	438
17	390	---	427	463	418	417	503	440	437
18	397	---	435	487	416	431	461	432	423
19	397	---	427	452	412	408	518	447	428
20	394	460	425	462	419	409	489	441	407
21	383	432	441	439	414	395	458	464	416
22	378	442	438	454	403	438	463	445	415
23	381	467	441	448	411	455	480	434	404
24	413	500	426	539	436	447	463	438	424
25	498	443	463	467	426	456	456	442	411
26	471	498	435	514	409	465	495	458	411
27	445	450	437	545	400	462	470	495	417
28	468	428	435	501	401	419	429	461	418
29	426		434	457	397	448	432	475	436
30	417		481	410	390	410	447	472	429
31	415		452		---		442	467	

8. ACKNOWLEDGEMENTS

A very special thanks to Frank Cowley and Donna Batehelor from SEL/SESC for their excellent work in the recovery of misplaced and mislabeled data tapes. Without their patient, methodical efforts the data necessary to compare satellites and complete the time series would not have been available.

9. REFERENCES

Cochran, William G., G. W. Snedecor, 1967, pages 329-330, Statistical Methods (6th Ed.)

Donnelly, R. F., R. N. Grubb and F. C. Cowley, 1977, Solar X-ray Measurements from SMS-1, SMS-2, and GOES-1 Information for Data Users, NOAA Technical Memorandum ERL SEL-48, NOAA ERL SEL, Boulder, Colorado 80303.

Donnelly, R. F., 1981, SMS-GOES Solar Soft X-Ray Measurements Part I. SMS-1, SMS-2, and GOES-1 Measurements from July 1, 1974, through December 31, 1976, NOAA Technical Memorandum ERL SEL-56, NOAA ERL SEL, Boulder, Colorado, 80303.

Donnelly, R. F. and S. D. Bouwer, 1981, SMS-GOES Solar Soft X-Ray Measurements Part II. SMS-2, GOES-1, GOES-2, and GOES-3 Measurements from January 1, 1977, through December 31, 1980, NOAA Technical Memorandum ERL SEL-57, NOAA ERL SEL, Boulder, Colorado, 80303.

Donnelly, R. F., 1982, Comparison of Nonflare Solar Soft X-Ray Flux with 10.7 cm Radio Flux, Accepted for publication by Journal of Geophysical Research.

Grubb, R. N., 1975, The SMS/GOES Space Environment Monitor Subsystem, NOAA Technical Memorandum ERL SEL-42, NOAA ERL SEL, Boulder, Colorado 80303.

Kreplin, R. W., K. P. Dere, D. M. Horan, and J. F. Meekins, 1977, The Solar Spectrum Below 10Å, pages 287-312, The Solar Output and Its Variation, ed. O. R. White.

Unzicker, A. and R. F. Donnelly, 1974, Calibration of X-Ray Ion Chambers for the Space Environment Monitoring System, NOAA Technical Report ERL 310-SEL 31, U. S. Government Printing Office, Washington, DC 20402.